

Non-Abelian Anyons and Interferometry

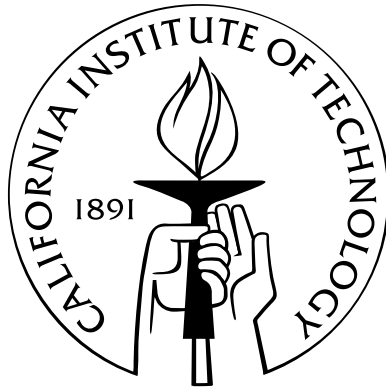
Thesis by

Parsa Hassan Bonderson

In Partial Fulfillment of the Requirements

for the Degree of

Doctor of Philosophy



California Institute of Technology

Pasadena, California

2007

(Defended 23 May, 2007)

© 2007

Parsa Hassan Bonderson

All Rights Reserved

To all my teachers,
especially the three who have been with me from the very beginning:
my parents, Mahrokh and Loren, and my sister, Roxana.

Acknowledgments

First and foremost, I would like to thank the members of my thesis defense committee: my advisor John Preskill for his guidance and support, and for giving me a chance and pointing me in the right direction when I was lost; Alexei Kitaev for providing inspiring and enlightening discussions; Kirill Shtengel for taking me under his wing and for all the help and advice he has given me; and Nai-Chang Yeh for her endless encouragement and enthusiasm. Also, I thank John Schwarz for his efforts and understanding during his time spent as my initial advisor at Caltech. I would like to recognize the hard work and affability of the Caltech staff, especially Donna Driscoll, Ann Harvey, and Carol Silberstein. I have had the pleasure and benefit of discussing physics, mathematics, and other interesting topics with Eddy Ardonne, Waheb Bishara, Dave DeConde, Mike Freedman, Tobe Hagge, Israel Klich, Chetan Nayak, Ed Rezayi, Ady Stern, and Zhenghan Wang. I would like to express my utmost appreciation to Kirill Shtengel and Joost Slingerland for the countless discussions and enjoyable collaborations that I have shared with them, and for all their efforts and aid. Without them, this work would not have been possible.

I am deeply grateful to all the friends I have made at Caltech and thank them for making my time there enjoyable. In particular, two of them deserve special mention: Auna Moser for capering and learning to appreciate/endure my shenanigans, and Megan Eckart for being my most cherished and dependable friend throughout our entire duration at Caltech. Finally, no panegyric could possibly capture the full extent of my appreciation for all of my family and friends, and the love and support they have always given me. Their impact on and significance in my life is immeasurable.

My graduate research has been supported in part by an NDSEG Fellowship, the NSF under Grants No. EIA-0086038, PHY-0456720, and PHY-99-07949, the NSA under ARO Grant No. W911NF-05-1-0294, the IQI at Caltech, the KITP at UCSB, and Microsoft Station Q.

Abstract

This thesis is primarily a study of the measurement theory of non-Abelian anyons through interference experiments. We give an introduction to the theory of anyon models, providing all the formalism necessary to apply standard quantum measurement theory to such systems. This formalism is then applied to give a detailed analysis of a Mach-Zehnder interferometer for arbitrary anyon models. In this treatment, we find that the collapse behavior exhibited by a target anyon in a superposition of states is determined by the monodromy of the probe anyons with the target. Such measurements may also be used to gain knowledge that would help to properly identify the anyon model describing an unknown system. The techniques used and results obtained from this model interferometer have general applicability, and we use them to also describe the interferometry measurements in a two point-contact interferometer proposed for non-Abelian fractional quantum Hall states. Additionally, we give the complete description of a number of important examples of anyon models, as well as their corresponding quantities that are relevant for interferometry. Finally, we give a partial classification of anyon models with small numbers of particle types.

Contents

Acknowledgments	iv
Abstract	v
1 Introduction	1
1.1 Exchange Statistics and Anyons	2
1.2 The Fractional Quantum Hall Effect	6
1.3 Overview	10
2 Anyon Models	13
2.1 Fusion	13
2.2 Bending and Tracing	20
2.3 Braiding	25
2.4 Physical States	29
2.5 Solving the Pentagon and Hexagon Equations	31
3 Mach-Zehnder Interferometer	40
3.1 One Probe	45
3.2 N Probes	49
3.3 Distinguishability	62
3.4 Probe Generalizations	63
4 Fractional Quantum Hall Two Point-Contact Interferometer	67
5 Examples	77
5.1 \mathbb{Z}_N	77
5.2 $D(\mathbb{Z}_N)$	79
5.3 $D'(\mathbb{Z}_2)$	80

5.4	$SU(2)_k$	81
5.5	Fib	82
5.6	Ising	83
5.7	Constructing New Models from Old	86
5.8	Anyon Models in the Physical World	89
A	Tabulating Anyon Models	94
A.1	Key to the Tables	94
	Bibliography	117

Chapter 1 Introduction

“A mathematician may say anything he pleases, but a physicist must be at least partially sane.” -Josiah Willard Gibbs (1839-1903).

In many ways, we are fortunate to be living in a universe with exactly three spatial dimensions. It keeps us from falling apart, allows us, if we are willing, to see things as they really are, makes it possible, perhaps with some practice, to communicate in a clear and coherent manner, and it provides some of the more advanced members of civilization with the ability to tie their shoes [1, 2].

Perhaps these frivolous statements deserve some explanation, or at least a translation from their seemingly nonsensical form into something physically meaningful. We begin by pointing out that Newton’s $1/r^2$ force-law [3], which arises for Gaussian central potentials associated with gravitational and electric point charges, is particular to three spatial dimensions. As shown in [4, 5], a Gaussian central potential in D dimensional space generates a $1/r^{D-1}$ force law, and this only permits stable orbits when $D = 3$. Indeed, this implies that without exactly three spatial dimensions, we would lose the stable orbits that keep our structure intact from astrophysical scales down to atomic scales. (Similar results arise from such considerations in the framework of general relativity [6].) Another point of clarification is that transmission of information signals via light or sound waves is only reverberation-free and distortionless for radiation in $D = 1, 3$ spatial dimensions [7]. Finally, another seemingly innocuous, but rather important, fact is that three is the exact number of dimensions that permits nontrivial knots to exist. Any fewer dimensions, and it is impossible to form a knot in a strand, since there is no “under” or “over,” just “next to.” Any more dimensions and there is too much spatial freedom, which will make knots unravel, since one can always move one strand past another by pushing it into one of the extra dimensions, where it may pass unhindered.

Knowing that three is an interesting dimensionality for space that grants some

rather nice properties, one might be inclined to ask whether three might also be an interesting dimensionality for *spacetime*. Indeed, this turns out to be the case, primarily because of the property regarding whether nontrivial knots are allowed to exist and the effect this has on particle statistics. In fact, it is exactly this property that requires particles in three (or more) spatial dimensions to exhibit only the well-known bosonic [8, 9] and fermionic [10, 11] statistics that play such a crucial role in the structure and interaction of matter in the universe. We will describe this in more detail in the next section, and then devote the rest of this thesis to systems with two spatial dimensions.

1.1 Exchange Statistics and Anyons

In quantum mechanics, the state of a system of N particles is given by a wavefunction $\Psi(x_1, \dots, x_N)$ for particle coordinates x_j (all internal quantum numbers labeling the state, such as spin, will be left implicit). In mathematical parlance, the wavefunction is a section of a vector bundle with fibre \mathbb{C}^k over the configuration space of the N particles. The modulus square of a wavefunction $|\Psi(x_1, \dots, x_N)|^2$ has the interpretation of probability density [12], so wavefunctions must be normalized (i.e. $\int |\Psi(x_1, \dots, x_N)|^2 dx_1 \dots dx_N = 1$). In order to preserve total probability, quantum evolutions must be represented by unitary transformations on the state space. The configuration space \mathcal{C}_N of N particles living in the spatial manifold M is given by

$$\mathcal{C}_N = \frac{M^N - \Delta_N}{G} \quad (1.1)$$

where $\Delta_N = \{(x_1, \dots, x_N) \in M^N : x_i = x_j \text{ for some } i, j\}$ is subtracted from M^N as a “hard-core” condition that prevents two or more particles from occupying the same point in space¹. To account for indistinguishability of identical particles (a characteristic property of quantum physics), one takes the quotient of $M^N - \Delta_N$ by the

¹This condition is dropped for bosons, which are allowed to occupy the same point in space and have trivial exchange statistics. Without this “hard-core” condition, the configuration space would always be simply-connected, and hence only permit trivial exchange statistics, as we will see.

action of the group G of permutations among identical particles. If all N particles are identical to each other (which we will take to be the case for now), then $G = S_N$ is the permutation group of N objects.

The N strand braid group on M is defined as $B_N(M) = \pi_1(\mathcal{C}_N)$, the fundamental group of configuration space [13] (though perhaps it should be called the “ N particle exchange group on M ,” when $\dim(M) \geq 3$). To understand this terminology, we note that $[\alpha] \in \pi_1(\mathcal{C}_N)$ are (homotopy equivalence classes of) loops in configuration space, specifying processes that begin and end in the same configuration of particles, up to interchanges of indistinguishable particles. Projecting the particles’ coordinates² for a representative path $\alpha(t)$ in \mathcal{C}_N , where $t \in [0, 1]$ may be thought of as time, into the spacetime $M \times [0, 1]$ gives the particles’ worldline trajectories for the exchange process $\alpha(t)$. These worldlines look like “braided” strands running from the $t = 0$ timeslice to the $t = 1$ timeslice (though for $\dim(M) \geq 3$, spacetime has enough dimensions to always permit the worldlines to be smoothly unbraided without intersecting them). Physical systems may be assumed to have configuration spaces that are path connected and locally simply connected.

Quantizing the system, we find that evolution operators are characterized by unitary representations of the fundamental group of configuration space $\pi_1(\mathcal{C}_N)$. This fact is laid bare in the path integral formalism [14] of quantum mechanics, where the physical interpretation as a “sum over paths” makes it clear that the propagator (evolution kernel) splits into contributions from homotopically inequivalent path sectors labeled by elements of $\pi_1(\mathcal{C}_N)$. Specifically, the propagator between the points $X_a, X_b \in \mathcal{C}_N$ at times t_a, t_b takes the form [15]:

$$K(X_b, t_b; X_a, t_a) = \sum_{[\alpha] \in \pi_1(\mathcal{C}_N)} U([\alpha]) K^{[\alpha\gamma]}(X_b, t_b; X_a, t_a) \quad (1.2)$$

where one must specify some arbitrary path γ in \mathcal{C}_N from $\gamma(t_a) = X_a$ to $\gamma(t_b) = X_b$ to define $K^{[\alpha\gamma]}$. The “weight factors” $U([\alpha])$ must, in general, comprise a unitary

²Actually, one must first lift $\alpha(t)$ from $\mathcal{C}_N \times [0, 1]$ to a representative in $M^N \times [0, 1]$ and then project the spatial coordinate of each particle.

representation of $\pi_1(\mathcal{C}_N)$ acting on the state space. From the perspective that $[\alpha] \in \pi_1(\mathcal{C}_N)$ parameterizes a particle exchange process, $U([\alpha])$ is the operator representing the “statistics” transformation of states due to the exchange specified by $[\alpha]$. It is often assumed that exchange statistics for physical systems correspond to direct sums of one-dimensional irreducible representations of $\pi_1(\mathcal{C}_N)$, but there is no reason *a priori* to make such a restriction. We will see that interesting, though so far empirically unsubstantiated, physical possibilities may occur with higher dimensional representations.

Since our universe appears very convincingly (to most people) to have three spatial dimensions, one usually considers $\dim M = 3$, and for most intents and purposes $M = \mathbb{R}^3$ is an accurate description. In this case, $\pi_1(\mathcal{C}_N) = S_N$, since all configurations of worldlines producing the same permutation of particle positions are homotopically equivalent. In fact, if M is any simply connected manifold with $\dim M \geq 3$, then $\pi_1(\mathcal{C}_N) = S_N$ [13]. The one-dimensional representations of S_N are simply the trivial (exchange has no effect) and alternating (exchange of a pair gives an overall sign change) representations, which, respectively correspond to the archetypal bosonic and fermionic exchange statistics. Multi-dimensional representations of S_N give rise to what is known as “parastatistics” [16], however, it has been shown that parastatistics can be replaced by bosonic and fermionic statistics, if a hidden degree of freedom (a non-Abelian isospin group) is introduced [17].

If the space manifold has $\dim M = 2$, then particles’ worldlines would exist in a $(2 + 1)$ -dimensional spacetime, where they cannot be continuously unbraided without intersecting them. Consequently, exchange statistics in two spatial dimensions, which were first considered in [18], are referred to as “braiding statistics.” When $M = \mathbb{R}^2$, we get $\pi_1(\mathcal{C}_N) = B_N$, Artin’s N strand braid group [19], which is the infinite order group generated by the counterclockwise half twists (and their clockwise half twist inverses)

$$R_i = \begin{array}{c} \diagup \quad \diagdown \\ i \quad i+1 \end{array}, \quad R_i^{-1} = \begin{array}{c} \diagdown \quad \diagup \\ i \quad i+1 \end{array} \quad (1.3)$$

exchanging strands i and $i + 1$, for $i = 1, \dots, N - 1$, subject to the relations

$$R_i R_j = R_j R_i \quad \text{for } |i - j| \geq 2 \quad (1.4)$$

$$R_i R_{i+1} R_i = R_{i+1} R_i R_{i+1}. \quad (1.5)$$

Diagrammatically, group multiplication is just stacking braids on top of each other, and the generator relations can be seen to simply require that the group elements behave as braids do, i.e. (for $|i - j| \geq 2$)

$$\begin{array}{c} \begin{array}{c} \text{---} \\ \diagdown \quad \diagup \\ \text{---} \end{array} \dots \begin{array}{c} \text{---} \\ \diagup \quad \diagdown \\ \text{---} \end{array} = \begin{array}{c} \text{---} \\ \diagup \quad \diagdown \\ \text{---} \end{array} \dots \begin{array}{c} \text{---} \\ \diagdown \quad \diagup \\ \text{---} \end{array} \\ R_i R_j \qquad R_j R_i \end{array} \quad (1.6)$$

$$\begin{array}{c} \begin{array}{c} \text{---} \\ \diagdown \quad \diagup \\ \text{---} \\ \diagdown \quad \diagup \\ \text{---} \end{array} = \begin{array}{c} \text{---} \\ \diagup \quad \diagdown \\ \text{---} \\ \diagdown \quad \diagup \\ \text{---} \end{array} . \\ R_i R_{i+1} R_i \qquad R_{i+1} R_i R_{i+1} \end{array} \quad (1.7)$$

The one-dimensional unitary representations of B_N are simply given by $D[R_j] = e^{i\theta}$ for all j , where the phase can take any value, $\theta \in [0, 2\pi)$. Because of this, particles with exchange statistics governed by the braid group have been dubbed “anyons” [20, 21]. Exchange statistics described by multi-dimensional irreducible representations of the braid group [22] give rise to what are referred to as non-Abelian anyons³ and non-Abelian (braiding) statistics.

In general, using arbitrary space manifolds M may introduce additional group generators and constraints to $\pi_1(\mathcal{C}_N)$, arising from the topological structure (such as non-trivial cycles) of M , see e.g. [23]. Additionally, one may also allow for different particle types by using $G = S_{N_1} \times \dots \times S_{N_m}$ (a subgroup of S_N), where the particles

³In this thesis, the term “anyon” will be used in reference to both the Abelian and non-Abelian varieties.

fall into m subsets of N_j identical particles that are distinguishable from those of the other subsets, giving rise to the “colored” braid group on M . Such generalizations for braiding statistics quickly become cumbersome using group representation theory, especially for multi-dimensional representations. Furthermore, one would typically like to consider systems in which there are processes that do not conserve particle number, a notion unsupported by the group theoretic language. To circumvent these shortcomings for systems with two spatial dimensions, one may switch over to the quantum field theoretic-type formalism of anyon models, in which the topological and algebraic properties of the anyonic system are described by category theory, rather than group theory. The structures of anyon models originated from conformal field theory (CFT) [24, 25] and Chern-Simons theory [26]. They were further developed in terms of algebraic quantum field theory [27, 28], and made mathematically rigorous in the language of braided tensor categories [29, 30, 31].

Of course, one might wonder whether any of this exotic braiding statistics is at all relevant to us, since we live in a universe with three spatial dimensions. Amazingly, it turns out that, even in our three-dimensional universe, we are capable of crafting physical systems that are *effectively* two dimensional and have “quasiparticles,” point-like localized coherent state excitations that behave like particles, that appear to possess braiding statistics. In fact, some of these are even strongly believed (though, thus far, experimentally unconfirmed) to be non-Abelian anyons! Physically, anyon models describe the topological behavior of quasiparticle excitations in two-dimensional, many-body systems with an energy gap that suppresses (non-topological) long-range interactions, and hence an anyon model is said to characterize a system’s “topological order.”

1.2 The Fractional Quantum Hall Effect

The fractional quantum Hall effect is the most prominent example of anyonic systems, so we will briefly review some relevant facts on the subject. (For a general introduction into the quantum Hall effect, see e.g. [32, 33, 34, 35].)

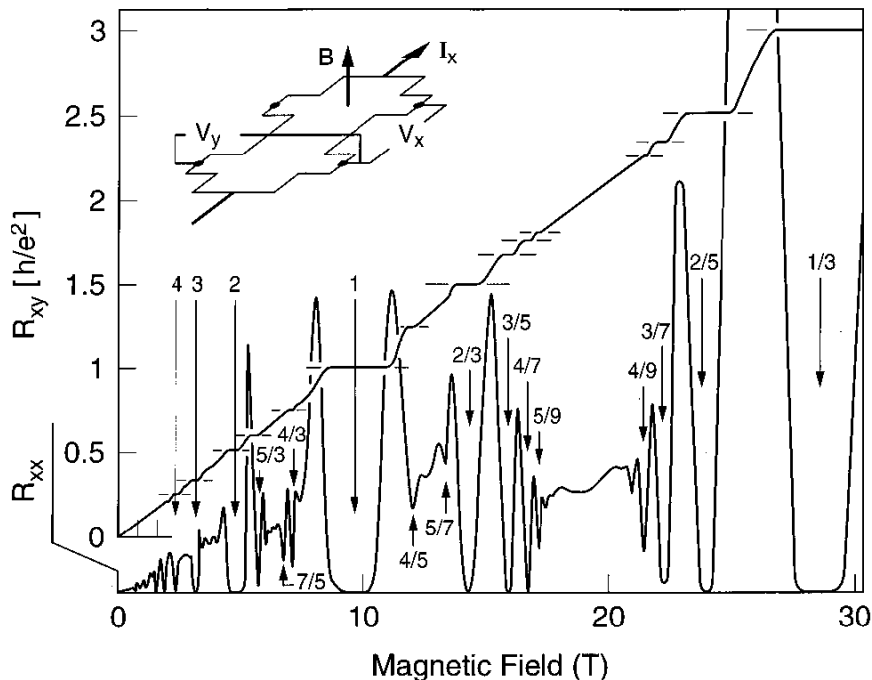


Figure 1.1: Composite view showing the Hall resistance $R_{xy} = V_y/I_x$ and the magnetoresistance $R_{xx} = V_x/I_x$ of a two-dimensional electron gas as a function of magnetic field ($n = 52.333 \times 10^{11} \text{ cm}^{-2}$, $T = 85 \text{ mK}$). The filling factor ν is indicated for the most prominent quantum Hall states (deep minima in R_{xx}). (From Refs. [36, 37].)

The quantum Hall effect (QHE) is an anomalous Hall effect that occurs in two dimensional electron gases (2DEGs) formed at the interface of a semiconductor and an insulator (such as in GaAs/AlGaAs heterostructures) when they are subjected to strong magnetic fields ($\sim 10 \text{ T}$) at very low temperatures ($\sim 10 \text{ mK}$). Under these conditions, the Hall resistance R_{xy} develops plateaus as a function of the applied magnetic field, instead of varying linearly, as semiclassical theory would predict.

These plateaus occur at values which are quantized to extreme precision in integer [38] or fractional [39] multiples of the fundamental conductance quantum $\frac{e^2}{h}$. These multiples are the filling fractions, usually denoted $\nu \equiv N_e/N_\phi$ where N_e is the number of electrons and N_ϕ is the number of fundamental flux quanta through the area occupied by the 2DEG at magnetic field corresponding to the center of a plateau. At the plateaus, the conductance tensor is off-diagonal, meaning a dissipationless transverse current flows in response to an applied electric field. In particular,

the electric field generated by threading an additional localized flux quantum through the system expels a net charge of νe , thus creating a quasihole. Consequently, charge and flux are intimately coupled together in the quantum Hall effect.

In the fractional quantum Hall (FQH) regime, electrons form an incompressible fluid state that supports localized excitations (quasiholes and quasiparticles) which, for the simplest cases, carry one magnetic flux quantum and, hence, fractional charge νe . This combination of fractional charge and unit flux implies that they are anyons, due to their mutual Aharonov–Bohm effect. The fractional charge of quasiparticles in the $\nu = \frac{1}{3}$ Laughlin state was first measured in 1995 [40]. Recently, a series of experiments purported to verify the fractional braiding statistics has been reported [41, 42, 43, 44, 45, 46]. The long-distance interactions between quasiholes in the bulk of the sample are purely topological and may be described by an anyon model.

Boundary excitations and currents of the Hall liquid are described by a $1 + 1$ dimensional conformal field theory whose topological order is the same as that of the bulk, when there is no edge reconstruction. These boundary excitations provide one way of coupling measurement devices to the 2DEG. A further connection between the physics of the bulk and CFT can be established following the observation in [47] that the microscopic trial wavefunction describing the ground state of the incompressible FQH liquid can be constructed from conformal blocks (CFT correlators). In particular, the renowned Laughlin wavefunction for the $\nu = 1/3$ state [48] given by

$$\Psi_{\text{GS}} = \prod_{j < k} (z_j - z_k)^3 \prod_j e^{-|z_j|^2/4} \quad (1.8)$$

where $z = (x + iy)/l$ with the magnetic length $l = \sqrt{\hbar/eB}$, can be interpreted as a conformal block of a free massless bosonic field. Without going into details, we mention that the quasihole wavefunctions (written in terms of electron coordinates) also have a similar CFT interpretation.

We are particularly interested in non-Abelian statistics, so we bring special attention to several observed plateaus in the second Landau level ($2 \leq \nu \leq 4$) that are expected to possess non-Abelian anyons, in particular $\nu = \frac{5}{2}$, $\frac{7}{2}$, and $\frac{12}{5}$ (also, possibly

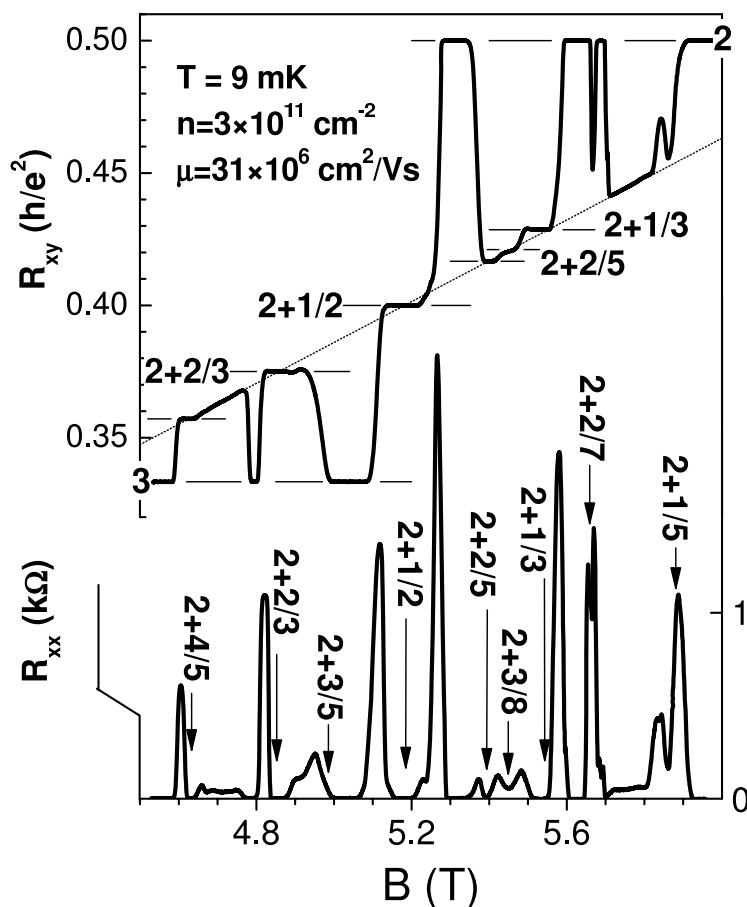


Figure 1.2: R_{xx} and R_{xy} between $\nu = 2$ and $\nu = 3$ at 9mK. Major FQHE states are marked by arrows. The horizontal lines show the expected Hall value of each FQHE state. The dotted line is the calculated classical Hall resistance.(From Ref. [52].)

$\nu = \frac{19}{8}$) [49, 50, 51, 52]. See Fig. 1.2.

Predictions of non-Abelian statistics in these states originated with the paper of Moore and Read [47], which employed a CFT construction to obtain the following trial wave function for the electronic ground state of $\nu = \frac{5}{2}$ Hall plateau:

$$\Psi_{\text{GS}} = \mathcal{A} \left(\frac{1}{z_1 - z_2} \frac{1}{z_3 - z_4} \dots \right) \prod_{j < k} (z_j - z_k)^2 \prod_j e^{-|z_j|^2/4} \quad (1.9)$$

with $\mathcal{A}(\dots)$ denoting the antisymmetrized sum over all possible pairings of electron coordinates. Later, this construction was generalized by Read and Rezayi to a series of

non-Abelian states, which include one at $\nu = \frac{12}{5}$ [53]. At least for $\nu = \frac{5}{2}$ (the Moore–Read state) and $\nu = \frac{12}{5}$ (the $k = 3, M = 1$ Read–Rezayi state), these wavefunctions were found to have very good overlap with the exact ground states obtained by numerical diagonalization of small systems [54, 55].

Detailed investigations of the braiding behavior of quasiholes of the Moore–Read state were carried out in Ref. [56], and of the $\nu = \frac{12}{5}$ state, as well as the other states in the Read–Rezayi series in Ref. [57]. Owing to the special feature of the Moore–Read state as a weakly-paired state of a $p_x + ip_y$ superconductor of composite fermions [58], alternative explicit calculations of the non-Abelian exchange statistics of quasiparticles were carried out in the language of unpaired, zero-energy Majorana modes associated with the vortex cores [59, 60]. (Unfortunately, this language does not readily adapt to give a similar interpretation for the other states in the Read–Rezayi series.)

1.3 Overview

In addition to the proposed fractional quantum Hall states that could host non-Abelian anyons [47, 53, 61], there are a number of other more speculative proposals of systems that may be able to exhibit non-Abelian braiding statistics. These include lattice models [62, 63], quantum loop gases [64, 65, 66, 67], string-net gases [68, 69, 70, 71], Josephson junction arrays [72], $p_x + ip_y$ superconductors [73, 74, 75], and rapidly rotating bose condensates [76, 77, 78]. Since non-Abelian anyons are representative of an entirely new and exotic phase of matter, their discovery would be of great importance, in and of itself. However, as additional motivation, non-Abelian anyons could also turn out to be an invaluable resource for quantum computing.

The idea to use the non-local, multi-dimensional state space shared by non-Abelian anyons as a place to encode qubits was put forth by Kitaev [62], and further developed in Refs. [79, 80, 81, 82, 83, 84, 85]. The advantage of this scheme, known as “topological quantum computing,” is that the non-local state space is impervious to local perturbations, so the qubit encoded there is “topologically” protected from errors. A

model for topological qubits in the Moore–Read state was proposed in Ref. [86], however braiding operations alone in this state are not computationally universal, severely limiting its usefulness in this regard. Nevertheless, one may still hope to salvage the situation by supplementing braiding in the Moore–Read state with topology changing operations [87, 88] or non-topologically protected operations [89] to produce universality. The greater hope, however, lies in the $k = 3$ Read–Rezayi state, for which the non-Abelian braiding statistics are essentially described by the computationally universal “Fibonacci” anyon model (see Chapter 5.5). Consequently, the efforts in “topological quantum compiling” (i.e. designing anyon braids that produce desired computational gates) for this anyon model [90, 91, 92] may be applied directly.

The primary focus of this thesis is to address the measurement theory of anyonic states. This provides a key element in detecting non-Abelian statistics and correctly identifying the topological order of a system. Furthermore, the ability to perform measurements of anyonic states is a crucial component of topological quantum computing, in particular for the purposes of qubit initialization and readout. Clearly, the most direct way of probing braiding statistics is through experiments that establish interference between different braiding operations. In this vein, we will consider interferometry experiments which probe braiding statistics via Aharonov–Bohm type interactions [93], where probe anyons exhibit quantum interference between homotopically distinct paths traveled around a target, producing distinguishable measurement distributions. This sort of experiment provides a quantum non-demolitional measurement [94] of the anyonic state of the target, and is ideally suited for the qubit readout procedure in topological quantum computing.

In Chapter 2, we provide an introduction to the theory of anyon models, giving all the essential background needed to understand the rest of the thesis, and establishing the connection with standard concepts of quantum information theory. Additionally, we describe methods and a program used to solve the Pentagon and Hexagon equations, the consistency equations that, in principle, determine all anyon models.

In Chapter 3, we analyze a Mach-Zehnder type interferometer for an arbitrary anyon model. We consider a target anyon allowed to be in a superposition of anyonic

states, and describe its collapse behavior resulting from interferometry measurements by probe anyons. We find that probe anyons will collapse any superpositions between states they can distinguish by monodromy, as well as remove any entanglement that they can detect between the target and outside anyons. We show how these measurements may be used to determine the target's anyonic charge and/or help identify the topological order of a system.

In Chapter 4, we consider a two point-contact interferometer designed for fractional quantum Hall systems. We give the evolution operator to all orders in tunneling, and apply the methods and results of Chapter 3 to describe how superpositions in the target anyon state collapse as a result of interferometry measurements, and how to determine the anyonic charge of the target. We give detailed predictions for the Moore–Read state and all the Read–Rezayi states, particularly the $k = 3$ state.

In Chapter 5, we give the complete description of a number of important examples of anyon models. For each of these, we also compute details related to the results of the interferometry experiments as analyzed in Chapter 3. These examples are also used to construct the anyon models describing the fractional quantum Hall states of interest.

In Appendix A, we tabulate the results of the program described in Chapter 2 that finds solutions to the Pentagon and Hexagon equations. This provides a partial classification of anyon models with small numbers of particle types, and may be helpful for the purposes of identification of topological phases.

Chapter 2 Anyon Models

In this chapter, we introduce the theory of anyon models, presenting all the relevant details that will be employed throughout this thesis. In mathematical terminology, anyon models are known as unitary braided tensor categories, but we will avoid descending too far into the abstract depths of category theory, and instead follow the relatively concrete approach found in Refs. [63, 95]. We hope to bring the language of anyon models into closer contact with the more traditional language of quantum information and measurement theory, and to fill in the missing concepts necessary for this connection.

2.1 Fusion

An anyon model has a finite set \mathcal{C} of superselection sector labels called topological or anyonic charges. These conserved charges obey a commutative, associative fusion algebra

$$a \times b = \sum_{c \in \mathcal{C}} N_{ab}^c c \quad (2.1)$$

where the fusion multiplicities N_{ab}^c are non-negative integers which indicate the number of different ways the charges a and b can be combined to produce the charge c . There is a unique trivial “vacuum” charge $1 \in \mathcal{C}$ for which $N_{a1}^c = \delta_{ac}$, and each charge a has a unique conjugate charge, or “antiparticle,” $\bar{a} \in \mathcal{C}$ such that $N_{a\bar{a}}^1 = \delta_{a\bar{a}}$. ($1 = \bar{1}$ and $\bar{\bar{a}} = a$.) The fusion multiplicities obey the relations

$$N_{ab}^c = N_{ba}^c = N_{b\bar{c}}^{\bar{a}} = N_{\bar{a}\bar{b}}^{\bar{c}} \quad (2.2)$$

$$\sum_e N_{ab}^e N_{ec}^d = \sum_f N_{af}^d N_{bc}^f \quad (2.3)$$

and a theory is non-Abelian if there is some a and b such that

$$\sum_c N_{ab}^c > 1. \quad (2.4)$$

The domain of a sum will henceforth be left implicit when it runs over all possible labels. If $\sum_c N_{ab}^c = 1$ for every b , then the charge a is Abelian. To each fusion product, there is assigned a fusion vector space V_{ab}^c with $\dim V_{ab}^c = N_{ab}^c$, and a corresponding splitting space V_c^{ab} , which is the dual space. We pick some orthonormal set of basis vectors $|a, b; c, \mu\rangle \in V_c^{ab}$ ($\langle a, b; c, \mu| \in V_{ab}^c$) for these spaces, where $\mu = 1, \dots, N_{ab}^c$. If $N_{ab}^c = 0$, then $V_c^{ab} = \emptyset$ and it clearly has no basis elements. We will sometimes use the notation $c \in \{a \times b\}$ to mean c such that $N_{ab}^c \neq 0$. Splitting and fusion spaces involving the vacuum charge have dimension one, and so we will leave their basis vector labels $\mu = 1$ implicit. The splitting of three anyons with charge a, b, c from the charge d corresponds to a space V_d^{abc} which can be decomposed into tensor products of two anyon splitting spaces by matching the intermediate charge. This can be done in two isomorphic ways

$$V_d^{abc} \cong \bigoplus_e V_e^{ab} \otimes V_d^{ec} \cong \bigoplus_f V_d^{af} \otimes V_f^{bc}. \quad (2.5)$$

To incorporate the notion of associativity at the level of splitting spaces, we need associativity constraints that essentially specify a set of isomorphisms between different decompositions that are to be considered simply a change of basis. These isomorphisms (called F -moves) are written as

$$|a, b; e, \alpha\rangle |e, c; d, \beta\rangle = \sum_{f, \mu, \nu} [F_d^{abc}]_{(e, \alpha, \beta)(f, \mu, \nu)} |b, c; f, \mu\rangle |a, f; d, \nu\rangle \quad (2.6)$$

and are unitary for anyon models ¹. F -symbols that includes vertices that are not permitted by fusion do not actually occur, since the corresponding splitting space has

¹One may think of fusion of anyonic charges as a generalization of tensor products of representations of groups. (The round brackets are used to group together indices into the multi-indices labeling each side of the transformation.) From this perspective, the F -symbols are the analog of $6j$ -symbols.

no basis elements. The same notion of associativity is, of course, true for fusion of three anyons, which is denoted in the same manner with kets. The associativity for fusion is given by F^\dagger , and together with unitarity, we have

$$\left[(F_d^{abc})^\dagger \right]_{(f,\mu,\nu)(e,\alpha,\beta)} = [F_d^{abc}]_{(e,\alpha,\beta)(f,\mu,\nu)}^* = \left[(F_d^{abc})^{-1} \right]_{(f,\mu,\nu)(e,\alpha,\beta)}. \quad (2.7)$$

For fusion and splitting of more anyons, one does the obvious iteration of such decompositions. Using the decomposition

$$\begin{aligned} V_{a'_1, \dots, a'_n}^{a_1, \dots, a_m} &\cong \bigoplus_{\substack{e_2, \dots, e_{m-1} \\ e'_2, \dots, e'_{n-1} \\ e}} V_{e_2}^{a_1 a_2} \otimes V_{e_3}^{e_2 a_3} \otimes \dots \otimes V_e^{e_{m-1} a_m} \\ &\quad \otimes V_{e'_{n-1} a'_n}^e \otimes \dots \otimes V_{e'_2 a'_3}^{e'_3} \otimes V_{a'_1 a'_2}^{e'_2} \end{aligned} \quad (2.8)$$

will be referred to as “the standard basis” representation. For this to be consistent for arbitrary numbers of anyons, one must obtain the same result when two distinct series of F -moves start and end in the same decompositions. This consistency is achieved by the constraint called the Pentagon equation

$$\begin{aligned} &\sum_{\delta} [F_e^{fcd}]_{(g,\beta,\gamma)(l,\delta,\nu)} [F_e^{abl}]_{(f,\alpha,\delta)(k,\lambda,\mu)} \\ &= \sum_{h,\sigma,\psi,\rho} [F_g^{abc}]_{(f,\alpha,\beta)(h,\sigma,\psi)} [F_e^{ahd}]_{(g,\sigma,\gamma)(k,\lambda,\rho)} [F_k^{bcd}]_{(h,\psi,\rho)(l,\mu,\nu)} \end{aligned} \quad (2.9)$$

One imposes the (physically mandatory) axiom that fusion and splitting with the vacuum charge does not change the state, which is equivalent to the condition that fusion/splitting with the vacuum commutes with the associativity moves. This is represented by the condition that F_d^{abc} is trivial (i.e. equal to 1 if allowed by fusion) when any of a, b, c are equal to 1^2 . We point out, however, that F_d^{abc} need not be trivial when d is the vacuum charge.

²There is a “gauge” choice that one makes in picking the basis states of the fusion/splitting spaces (discussed more in Chapter 2.5). If one chooses not to believe in this as a physical axiom, one may instead recognize that this condition can always be imposed consistently as a “gauge” choice in defining the basis states.

An important quantity known as the quantum dimension d_a of a charge a may be found from the fusion multiplicities by considering the asymptotic scaling of the dimension of the fusion space of n anyons of charge a when n is taken to be large

$$\dim \left(\sum_{c_n} V_{a\dots a}^{c_n} \right) = \sum_{c_2, \dots, c_n} N_{aa}^{c_2} N_{c_2 a}^{c_3} \dots N_{c_{n-1} a}^{c_n} \sim d_a^n. \quad (2.10)$$

Though this gives an intuition for its name, the quantum dimension will, however, be defined by

$$d_a = d_{\bar{a}} = \left| [F_a^{a\bar{a}a}]_{1,1} \right|^{-1}. \quad (2.11)$$

(That Eq. (2.10) follows from this definition may be seen from Eq. (2.36), which, by the Perron-Frobenius theorem, indicates that d_a is the largest eigenvalue of N_{ab}^c when treated as a matrix in the indices b, c .) From unitarity of anyon models, we have $d_a \geq 1$, with equality iff a is Abelian (i.e. fusion with any other charge has exactly one fusion channel). The total quantum dimension is defined as

$$\mathcal{D} = \sqrt{\sum_a d_a^2}. \quad (2.12)$$

It is extremely useful to employ a diagrammatic formalism for anyon models. Each anyonic charge label is associated with an oriented line. It is useful in some contexts to think of these lines as the anyons' worldlines (we will consider time as increasing in the upward direction), however, such an interpretation is not necessary nor even always appropriate. Reversing the orientation of a line is equivalent to conjugating the charge labeling it, i.e.

$$\begin{array}{c} \uparrow \\ a \end{array} = \begin{array}{c} \downarrow \\ \bar{a} \end{array}. \quad (2.13)$$

The fusion and splitting states are assigned to trivalent vertices with the appropriately corresponding fusion/splitting of anyonic charges:

$$(d_c/d_a d_b)^{1/4} \begin{array}{c} c \\ \uparrow \\ \mu \\ \swarrow \quad \searrow \\ a \quad b \end{array} = \langle a, b; c, \mu | \in V_{ab}^c, \quad (2.14)$$

$$(d_c/d_a d_b)^{1/4} \begin{array}{c} a \nearrow \\ \mu \\ c \uparrow \end{array} \begin{array}{c} \searrow b \\ \end{array} = |a, b; c, \mu\rangle \in V_c^{ab}, \quad (2.15)$$

where the normalization factors $(d_c/d_a d_b)^{1/4}$ are included so that diagrams are in the isotopy invariant convention throughout this thesis. Isotopy invariance means that the value of a (labeled) diagram is not changed by continuous deformations, so long as open endpoints are held fixed and lines are not passed through each other or around open endpoints. Open endpoints should be thought of as ending on some boundary (e.g. a timeslice or an edge of the system) through which isotopy is not permitted. Building in isotopy invariance is a bit more complicated than just making this normalization change, but we will come back to these details later in the chapter. These normalization factors leave the F -symbols unchanged in the conversion to diagrams

$$\begin{array}{c} a \nearrow \\ \alpha \\ e \\ \beta \\ d \searrow \end{array} \begin{array}{c} b \nearrow \\ \\ c \nearrow \end{array} = \sum_{f, \mu, \nu} [F_d^{abc}]_{(e, \alpha, \beta)(f, \mu, \nu)} \begin{array}{c} a \nearrow \\ \\ \nu \\ d \searrow \end{array} \begin{array}{c} b \nearrow \\ f^\mu \\ c \nearrow \end{array}. \quad (2.16)$$

Any diagrammatic equation, such as this, is also valid as a local relation within larger, more complicated diagrams. The Pentagon equation (2.9) is expressed diagrammatically in Fig. 2.1.

The property that fusion/splitting with the vacuum is trivial is manifested diagrammatically as the ability to move, add, and delete vacuum lines from diagrams at will. (There is a subtlety in making this compatible with isotopy invariance that we will describe shortly.) Inner products are formed diagrammatically by stacking vertices so the fusing/splitting lines connect

$$\begin{array}{c} c \uparrow \\ \mu \\ a \nearrow \\ \mu' \\ c' \uparrow \end{array} \begin{array}{c} \searrow b \\ \end{array} = \delta_{c, c'} \delta_{\mu, \mu'} \sqrt{\frac{d_a d_b}{d_c}} \begin{array}{c} | \\ c \end{array} \quad (2.17)$$

and this generalizes to more complicated diagrams. An important feature of this relation is that it diagrammatically encodes charge conservation, and, in particular,

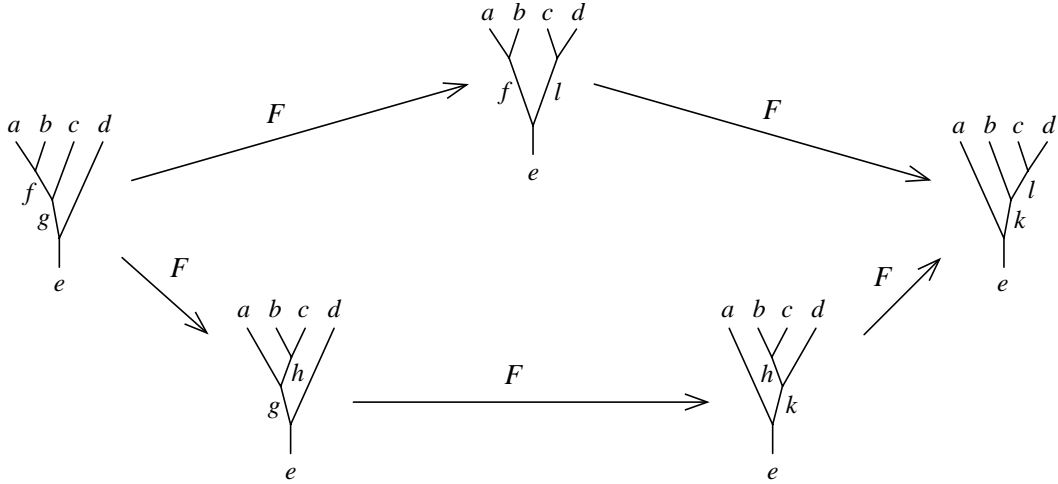
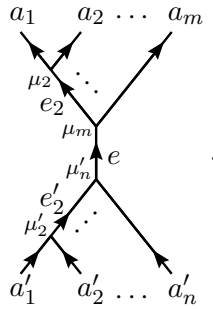


Figure 2.1: The Pentagon equation enforces the condition that different sequences of F -moves from the same starting fusion basis decomposition to the same ending decomposition gives the same result. Eq. (2.9) is obtained by imposing the condition that the above diagram commutes.

forbids tadpole diagrams.

In general, operators may be formed by taking linear combinations of fusion/splitting diagrams that conserve charge, which can be specified in terms of the standard basis elements of the fusion/splitting spaces $V_{a'_1, \dots, a'_n}^{a_1, \dots, a_m}$:



The identity operator on a pair of anyons with charges a and b respectively is

$$\mathbb{I}_{ab} = \sum_{c, \mu} |a, b; c, \mu\rangle \langle a, b; c, \mu| \tag{2.18}$$

or, written diagrammatically

$$\begin{array}{c} a \\ \uparrow \\ \uparrow \\ \uparrow \\ b \end{array} = \sum_{c,\mu} \sqrt{\frac{d_c}{d_a d_b}} \begin{array}{c} a \quad b \\ \swarrow \quad \searrow \\ c^\mu \\ \swarrow \quad \searrow \\ a \quad b \end{array}, \quad (2.19)$$

We introduce the notation

$$\begin{array}{c} A_1 \quad A_m \\ \uparrow \quad \dots \quad \uparrow \\ \boxed{X} \\ \uparrow \quad \dots \quad \uparrow \\ A'_1 \quad A'_n \end{array} = X \in V_{A'_1, \dots, A'_n}^{A_1, \dots, A_m} = \sum_{\substack{a_1, \dots, a_m \\ a'_1, \dots, a'_n}} V_{a'_1, \dots, a'_n}^{a_1, \dots, a_m} \quad (2.20)$$

where a capitalized anyonic charge label means a (direct) sum over all possible charges, so that the operator X is defined for acting on any n anyon input and m anyon output. The indices on operators will be left implicit when they are contextually clear (and unnecessary). If one wants to consider operators that do not conserve anyonic charge, this must be done by introducing anyon charge lines that leave the system on which the operator acts, which, in fact, is really just considering a larger combined system in which charge actually is conserved. Conjugation of a diagram is carried out by simultaneously reflecting the diagram across the xy -plane and reversing the orientation of arrows.

Tensoring together two operators (on separate sets of anyons) is simply executed by juxtaposition of their diagrams:

$$\begin{array}{c} \uparrow \dots \uparrow \uparrow \dots \uparrow \\ \boxed{X \otimes Y} \\ \uparrow \dots \uparrow \uparrow \dots \uparrow \end{array} = \begin{array}{c} \uparrow \dots \uparrow \\ \boxed{X} \\ \uparrow \dots \uparrow \end{array} \begin{array}{c} \uparrow \dots \uparrow \\ \boxed{Y} \\ \uparrow \dots \uparrow \end{array} \quad (2.21)$$

The associativity relations may then be used to re-write the resulting tensor product in the standard basis, however, it is often more convenient not to re-write it as such.

2.2 Bending and Tracing

The first requirement for isotopy invariance is the ability to introduce and remove bends in a line. Bending a line horizontally (so that the line always flows upward) is trivial, but a complication arises when a line is bent vertically. The F -move associated with this type of bending is

$$\begin{array}{c} \uparrow \\ \cdot 1 \\ \swarrow \quad \searrow \\ a \quad \bar{a} \\ \nwarrow \quad \nearrow \\ \cdot 1 \\ \uparrow \end{array} a = [F_a^{a\bar{a}a}]_{1,1} \begin{array}{c} \uparrow \\ \cdot 1 \\ \swarrow \quad \searrow \\ a \quad \bar{a} \\ \nwarrow \quad \nearrow \\ \cdot 1 \\ \uparrow \end{array} a = d_a [F_a^{a\bar{a}a}]_{1,1} \begin{array}{c} \uparrow \\ a \end{array} \quad (2.22)$$

(using Eq. (2.17) twice in the last step). In general, the quantity

$$[F_a^{a\bar{a}a}]_{1,1} = \frac{\varkappa_a}{d_a} \quad (2.23)$$

has a non-trivial phase $\varkappa_a = \varkappa_a^*$, which is why one needs more than just vertex normalization to generate isotopy invariance for this kind of bending. Though one may always make a consistent gauge choice such that $\varkappa_a = 1$ for all a that are not self-dual, for the charges a that are self-dual ($a = \bar{a}$), $\varkappa_a = \pm 1$ is a gauge invariant quantity, known as the Frobenius-Schur indicator. For isotopy invariance, one follows the prescription that when a vacuum line is removed from the bottom of a splitting vertex or from the top of a fusion vertex, it is replaced with a right-directed flag

$$\begin{array}{c} 1 \\ \vdots \\ \swarrow \quad \searrow \\ a \quad \bar{a} \end{array} = \begin{array}{c} \curvearrowright \\ a \quad \bar{a} \end{array} = \varkappa_a \begin{array}{c} \curvearrowleft \\ a \quad \bar{a} \end{array} \quad (2.24)$$

$$\begin{array}{c} \swarrow \quad \searrow \\ a \quad \bar{a} \\ \vdots \\ 1 \end{array} = \begin{array}{c} \curvearrowright \\ a \quad \bar{a} \end{array} = \varkappa_a^* \begin{array}{c} \curvearrowleft \\ a \quad \bar{a} \end{array} . \quad (2.25)$$

where “cups” and “caps” with left-directed flags are defined in terms of those with right-directed flags by multiplication with the \varkappa_a . From this, isotopy involving vertical bending is defined as introducing or removing alternating cap-cup pairs with opposing

flags:

$$\begin{array}{c} a \quad \bar{a} \quad a \\ \curvearrowright \quad \curvearrowleft \quad \curvearrowright \\ \hline a \\ \hline \end{array} = \begin{array}{c} \curvearrowleft \quad \curvearrowright \\ \hline a \\ \hline \end{array} = \begin{array}{c} \curvearrowleft \quad \curvearrowright \\ \hline a \\ \hline \end{array}. \quad (2.26)$$

In diagrams when cups and caps are paired up with opposing flags, these flags may be left implicit, and we will do so from now on. (In fact, these important flags are typically paired up properly, so they usually do not show up explicitly.) Combining this with Eq. (2.17) with $c = 1$ we see that an unknotted loop carrying charge a evaluates to its quantum dimension

$$a \circlearrowleft = d_a. \quad (2.27)$$

The effect on a splitting vertex of bending a line down is that it is rotated to become a fusion vertex. More precisely, bending to the left and to the right, respectively, give the maps

$$\begin{array}{c} a \quad b \\ \curvearrowleft \quad \curvearrowright \\ \mu \quad c \\ \hline \bar{a} \end{array} = \sum_{\nu} [A_c^{ab}]_{\mu\nu} \begin{array}{c} b \\ \curvearrowright \\ \nu \\ \hline \bar{a} \quad c \end{array} \quad (2.28)$$

$$\begin{array}{c} a \quad b \\ \curvearrowright \quad \curvearrowleft \\ \mu \quad c \\ \hline \bar{b} \end{array} = \sum_{\nu} [B_c^{ab}]_{\mu\nu} \begin{array}{c} a \\ \curvearrowright \\ \nu \\ \hline c \quad \bar{b} \end{array}, \quad (2.29)$$

where

$$[A_c^{ab}]_{\mu\nu} = \sqrt{\frac{d_a d_b}{d_c}} \mathcal{X}_a^* [F_b^{\bar{a}ab}]_{1,(c,\mu,\nu)}^* \quad (2.30)$$

$$[B_c^{ab}]_{\mu\nu} = \sqrt{\frac{d_a d_b}{d_c}} [F_b^{ab\bar{b}}]_{(c,\mu,\nu),1} \quad (2.31)$$

are unitary in μ, ν (though it may not be obvious from these expressions).

We can now write the F -move with one of its legs bent down

$$\begin{array}{c} a \quad b \\ \uparrow \quad \uparrow \\ \alpha \quad e \quad \beta \\ \downarrow \quad \downarrow \\ c \quad d \end{array} = \sum_{f,\mu,\nu} [F_{cd}^{ab}]_{(e,\alpha,\beta)(f,\mu,\nu)} \begin{array}{c} a \quad b \\ \curvearrowright \quad \curvearrowleft \\ f \quad \mu \\ \nu \\ \hline c \quad d \end{array} \quad (2.32)$$

$$[F_{cd}^{ab}]_{(e,\alpha,\beta)(f,\mu,\nu)} = \sum_{\alpha',\nu'} \left[(A_e^{\bar{c}a})^{-1} \right]_{\alpha\alpha'} [F_d^{\bar{c}ab}]_{(e,\alpha',\beta)(f,\mu,\nu')} [A_d^{\bar{e}f}]_{\nu'\nu}, \quad (2.33)$$

which is also a unitary transformation. Combined with Eq. (2.19), this gives

$$[F_{ab}^{ab}]_{1,(c,\mu,\nu)} = \sqrt{\frac{d_c}{d_a d_b}} \delta_{\mu,\nu}, \quad (2.34)$$

$$[F_{cd}^{ab}]_{(e,\alpha,\beta)(f,\mu,\nu)} = \sqrt{\frac{d_e d_f}{d_a d_d}} [F_f^{ceb}]_{(a,\alpha,\mu)(d,\beta,\nu)}^*. \quad (2.35)$$

Using Eq. (2.19) and isotopy, we get the important relation

$$d_a d_b = a \circlearrowleft b = \sum_{c,\mu} \sqrt{\frac{d_c}{d_a d_b}} a \circlearrowleft_{\mu}^c b = \sum_c N_{ab}^c d_c. \quad (2.36)$$

Inverting F , we find:

$$\left[(F_{ab}^{ab})^{-1} \right]_{(c,\mu,\nu),1} = \sqrt{\frac{d_c}{d_a d_b}} \delta_{\mu,\nu}, \quad (2.37)$$

$$\sum_{c,\mu} [F_{ab}^{ab}]_{(e,\alpha,\beta)(c,\mu,\mu)} \sqrt{d_c} = \sqrt{d_a d_b} \delta_{e,1} \quad (2.38)$$

The trace on operators formed from bras and ket is defined in the usual way; e.g. for a two anyon operator

$$\text{Tr} [|a, b; c, \mu\rangle \langle a', b'; c, \mu'|] = \delta_{a,a'} \delta_{b,b'} \delta_{\mu,\mu'}. \quad (2.39)$$

To translate the trace into the diagrammatic formalism, one defines the *quantum* trace, denoted $\widetilde{\text{Tr}}$, by closing the diagram with loops (with properly paired flags) that match the outgoing lines with the respective incoming lines at the same position

$$\widetilde{\text{Tr}} X = \widetilde{\text{Tr}} \left[\begin{array}{c} \begin{array}{ccc} A_1 & \dots & A_n \\ \uparrow & & \uparrow \\ \boxed{X} \\ \uparrow & & \uparrow \\ A'_1 & \dots & A'_n \end{array} \end{array} \right] = \begin{array}{c} \begin{array}{ccc} A_1 & \dots & A_n \\ \uparrow & & \uparrow \\ \boxed{X} \\ \uparrow & & \uparrow \\ \dots & & \dots \end{array} \end{array}. \quad (2.40)$$

Connecting the endpoints of two lines labeled by different anyonic charges violates charge conservation, so such diagrams evaluate to zero. The operator $X \in V_{A'_1 \dots A'_n}^{A_1 \dots A_n}$ may be written as

$$X = \sum_c X_c, \quad X_c \in V_c^{A_1 \dots A_n} \otimes V_{A'_1 \dots A'_n}^c \quad (2.41)$$

(note that this decomposition is basis independent), which may be used to relate the trace and the quantum trace via

$$\mathrm{Tr} X = \sum_c \frac{1}{d_c} \widetilde{\mathrm{Tr}} X_c, \quad \widetilde{\mathrm{Tr}} X = \sum_c d_c \mathrm{Tr} X_c. \quad (2.42)$$

We also need to define the *partial* traces for anyons. At this point, we only define them with respect to the planar fusion structure, i.e. in terms of the $(1+1)$ -dimensional diagrams, but after we introduce braiding, we will return to address issues that arise from the full $(2+1)$ -dimensional structure. In order to take the partial trace of a single anyon B , the planar structure requires that it must be one of the two outer anyons (i.e. the first or last in the lineup). Physically, this corresponds to the fact that one cannot treat the subsystem excluding B as independent of B if this anyon is still located in the midst of the remaining anyons. The partial quantum trace over B of an operator $X \in V_{A'_1, \dots, A'_n, B'}^{A_1, \dots, A_n, B}$ is defined by looping only the line for anyon B back on itself

$$\widetilde{\mathrm{Tr}}_B X = \begin{array}{c} \begin{array}{c} A_1 \quad \dots \quad A_n \\ \uparrow \quad \dots \quad \uparrow \\ \boxed{X} \\ \uparrow \quad \dots \quad \uparrow \\ A'_1 \quad \dots \quad A'_n \end{array} \quad \begin{array}{c} \curvearrowright \\ B \end{array} \end{array} \quad (2.43)$$

and for $X \in V_{B', A'_1, \dots, A'_n}^{B, A_1, \dots, A_n}$ as

$$\widetilde{\mathrm{Tr}}_B X = \begin{array}{c} \begin{array}{c} A_1 \quad \dots \quad A_n \\ \uparrow \quad \dots \quad \uparrow \\ \boxed{X} \\ \uparrow \quad \dots \quad \uparrow \\ A'_1 \quad \dots \quad A'_n \end{array} \quad \begin{array}{c} \curvearrowleft \\ B \end{array} \end{array}. \quad (2.44)$$

To relate the partial quantum trace to the partial trace, we implement factors for the quantum dimensions of the overall charges of the operator before *and* after the partial trace

$$\mathrm{Tr}_B X = \sum_{c,f} \frac{d_f}{d_c} \left[\widetilde{\mathrm{Tr}}_B X_c \right]_f, \quad \widetilde{\mathrm{Tr}}_B X = \sum_{c,f} \frac{d_c}{d_f} [\mathrm{Tr}_B X_c]_f, \quad (2.45)$$

where

$$\widetilde{\mathrm{Tr}}_B X_c = \sum_f \left[\widetilde{\mathrm{Tr}}_B X_c \right]_f, \quad \left[\widetilde{\mathrm{Tr}}_B X_c \right]_f \in V_f^{A_1, \dots, A_n} \otimes V_{A'_1, \dots, A'_n}^f. \quad (2.46)$$

The partial trace and partial quantum trace over the subsystem of anyons $B = \{B_1, \dots, B_n\}$ that are sequential outer lines (on either, possibly alternating, sides) of an operator is defined by iterating the partial quantum trace on the B anyons

$$\mathrm{Tr}_B = \mathrm{Tr}_{B_1} \dots \mathrm{Tr}_{B_n}, \quad \widetilde{\mathrm{Tr}}_B = \widetilde{\mathrm{Tr}}_{B_1} \dots \widetilde{\mathrm{Tr}}_{B_n} \quad (2.47)$$

Iterating these over all the anyons of a system returns the trace and quantum trace, respectively, as they should.

Using Eq. (2.37) and the fact that tadpole diagrams evaluate to zero, we have

$$\begin{aligned} \widetilde{\mathrm{Tr}}_B \left[\begin{array}{c} a \quad b \\ \diagdown \quad / \\ c \quad \mu \\ / \quad \diagdown \\ a' \quad b' \end{array} \right] &= \begin{array}{c} a \quad b \\ \diagdown \quad / \\ c \quad \mu \\ / \quad \diagdown \\ a' \quad b' \end{array} \text{ with a loop } = \sum_{\epsilon, \alpha, \beta} \left[(F_{a'b'}^{ab})^{-1} \right]_{(c, \mu, \mu')(\epsilon, \alpha, \beta)} \begin{array}{c} a \\ \alpha \\ \leftarrow e \\ \beta \\ \rightarrow \\ a' \end{array} \text{ with a loop } \\ &= \left[(F_{ab}^{ab})^{-1} \right]_{(c, \mu, \mu'), 1} a \uparrow \text{ with a loop } b = \sqrt{\frac{d_b d_c}{d_a}} \delta_{\mu, \mu'} \uparrow a. \quad (2.48) \end{aligned}$$

Applying this to three anyon standard basis vectors gives

$$\begin{aligned} \widetilde{\text{Tr}}_B [|a_1, a_2; f, \mu\rangle |f, b; c, \nu\rangle \langle f', b'; c, \nu'| \langle a'_1, a'_2; f', \mu'|] \\ = \delta_{b,b'} \delta_{f,f'} \delta_{\nu,\nu'} \frac{d_c}{d_f} |a_1, a_2; f, \mu\rangle \langle a'_1, a'_2; f, \mu'| \end{aligned} \quad (2.49)$$

$$\begin{aligned} \text{Tr}_B [|a_1, a_2; f, \mu\rangle |f, b; c, \nu\rangle \langle f', b'; c, \nu'| \langle a'_1, a'_2; f', \mu'|] \\ = \delta_{b,b'} \delta_{f,f'} \delta_{\nu,\nu'} |a_1, a_2; f, \mu\rangle \langle a'_1, a'_2; f, \mu'|, \end{aligned} \quad (2.50)$$

and this similarly generalizes when dealing with more anyons. Since this seems to indicate that the partial trace has the appropriate behavior with respect to bras and kets, one might think that it is the usual notion of partial trace, but things are a bit more subtle than this, since these bras and kets do not have the usual tensor product structure. On the other hand, when considering tensor products of operators, it is the partial quantum trace that behaves in the appropriate manner for a partial traces (i.e. as in the usual basis independent definition of partial trace). Specifically, tracing over the set of anyons B on which the operator Y acts, we have

$$\widetilde{\text{Tr}}_B [X \otimes Y] = X \widetilde{\text{Tr}} Y \quad (2.51)$$

$$\text{Tr}_B [X \otimes Y] = \sum_{a,b,c} N_{ab}^c X_a \text{Tr} Y_b. \quad (2.52)$$

2.3 Braiding

The unitary braiding operations of pairs of anyons, also called R -moves, are written as

$$R_{ab} = \begin{array}{c} \nearrow \quad \nearrow \\ a \quad b \\ \searrow \quad \searrow \end{array}, \quad R_{ab}^\dagger = R_{ab}^{-1} = \begin{array}{c} \nearrow \quad \nearrow \\ b \quad a \\ \searrow \quad \searrow \end{array}, \quad (2.53)$$

which are defined through their application to basis vectors:

$$R_{ab} |a, b; c, \mu\rangle = \sum_{\nu} [R_c^{ab}]_{\mu\nu} |b, a; c, \nu\rangle \quad (2.54)$$

$$\begin{array}{c} \nearrow \quad \nearrow \\ b \quad a \\ \searrow \quad \searrow \\ \uparrow \mu \\ c \end{array} = \sum_{\nu} [R_c^{ab}]_{\mu\nu} \begin{array}{c} \nearrow \quad \nearrow \\ b \quad a \\ \searrow \quad \searrow \\ \uparrow \nu \\ c \end{array} \quad (2.55)$$

and similarly for R^{-1} , which, by unitarity, satisfy $\left[(R_c^{ab})^{-1}\right]_{\mu\nu} = [R_c^{ba}]_{\nu\mu}^*$. The braiding operator may be represented in terms of planar diagrams as

$$R_{ab} = \sum_{c,\mu,\nu} \sqrt{\frac{d_c}{d_a d_b}} [R_c^{ab}]_{\mu\nu} \begin{array}{c} b \swarrow \quad \nearrow a \\ \quad \nu \\ \quad \uparrow \\ \quad \mu \\ \quad \downarrow \\ a \swarrow \quad \nearrow b \end{array} . \quad (2.56)$$

For braiding to be consistent with fusion, it must satisfy the Hexagon equations

$$\begin{aligned} & \sum_{\lambda,\gamma} [R_e^{ca}]_{\alpha\lambda} [F_d^{acb}]_{(e,\lambda,\beta)(g,\mu,\gamma)} [R_g^{cb}]_{\gamma\nu} \\ = & \sum_{f,\sigma,\delta,\psi} [F_d^{cab}]_{(e,\alpha,\beta)(f,\sigma,\delta)} [R_d^{cf}]_{\sigma\psi} [F_d^{abc}]_{(f,\delta,\psi)(g,\mu,\nu)} \end{aligned} \quad (2.57)$$

and

$$\begin{aligned} & \sum_{\lambda,\gamma} [(R_e^{ac})^{-1}]_{\alpha\lambda} [F_d^{acb}]_{(e,\lambda,\beta)(g,\mu,\gamma)} [(R_g^{bc})^{-1}]_{\gamma\nu} \\ = & \sum_{f,\sigma,\delta,\psi} [F_d^{cab}]_{(e,\alpha,\beta)(f,\sigma,\delta)} \left[(R_d^{fc})^{-1} \right]_{\sigma\psi} [F_d^{abc}]_{(f,\delta,\psi)(g,\mu,\nu)} \end{aligned} \quad (2.58)$$

which essentially impose the property that lines may be passed over or under vertices respectively (i.e. braiding commutes with fusion), and implies the usual Yang-Baxter relation for braids. These relations are represented diagrammatically in Fig. 2.2. The F -symbols and R -symbols completely specify an anyon model, and a theorem known as Mac Lane coherence [96] tells us that no further consistency conditions are needed beyond the Pentagon and Hexagon equations.

The fact that braiding with the vacuum is trivial is given by the condition

$$R_a^{a1} = R_b^{1b} = 1 \quad (2.59)$$

which follows from the Hexagon equations combined with the triviality of fusion with

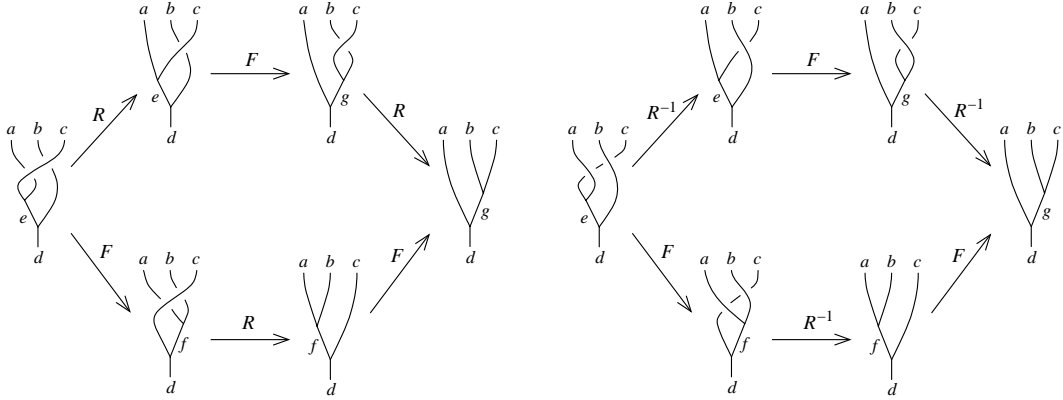


Figure 2.2: The Hexagon equations enforce the condition that braiding is compatible with fusion, in the sense that different sequences of F -moves and R -moves from the same starting configuration to the same ending configuration give the same result. Eqs. (2.57) and (2.58) are obtained by imposing the condition that the above diagram commutes.

vacuum. The braiding matrices satisfy the ribbon property

$$\sum_{\lambda} [R_c^{ab}]_{\mu\lambda} [R_c^{ba}]_{\lambda\nu} = \frac{\theta_c}{\theta_a\theta_b} \delta_{\mu,\nu} \quad (2.60)$$

where θ_a is a root of unity called the topological spin of a , defined by

$$\theta_a = \theta_{\bar{a}} = d_a^{-1} \widetilde{\text{Tr}} R_{aa} = \sum_{c,\mu} \frac{d_c}{d_a} [R_c^{aa}]_{\mu\mu} = \varkappa_a [R_1^{\bar{a}a}]^* = \frac{1}{d_a} \text{Diagram} \quad (2.61)$$

When applicable, this is related to s_a , the (ordinary angular momentum) spin or CFT conformal scaling dimension of a , by

$$\theta_a = e^{i2\pi s_a}. \quad (2.62)$$

The topological S -matrix is defined by

$$S_{ab} = \mathcal{D}^{-1} \widetilde{\text{Tr}} [R_{ba} R_{ab}] = \mathcal{D}^{-1} \sum_c N_{ab}^c \frac{\theta_c}{\theta_a\theta_b} d_c = \frac{1}{\mathcal{D}} \text{Diagram} \quad (2.63)$$

One can see from this that $S_{ab} = S_{ba} = S_{\bar{a}\bar{b}}^*$ and $d_a = S_{1a}/S_{11}$. A useful property for

removing loops from lines is

$$\begin{array}{c} \uparrow b \\ \circlearrowleft \\ \downarrow a \end{array} = \frac{S_{ab}}{S_{1b}} \begin{array}{c} \uparrow b \\ | \\ \downarrow a \end{array} \quad (2.64)$$

A UBTC is “modular” and corresponds to a TQFT (topological quantum field theory), if its monodromy is non-degenerate, i.e. for each $a \neq 1$, there is some b such that $R_{ba}R_{ab} \neq \mathbb{I}_{ab}$, which is the case iff the topological S -matrix is unitary. For such theories, the S -matrix, together with $T_{ab} = \theta_a \delta_{ab}$ represent the generators of the modular group $\text{PSL}(2, \mathbb{Z})$.

The monodromy scalar component

$$M_{ab} = \frac{\widetilde{\text{Tr}}[R_{ba}R_{ab}]}{\widetilde{\text{Tr}}\mathbb{I}_{ab}} = \frac{1}{d_a d_b} \begin{array}{c} \circlearrowleft \\ \circlearrowright \\ \downarrow a \end{array} \begin{array}{c} \uparrow b \\ | \\ \downarrow a \end{array} = \frac{S_{ab}S_{11}}{S_{1a}S_{1b}} \quad (2.65)$$

is an important quantity, typically arising in interference terms, such as those occurring in experiments that probe anyonic charge. It is the identity coefficient of the full braid (monodromy) operation, and so may also be written as

$$M_{ab} = \sum_{(f,\mu,\nu)} [B_b^{\bar{a}ba}]_{1,(f,\mu,\nu)} [B_b^{\bar{a}ab}]_{(f,\mu,\nu),1} \quad (2.66)$$

the 1, 1 component of the B^2 operator, where

$$\begin{array}{c} a \\ \swarrow \\ \alpha \\ \searrow \\ e \\ \downarrow \\ \beta \\ \downarrow \\ d \end{array} \begin{array}{c} b \\ \uparrow \\ \downarrow \\ c \end{array} = \sum_{(f,\mu,\nu)} [B_d^{abc}]_{(e,\alpha,\beta)(f,\mu,\nu)} \begin{array}{c} a \\ \swarrow \\ \mu \\ \searrow \\ f \\ \downarrow \\ \nu \\ \downarrow \\ d \end{array} \begin{array}{c} b \\ \uparrow \\ \downarrow \\ c \end{array} \quad (2.67)$$

$$[B_d^{abc}]_{(e,\alpha,\beta)(f,\mu,\nu)} = \sum_{g,\gamma,\delta,\eta} [F_d^{acb}]_{(e,\alpha,\beta)(g,\gamma,\delta)} [R_g^{cb}]_{\gamma\eta} [(F_d^{abc})^{-1}]_{(g,\eta,\delta)(f,\mu,\nu)} \quad (2.68)$$

Braiding the same configuration clockwise instead of counterclockwise (using R_{bc}^{-1} instead of R_{cb} on the left hand side), we have $\left[(B_d^{acb})^{-1} \right]_{(e,\alpha,\beta)(f,\mu,\nu)} = [B_d^{acb}]_{(f,\mu,\nu)(e,\alpha,\beta)}^*$. Because the B -move is a unitary operator, we must have $|M_{ab}| \leq 1$. When $|M_{ab}| = 1$,

only the 1, 1 element of B^2 is non-zero, hence

$$\begin{array}{c} a \backslash \\ \curvearrowright \\ \curvearrowleft \\ a \end{array} \begin{array}{c} b \\ / \\ \curvearrowright \\ b \end{array} = M_{ab} \begin{array}{c} a \\ | \\ \uparrow \\ a \end{array} \begin{array}{c} b \\ | \\ \uparrow \\ b \end{array} \quad (2.69)$$

so that the braiding of a and b is Abelian. The monodromy of a and b is trivial if $M_{ab} = 1$. If $N_{ab}^c \neq 0$ and $|M_{be}| = 1$ for some e , then the relation

$$M_{ce} = M_{ae}M_{be} \quad (2.70)$$

follows from the diagram

$$\begin{array}{c} c \\ \uparrow \\ e \\ \uparrow \\ \mu \\ \uparrow \\ a \end{array} \begin{array}{c} \curvearrowright \\ \curvearrowleft \\ b \\ \uparrow \\ \mu \\ \uparrow \\ b \end{array} = M_{be} \begin{array}{c} c \\ \uparrow \\ \mu \\ \uparrow \\ a \end{array} \begin{array}{c} \curvearrowright \\ \curvearrowleft \\ e \\ \uparrow \\ \mu \\ \uparrow \\ b \end{array} \quad (2.71)$$

2.4 Physical States

Now that we have the full $(2+1)$ -dimensional structure of anyon models, we finish defining the partial trace and partial quantum trace, which will be used to help describe physical state in anyonic systems. With the ability to braid, one also gains the ability to trace over any anyon in a system (not just those situated at one of the two outer positions of a planar diagram). To do so, one simply uses a series of braiding operations to move the anyon to one of the outside positions, at which point the planar definition of partial traces given earlier may be applied. However, an important point is that the series of braids one applies before tracing is not arbitrary, and in general, altering the series of braids will give a different outcome. Physically, the series of braiding operations that is applied before (planar) tracing an anyon specifies the path (with respect to the other anyons) by which the traced anyon is removed from the system in consideration. From this perspective, the planar partial trace is not unique (indeed, even an anyon already at one of the outer positions may

be given nontrivial braiding with the other anyons). To be uniquely defined, the definitions of partial trace and partial quantum trace of an anyon B must include the path by which B is removed from the system. In this paper, the path will always be specified implicitly (i.e. either it will be the trivial path corresponding to planar tracing, or we will diagrammatically indicate the removal path of the anyon being traced out).

The density matrix for an arbitrary two anyon system is

$$\begin{aligned} \rho &= \sum_{\substack{a,a',b,b' \\ c,\mu,\mu'}} \rho_{(a,b,c,\mu)(a',b',c,\mu')} \frac{1}{d_c} |a, b; c, \mu\rangle \langle a', b'; c, \mu'| \\ &= \sum_{\substack{a,a',b,b' \\ c,\mu,\mu'}} \frac{\rho_{(a,b,c,\mu)(a',b',c,\mu')}}{(d_a d_b d_{a'} d_{b'} d_c^2)^{1/4}} \begin{array}{c} a \nearrow \quad b \nearrow \\ \quad \quad \quad \mu \\ \quad \quad \quad \nearrow \\ c \quad \quad \quad \mu' \\ \quad \quad \quad \searrow \\ a' \searrow \quad b' \searrow \end{array} . \end{aligned} \quad (2.72)$$

which is normalized so that satisfying the trace condition takes the form

$$\widetilde{\text{Tr}}[\rho] = \sum_{a,b,c,\mu} \rho_{(a,b,c,\mu)(a,b,c,\mu)} = 1 \quad (2.73)$$

The factor $1/d_c$ could, of course, be absorbed into $\rho_{(a,b,c,\mu)(a',b',c,\mu')}$ (as a matter of convention), but then the d_c would appear in the summand of Eq. (2.73). The overall charge c must match up between the bra and the ket because of charge conservation. One can understand this, as well as the factor of $1/d_c$, by thinking of this density matrix as $\rho = \widetilde{\text{Tr}}_{\overline{C}}[\rho']$, the partial quantum trace over \overline{C} of a density matrix that describes the actual entire system

$$\begin{aligned} \rho' &= \sum_{\substack{a,b,c,\mu \\ a',b',c',\mu'}} \rho_{(a,b,c,\mu)(a',b',c',\mu')} |a, b; c, \mu\rangle |c, \bar{c}; 1\rangle \langle c', \bar{c}'; 1| \langle a', b'; c', \mu'| \\ &= \sum_{\substack{a,b,c,\mu \\ a',b',c',\mu'}} \frac{\rho_{(a,b,c,\mu)(a',b',c',\mu')}}{(d_a d_b d_c d_{a'} d_{b'} d_{c'})^{1/4}} \begin{array}{c} a \nearrow \quad b \nearrow \quad \bar{c} \\ \quad \quad \quad \mu \\ \quad \quad \quad \nearrow \\ c \quad \quad \quad \mu' \\ \quad \quad \quad \searrow \\ a' \searrow \quad b' \searrow \quad \bar{c}' \end{array} \end{aligned} \quad (2.74)$$

which only has vacuum overall charge. In other words, the entire system really has trivial total anyonic charge, but by restricting our attention to some subset of anyons, we have a reduced subsystem with overall charge c . Tracing over the \overline{C} anyon (which imposes $c = c'$) physically represents the fact that it is no longer included in the system of interest, and cannot be brought back to interact with the A and B anyons. Because of this, we are restricted to a subsystem which may only have incoherent superpositions of different overall charges c (i.e. one must keep track of the \overline{C} anyon to allow access to coherent superpositions). The manifestation of this property in ρ is exhibited by the charge c matching in the bra and the ket (or diagrammatically as the charge c line connecting μ and μ'). The generalization to density matrices of arbitrary numbers of anyons should be clear.

When considering the combination of two sets of anyons $A = \{A_1, \dots, A_m\}$ and $B = \{B_1, \dots, B_n\}$, we say the anyons of system A are *unentangled* with those of system B if the density matrix of the combined system is the tensor product (in some basis, and up to introduction/removal path braiding) of density matrices of the two systems $\rho^{AB} = \rho^A \otimes \rho^B$ (which is represented diagrammatically by there being no non-trivial charge line connecting the anyons of system A with those of system B). This essentially means the creation histories of the two different systems do not involve each other.

2.5 Solving the Pentagon and Hexagon Equations

One may, in principle, find all anyon models with a given set of fusion rules by solving the Pentagon and Hexagon equations. However, the number of variables and equations involved grows rapidly with the number of anyonic charges. Even for an Abelian theory with N charges, the number of variables in the Pentagon equation (i.e. the number of F -symbols) equals N^3 , while the number of equations equals N^4 . In general, this makes solving the equations by hand impractical. Still, using Mathematica, we were able to solve the equations for many interesting fusion rules, including the ones tabulated in Appendix A. In this section, we explain some of the

techniques we used to do so.

The Pentagon and Hexagon equations are multivariate polynomial equations and we can use the standard techniques for such systems of equations to attempt a solution. In particular, it is well known that any system of polynomial equations with only finitely many solutions can be solved algorithmically by finding a suitable Gröbner basis [97, 98] which brings the system into an “upper triangular” form. The Pentagon and Hexagon equations never have a finite number of solutions, because they have a gauge freedom associated with each distinct vertex that amounts to the choice of basis vectors. Using the notation where $[u_c^{ab}]_{\mu,\mu'}$ is the invertible change of basis transformation for the fusion space V_c^{ab} , i.e. $|\mu\rangle = \sum_{\mu'} [u_c^{ab}]_{\mu\mu'} |\mu'\rangle$ for $|\mu\rangle \in V_c^{ab}$, this gauge freedom, which takes the form

$$\begin{aligned} & [F_d^{abc}]'_{(e,\alpha',\beta')(f,\mu',\nu')} \\ &= \sum_{\alpha,\beta,\mu,\nu} [(u_e^{ab})^{-1}]_{\alpha'\alpha} [(u_d^{ec})^{-1}]_{\beta'\beta} [F_d^{abc}]_{(e,\alpha,\beta)(f,\mu,\nu)} [u_d^{af}]_{\mu\mu'} [u_f^{bc}]_{\nu\nu'} \end{aligned} \quad (2.75)$$

$$[R_c^{ab}]'_{\mu'\nu'} = \sum_{\mu,\nu} [(u_c^{ab})^{-1}]_{\mu'\mu} [R_c^{ab}]_{\mu\nu} [u_c^{ba}]_{\nu\nu'} \quad (2.76)$$

preserves the Pentagon and Hexagon equations. If one wants to ensure that the F -moves and R -moves are always represented by unitary matrices, then one must require that the bases for the splitting spaces are orthonormal, and the basis transformations above should be unitary. However, this is not necessary to preserve the Pentagon and Hexagon equations and we will not require it in the following. The presence of this gauge symmetry means that whenever a solution to the Pentagon and/or Hexagon equations exists, there is, in fact, a family of gauge equivalent solutions, parameterized by $[u_c^{ab}]_{\mu\mu'}$. A sort of converse to this statement is given by a theorem called Ocneanu rigidity [99, 63], which states that for any set of fusion rules, there are only finitely many gauge equivalence classes of solutions to the Pentagon equations and similarly only finitely many gauge equivalence classes of solutions to the Pentagon/Hexagon system of equations. This means that if we can fix the gauge, that is, if we can put restrictions on the F -symbols and R -symbols which may be achieved by a choice of

gauge and which eliminate further gauge freedom, then we will have only finitely many solutions to the Pentagon and Hexagon equations for these gauge fixed F -symbols and R -symbols and these equations can, in principle, be solved algorithmically.

2.5.1 Fixing the Gauge

To make the task of finding solutions easier, we will restrict ourselves here to fusion rules for which all fusion coefficients N_{ab}^c are equal to 0 or 1. We will call such fusion rules *multiplicity-free*. Most anyon models that occur in physical contexts are of this type. For multiplicity-free fusion rules, the nontrivial splitting spaces are all one-dimensional and, as a result, we may drop the Greek indices (basis labels) from the F -symbols, R -symbols and gauge transformation matrices. R and u now become nonzero complex numbers R_c^{ab} and u_c^{ab} . The Pentagon and Hexagon equations, Eqs. (2.9), (2.57), and (2.58), now simplify to

$$[F_e^{fcd}]_{gl} [F_e^{abl}]_{fk} = \sum_h [F_g^{abc}]_{fh} [F_e^{ahd}]_{gk} [F_k^{bcd}]_{hl} \quad (2.77)$$

$$R_e^{ac} [F_d^{acb}]_{eg} R_g^{bc} = \sum_f [F_d^{cab}]_{ef} R_d^{fc} [F_d^{abc}]_{fg} \quad (2.78)$$

$$(R_e^{ca})^{-1} [F_d^{acb}]_{eg} (R_g^{cb})^{-1} = \sum_f [F_d^{cab}]_{ef} (R_d^{cf})^{-1} [F_d^{abc}]_{fg}. \quad (2.79)$$

Under a gauge transformation, the F -symbols and R -symbols become

$$[F_d^{abc}]'_{ef} = \frac{u_d^{af} u_f^{bc}}{u_e^{ab} u_d^{ec}} [F_d^{abc}]_{ef} \quad (2.80)$$

$$[R_c^{ab}]' = \frac{u_c^{ba}}{u_c^{ab}} R_c^{ab}. \quad (2.81)$$

Now a simple strategy for fixing the gauge presents itself: we can eliminate the gauge freedom by setting certain F -symbols and R -symbols equal to a numerical value (for example, equal to 1). If a (non-invariant) F -symbol is initially non-zero, then we can set it equal to 1 by appropriately choosing one of the gauge factors appearing in the equation above. After setting $[F_d^{abc}]_{ef} = 1$, we have to keep the ratio $\frac{u_d^{af} u_f^{bc}}{u_e^{ab} u_d^{ec}}$

fixed in any further gauge transformation in order not to change $[F_d^{abc}]_{ef}$. In this way, we can proceed to fix more F -symbols until no further gauge freedom for the F -symbols exists, ensuring there will only be finitely many solutions to these gauge fixed Pentagon equations. Afterwards, we may do the same for the Hexagon equations, if there is any applicable gauge freedom left. The only problem with this scheme is that we must know in advance which F -symbols (if any) are equal to 0. Before dealing with this issue, let us assume it is known which F -symbols equal 0, and describe the gauge fixing procedure for the Pentagon equations in a bit more detail.

To fix the gauge for the F -symbols, we look at Eq. (2.80) and pick one of these which is linear in one of the gauge factors. In this equation, we set the transformed F -symbol equal to 1 and then we solve for the linearly occurring gauge factor. We substitute the solution back into the full set of equations, eliminating the fixed gauge factor. Then we repeat the procedure with another gauge factor which occurs linearly in a different equation, and continue iterating this step. At any point during this process, the gauge equations will still be in a form similar to the original: namely F' is seen to be equal to a product of (positive and negative) integer powers of F -symbols and gauge factors. For many theories with small numbers of particles, this procedure of solving linear equations and back-substitution can be carried through until no more free gauge factors appear on the right hand side of the equations. When this happens, the gauge is completely fixed as far as the F -symbols are concerned (there may still be gauge factors which have not been fixed, but the ratios of gauge factors that occur in the F -symbols' transformations are, indeed, fixed). However, in general, we may run out of equations that are linear in the gauge factors before the gauge is fully fixed. In such cases, one can continue the process using quadratic or higher order equations in the gauge factors. Such equations do not have unique solutions and so it may be necessary to keep track of the tree of possible subsequent solutions in order to make sure that a consistent overall gauge fixing emerges. Also, arbitrary choices of solutions to higher-order equations for gauge factors may lead to a residual finite gauge group. This is not a problem in solving the Pentagon equations, since the number of solutions will still be finite, but it must be tracked in order to

correctly count non-isomorphic (gauge inequivalent) anyon models after obtaining the solutions. Using this procedure and a similar procedure for the gauge freedom in the R -symbols, we have been able to automate gauge fixing for all the fusion rules we have solved using our program.

2.5.2 Finding Zeros

In order to be able to fix the gauge, we need to know which F -symbols are equal to 0 before solving the Pentagon equations themselves. For unitary anyon models, this appears to always be possible. In fact, using unitarity, we can write down a set of equations for the absolute values of the F -symbols which, in all the examples we have calculated, has only finitely many solutions. We have

$$\sum_e \left| [F_d^{abc}]_{ef} \right|^2 = \sum_f \left| [F_d^{abc}]_{ef} \right|^2 = 1 \quad (2.82)$$

as a special case of unitarity. Secondly, in unitary anyon models, it is possible [see Eq. (2.34)] to make a gauge choice so that

$$\left| [F_c^{a\bar{a}c}]_{1f} \right|^2 = \frac{d_f}{d_a d_c} \quad \text{and} \quad \left| [F_a^{abb}]_{e1} \right|^2 = \frac{d_e}{d_a d_b}. \quad (2.83)$$

In order to make use of this equation, we must know the quantum dimensions of the particles (without first calculating the F -symbols). This is not too much of a problem, since for unitary theories, d_a is the Perron-Frobenius eigenvalue of the integer matrix N_{ab}^c . Thirdly, in any unitary gauge, we must have

$$\left| [F_d^{abc}]_{ef} \right|^2 = 1 \quad (2.84)$$

whenever e and f are the unique labels allowed by fusion (given a , b , c , and d), since in these cases, the F -move is a unitary map between one-dimensional spaces.

Finally, some of the Pentagon equations Eq. (2.77) have only one term in the sum over h on the right hand side. Taking absolute value squared on both sides of those

Pentagon equations we obtain

$$\left| [F_e^{fcd}]_{gl} \right|^2 \left| [F_e^{abl}]_{fk} \right|^2 = \left| [F_g^{abc}]_{fh} \right|^2 \left| [F_e^{ahd}]_{gk} \right|^2 \left| [F_k^{bcd}]_{hl} \right|^2. \quad (2.85)$$

The equations for the absolute values of the F -symbols we have mentioned up to now determine a finite set of solutions for the F -symbols in all examples we have looked at. We are investigating whether this is true in general. If one is only interested in anyon models with braiding, one may add extra equations coming from the Hexagons which have only one term in the summation over f [cf. Eqs. (2.78) and (2.79)]. Note that these equations will also involve only F -symbols, since in any unitary gauge the absolute values of all R -symbols equals 1, for multiplicity-free fusion rules.

In solving the equations we have given for the absolute values of the F -symbols, it is useful to note that many of the equations are of the form

$$A \left| [F_d^{abc}]_{ef} \right|^2 = B, \quad (2.86)$$

where A is a numerical factor given in terms of previously fixed F -symbols and B is an expression that depends only on F -symbols other than $[F_d^{abc}]_{ef}$. After recursively eliminating variables using equations of this type, we often arrive at a set of equations that can be solved using Mathematica's standard equation-solving routines.

Note that any solution found here gives the absolute values of the F -symbols as they would occur in a unitary gauge. These absolute values are not invariant under general (non-unitary) gauge transformations. On the other hand, whether or not an F -symbol in a multiplicity-free theory is zero is a gauge-invariant property.

2.5.3 Solving the Gauge Fixed Pentagon and Hexagon Equations

Once the gauge is fixed, one may, in principle, solve the equations algorithmically, using, for example, the techniques based on Gröbner bases that are implemented in standard algebra packages, like Mathematica. However, the algorithms involved

scale at least exponentially, both in space and in time, as a function of the number of variables, the number and degree of the equations, and the number of solutions to the equations. This means that even after gauge-fixing, some preprocessing is still necessary before Gröbner basis techniques may be applied. Fortunately, it turns out that the structure of the Pentagon and Hexagon equations allows for a drastic reduction of the numbers of variables and equations by elementary means. Two subtypes of equations are responsible for this. First of all, there are typically many equations that are linear in at least one of the variables. Heuristically, one would expect this, because there are many equations and many more variables than can occur in any one equation (e.g. for the Pentagon equations, an upper bound for the number of variables in an equation is 2 plus 3 times the maximal number of fusion channels). Secondly, there are often many equations that have only two terms, because the sums on the right hand sides of the equations have only a single term. Both types of equations are very useful in reducing the number of variables, because they are usually easy to solve. In the case of a linear equation one can always solve for the linearly occurring variable if it occurs in only one of the terms. Since we use that we already know which F -symbols are zero, we do not have to worry about the possibility that the term with the linearly occurring variable is equal to zero. In the case of an equation with two terms, one may solve for any variable for which the two terms have different order, again using knowledge that both terms are non-zero.

Linear equations involving more than two terms have the drawback that repeated back-substitution of the solutions to such equations quickly increases the number of terms in the remaining equations. This places a heavy burden on the memory, causing the equations themselves to become very long, and slowing down the search for a Gröbner basis. Two-term equations which are not linear have the disadvantage of having multiple solutions, and each solution has to be substituted in order to be sure that one finds all solutions to the full set of equations. Because of this, we start the elimination of variables using the equations which are linear and have only two terms. This reduction step alone turns out to be very powerful, and, for the theories we have solved, it often reduced the number of variables by as much as a factor 50.

After this first reduction step, we use Mathematica's various simplification routines to bring the equations to a standard form. In this way, dependent equations can become identical, often leading to a substantial reduction in the number of equations (for example, for $SU(3)_7$ fusion rules, we have 4911 distinct gauge fixed Pentagon equations before the substitution step and 280 distinct equations after substitution and simplification).

We continue the process of variable elimination by solving further linear equations until we run out. These elimination steps usually consume most of the computer time involved in solving the equations, since the number of terms per equation tends to grow exponentially with the number of variables eliminated (the number of equations simultaneously decreases, but usually not enough to compensate). The speed of this growth is linked to the maximal (or typical) number of fusion channels allowed by the fusion rules, since this number determines the number of terms in the summations that occur in the Pentagon and Hexagon equations. As a result, theories with fewer fusion channels may be much easier to solve than theories with more fusion channels, even if the former have more anyonic charges.

After these elementary steps, we usually have only a small number of variables left (less than 5 for all theories tabulated in Appendix A) and in the simpler cases the equations may now be directly solved by Mathematica's standard algebraic equation reduction routines. For the more difficult theories we have solved, one further trick is necessary: to select some subset of the equations that is small and simple enough to be solved, and yet restrictive enough to lead to a discrete set of solutions. This may take some experimentation, but, due to the reduced number of variables, it is usually not a difficult task. Finally, one checks to determine which of the solutions of this subset of the equations actually solves the full equations.

Clearly, improvements to our program can still be made. We intend to extend the program to take more advantage of non-linear, two-term equations, as we hope this will improve our success at solving the equations for fusion rules with many fusion channels. Also, we have not yet made any effort to improve the efficacy of the more advanced solution algorithms used by Mathematica's equation-reduction

routines, for example, by choosing a better ordering on the polynomials. The tables in Appendix A were all produced using a single Dell Inspiron 6400 laptop computer, and most of them represent only a modest amount of computing time. With better computing resources and enough motivation, much more extensive tabulation should be possible.

Chapter 3 Mach-Zehnder Interferometer

In this chapter, we consider, in detail, a Mach-Zehnder type interferometer [100, 101] (see Fig. 3.1) for quasiparticles with (possibly non-Abelian) anyonic braiding statistics, greatly extending the analysis begun in Ref. [102]. This will serve as a prototypic model of interferometry experiments with anyons, and the methods used in its analysis readily apply to other classes of interferometers (e.g. the FQH two point-contact interferometer considered in Chapter 4). This interferometer was also considered for non-Abelian anyons in Ref. [103], but only for anyon models described by a discrete gauge theory-type formalism in which individual particles are assumed to have internal Hilbert spaces, and for probe anyons that are all identical and have trivial self-braiding. Unfortunately, this excludes perhaps the most important class of anyon models – those describing the fractional quantum Hall states – so we must dispense with such restrictions. We abstract to an idealized system that supports an arbitrary anyon model and also allows for a number of desired manipulations to be effected. Specifically, without concern for ways to physically actualize them, we posit the experimental abilities to: (1) produce, isolate, and position desired anyons, (2) provide anyons with some manner of propulsion to produce a beam of probe anyons, (3) construct lossless beam-splitters and mirrors, and (4) detect the presence of a probe anyon at the output legs of the interferometer.

The target anyon A is the composite of all anyons A_1, A_2, \dots located inside the central interferometry region, and so may be in a superposition of states with different total anyonic charges. Since these anyons are treated collectively by the experiment, we ignore their individuality and consider them as a single anyon A capable of charge superposition. We will assume the probe anyons, B_1, \dots, B_N may each also be treated as capable of charge superposition (though this would certainly be more difficult to physically realize). The probe anyons are sent as a beam into the interferometer through two possible input channels. They pass through a beam splitter

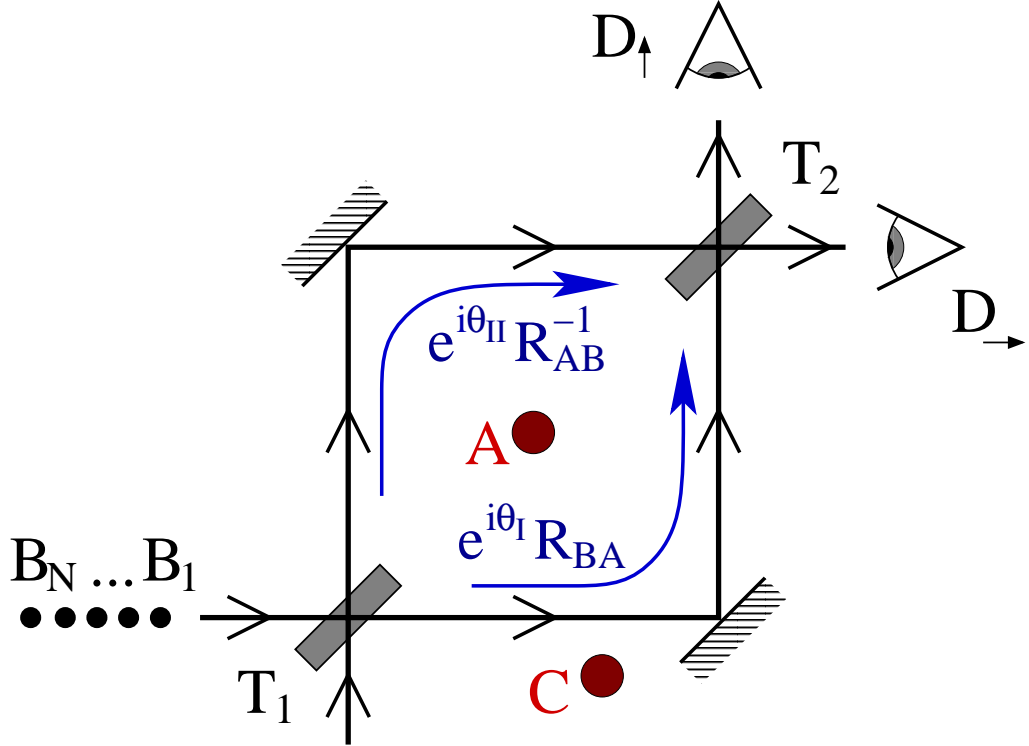


Figure 3.1: A Mach-Zehnder interferometer for an anyonic system. (These systems are effectively 2-dimensional, so the 3rd through 9th and/or 10th spatial dimensions are suppressed in this figure.) The target anyon(s) A in the central region shares entanglement only with the anyon(s) C outside this region. A beam of probe anyons B_1, \dots, B_N is sent through the interferometer, where T_j are beam splitters, and detected at one of the two possible outputs by D_s .

T_1 , are reflected by mirrors around the central target region, pass through a second beam splitter T_2 , and then are detected at one of the two possible output channels by the detectors D_s . When a probe anyon B passes through the bottom path of the interferometer, the state acquires the phase $e^{i\theta_I}$, which results from background Aharonov-Bohm interactions [93], path length differences, phase shifters, etc., and is also acted upon by the braiding operator R_{BA} , which is strictly due to the braiding statistics between the probe and target anyons. Similarly, when the probe passes through the top path of the interferometer, the state acquires the phase $e^{i\theta_{II}}$ and is acted on by R_{AB}^{-1} .

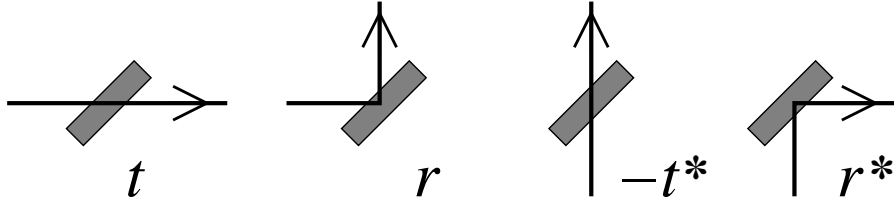


Figure 3.2: The transmission and reflection coefficients for a beam splitter.

Using the two-component vector notation

$$\begin{pmatrix} 1 \\ 0 \end{pmatrix} = |\rightarrow\rangle, \quad \begin{pmatrix} 0 \\ 1 \end{pmatrix} = |\uparrow\rangle \quad (3.1)$$

to indicate the direction (horizontal or vertical) a probe anyon is traveling through the interferometer at any point, the lossless beam splitters (see Fig. 3.2) are represented by

$$T_j = \begin{bmatrix} t_j & r_j^* \\ r_j & -t_j^* \end{bmatrix} \quad (3.2)$$

(for $j = 1, 2$), where $|t_j|^2 + |r_j|^2 = 1$ [104]. We note that these matrices could be multiplied by overall phases without affecting any of the results, since such phases are not distinguished by the two paths.

When considering operations involving non-Abelian anyons, it is important to keep track of all other anyons with which there is non-trivial entanglement. Indeed, if these additional particles are not tracked or are physically inaccessible, one should trace them out of the system, forgoing the ability to use them to form coherent superpositions of anyonic charge. We assume that the target anyon has no initial entanglement with the probe anyons, so their systems will be combined as tensor products, with no non-trivial charge lines connecting them before they interact in the interferometer.

The target system involves the target anyon A and the anyon C which is the only one entangled with A that is kept physically accessible. Recall that these anyons may really represent multiple quasiparticles that are being treated collectively, but as long

as we are not interested in operations involving the individual quasiparticles, they can be treated as a single anyon. The density matrix of the target system is

$$\begin{aligned}
\rho^A &= \sum_{a,a',c,c',f,\mu,\mu'} \rho_{(a,c;f,\mu),(a',c';f,\mu')}^A \frac{1}{d_f} |a, c; f, \mu\rangle \langle a', c'; f, \mu'| \\
&= \sum_{a,a',c,c',f,\mu,\mu'} \frac{\rho_{(a,c;f,\mu),(a',c';f,\mu')}^A}{(d_a d_{a'} d_c d_{c'} d_f^2)^{1/4}} \begin{array}{c} a \swarrow \quad \searrow c \\ \quad \uparrow \mu \\ f \quad \uparrow \mu' \\ \quad \swarrow \quad \searrow \\ a' \swarrow \quad \searrow c' \end{array} \quad (3.3)
\end{aligned}$$

We will assume that the probe anyons are also not entangled with each other, and that they are all identical (or, more accurately, belong to an ensemble of particles all described by the density matrix ρ^B). We will consider generalizations of the probe anyons in Chapter 3.4. Such generalizations complicate the bookkeeping of the calculation, but will have qualitatively similar results. A probe system involves the probe anyon B , which is sent through the interferometer entering the horizontal leg $s \Rightarrow$, and the anyon D which is entangled with B and will be sent off to the (left) side. We will write the directional index s of the probe particle as a subscript on its anyonic charge label, i.e. b_s . The density matrix of a probe system is

$$\begin{aligned}
\rho^B &= \sum_{b,b',d,d',h,\lambda,\lambda'} \rho_{(d,b_\rightarrow;h,\lambda),(d',b'_\rightarrow;h,\lambda')}^B \frac{1}{d_h} |d, b_\rightarrow; h, \lambda\rangle \langle d', b'_\rightarrow; h, \lambda'| \\
&= \sum_{b,b',d,d',h,\lambda,\lambda'} \frac{\rho_{(d,b_\rightarrow;h,\lambda),(d',b'_\rightarrow;h,\lambda')}^B}{(d_d d_{d'} d_b d_{b'} d_h^2)^{1/4}} \begin{array}{c} d \swarrow \quad \searrow b_\rightarrow \\ \quad \uparrow \lambda \\ h \quad \uparrow \lambda' \\ \quad \swarrow \quad \searrow \\ d' \swarrow \quad \searrow b'_\rightarrow \end{array} \quad (3.4)
\end{aligned}$$

The unitary operator representing a probe anyon passing through the interferometer is given by

$$U = T_2 \Sigma T_1 \quad (3.5)$$

$$\Sigma = \begin{bmatrix} 0 & e^{i\theta_{11}} R_{AB}^{-1} \\ e^{i\theta_{11}} R_{BA} & 0 \end{bmatrix}. \quad (3.6)$$

This can be written diagrammatically as

$$\begin{array}{c} A \\ \text{---} \\ \boxed{U} \\ \text{---} \\ B_{s'} \end{array} \begin{array}{c} B_s \\ \text{---} \\ \text{---} \\ A \end{array} = e^{i\theta_I} \begin{bmatrix} t_1 r_2^* & r_1^* r_2^* \\ -t_1 t_2^* & -r_1^* t_2^* \end{bmatrix} \begin{array}{c} \nearrow \\ \searrow \\ B \end{array} \begin{array}{c} \nearrow \\ \searrow \\ A \end{array} + e^{i\theta_{II}} \begin{bmatrix} r_1 t_2 & -t_1^* t_2 \\ r_1 r_2 & -t_1^* r_2 \end{bmatrix} \begin{array}{c} \nearrow \\ \searrow \\ B \end{array} \begin{array}{c} \nearrow \\ \searrow \\ A \end{array}. \quad (3.7)$$

The position of the anyon C with respect to the other anyons must be specified, and we will take it to be located below the central interferometry region and slightly to the right of A . (The specification ‘‘slightly to the right’’ merely indicates how the diagrams are to be drawn, and has no physical consequence.) For this choice of positioning, the operator

$$V = \begin{bmatrix} R_{CB}^{-1} & 0 \\ 0 & R_{CB}^{-1} \end{bmatrix} \quad (3.8)$$

represents the braiding of C with the probe¹. We do not bother drawing a similar diagrammatic representation for V , since it is a simple braid, in this case.

After a probe anyon B is measured at one of the detectors, it no longer interests us, and we remove it along with its entangled pair D from the vicinity of the target anyon system. Mathematically, this means we take the tensor product of the probe and target systems, evolve them with VU (which sends the probe through the interferometer) to get

$$\rho = VU (\rho^B \otimes \rho^A) U^\dagger V^\dagger, \quad (3.9)$$

apply the usual orthogonal measurement collapse projection

$$\Pr(s) = \widetilde{\text{Tr}}[\rho \Pi_s] \quad (3.10)$$

¹If the anyon C was instead located above the central interferometer region, we would have

$$V = \begin{bmatrix} R_{BC} & 0 \\ 0 & R_{BC} \end{bmatrix},$$

which leads to a similar evaluation. If it were located between the output legs of the interferometer, we would instead have

$$V = \begin{bmatrix} R_{BC} & 0 \\ 0 & R_{CB}^{-1} \end{bmatrix},$$

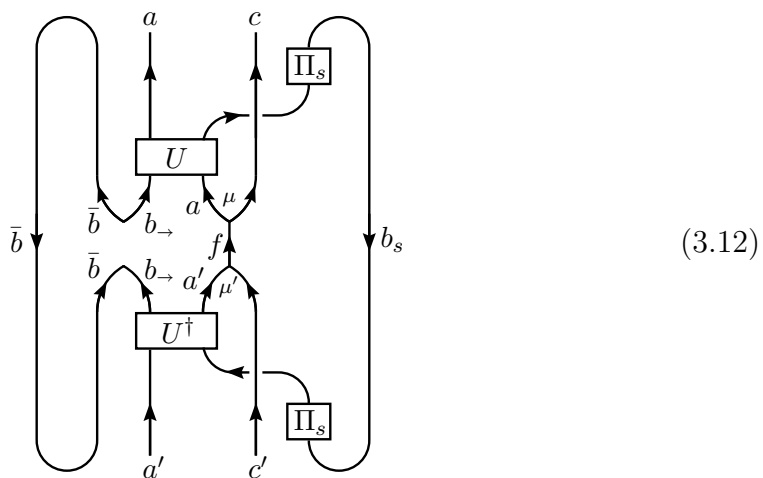
and the resulting evaluation becomes complicated. One could also envision far more complicated situations, such as having the anyons entangled with A distributed between all three of these locations, but we will not delve into this.

$$\rho \mapsto \frac{1}{\Pr(s)} \Pi_s \rho \Pi_s \quad (3.11)$$

with $\Pi_s = |s\rangle\langle s|$ for the outcome s , and then finally trace out the anyons B and D . Since the probe anyons are all initially unentangled, we may obtain their effect on the target system by considering that of each probe individually.

3.1 One Probe

We begin by considering the effect of a single probe with definite anyonic charge b , i.e. $\rho^b = |\bar{b}, b_{\rightarrow}; 1\rangle\langle \bar{b}, b_{\rightarrow}; 1|$, and return to general ρ^B immediately afterwards. For a particular component of the target anyons' density matrix, the relevant diagram that must be evaluated for a single probe measurement is



For the outcome $s \Rightarrow$, this is

$$\begin{aligned}
& \begin{array}{c} a \quad c \\ \uparrow \quad \uparrow \\ U \\ \downarrow \quad \downarrow \\ a \quad c \\ \leftarrow \quad \rightarrow \\ f \quad \mu \\ \downarrow \quad \downarrow \\ a' \quad c' \\ \uparrow \quad \uparrow \\ U^\dagger \\ \downarrow \quad \downarrow \\ a' \quad c' \end{array} = \sum_{(e,\alpha,\beta)} [(F_{a'c'}^{ac})^{-1}]_{(f,\mu,\mu')(e,\alpha,\beta)} \begin{array}{c} a \quad c \\ \uparrow \quad \uparrow \\ U \\ \downarrow \quad \downarrow \\ a \quad c \\ \leftarrow \quad \rightarrow \\ \alpha \quad \beta \\ \downarrow \quad \downarrow \\ a' \quad c' \\ \uparrow \quad \uparrow \\ U^\dagger \\ \downarrow \quad \downarrow \\ a' \quad c' \end{array} \\
& = \sum_{(e,\alpha,\beta)} [(F_{a'c'}^{ac})^{-1}]_{(f,\mu,\mu')(e,\alpha,\beta)} \\
& \quad \times \left\{ |t_1|^2 |r_2|^2 \begin{array}{c} a \quad c \\ \uparrow \quad \uparrow \\ \alpha \quad \beta \\ \leftarrow \quad \rightarrow \\ e \quad b \\ \downarrow \quad \downarrow \\ a' \quad c' \end{array} + t_1 r_1^* r_2^* t_2^* e^{i(\theta_1 - \theta_{II})} \begin{array}{c} a \quad c \\ \uparrow \quad \uparrow \\ \alpha \quad \beta \\ \leftarrow \quad \rightarrow \\ e \quad b \\ \downarrow \quad \downarrow \\ a' \quad c' \end{array} \right. \\
& \quad \left. + t_1^* r_1 t_2 r_2 e^{-i(\theta_1 - \theta_{II})} \begin{array}{c} a \quad c \\ \uparrow \quad \uparrow \\ \alpha \quad \beta \\ \leftarrow \quad \rightarrow \\ e \quad b \\ \downarrow \quad \downarrow \\ a' \quad c' \end{array} + |r_1|^2 |t_2|^2 \begin{array}{c} a \quad c \\ \uparrow \quad \uparrow \\ \alpha \quad \beta \\ \leftarrow \quad \rightarrow \\ e \quad b \\ \downarrow \quad \downarrow \\ a' \quad c' \end{array} \right\} \\
& = d_b \sum_{(e,\alpha,\beta)} [(F_{a'c'}^{ac})^{-1}]_{(f,\mu,\mu')(e,\alpha,\beta)} p_{aa'e,b}^{\rightarrow} \begin{array}{c} a \quad c \\ \uparrow \quad \uparrow \\ \alpha \quad \beta \\ \leftarrow \quad \rightarrow \\ e \quad b \\ \downarrow \quad \downarrow \\ a' \quad c' \end{array} \\
& = d_b \sum_{\substack{(e,\alpha,\beta) \\ (f',\nu,\nu')}} [(F_{a'c'}^{ac})^{-1}]_{(f,\mu,\mu')(e,\alpha,\beta)} [F_{a'c'}^{ac}]_{(e,\alpha,\beta)(f',\nu,\nu')} p_{aa'e,b}^{\rightarrow} \begin{array}{c} a \quad c \\ \swarrow \quad \searrow \\ \nu \quad \nu' \\ \swarrow \quad \searrow \\ a' \quad c' \end{array} \quad (3.13)
\end{aligned}$$

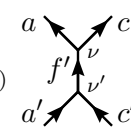
where we have defined

$$\begin{aligned}
p_{aa'e,b}^{\rightarrow} &= |t_1|^2 |r_2|^2 M_{eb} + t_1 r_1^* r_2^* t_2^* e^{i(\theta_1 - \theta_{II})} M_{ab} \\
&\quad + t_1^* r_1 t_2 r_2 e^{-i(\theta_1 - \theta_{II})} M_{a'b}^* + |r_1|^2 |t_2|^2
\end{aligned} \quad (3.14)$$

and have used Eqs. (2.64,2.65) to remove the b loops. A similar calculation for the $s = \uparrow$ outcome gives

$$p_{aa'e,b}^\uparrow = |t_1|^2 |t_2|^2 M_{eb} - t_1 r_1^* r_2^* t_2^* e^{i(\theta_1 - \theta_{II})} M_{ab} - t_1^* r_1 t_2 r_2 e^{-i(\theta_1 - \theta_{II})} M_{a'b}^* + |r_1|^2 |r_2|^2. \quad (3.15)$$

From this, inserting the appropriate coefficients and normalization factors, we find the reduced density matrix of the target anyons after a single probe measurement with outcome s :

$$\begin{aligned} \rho^A(s) &= \frac{1}{\text{Pr}(s)} \widetilde{\text{Tr}}_{\bar{B},B} [\Pi_s \rho \Pi_s] \\ &= \sum_{\substack{a,a',c,c',f,\mu,\mu' \\ (e,\alpha,\beta),(f',\nu,\nu')}} \frac{\rho_{(a,c;f,\mu),(a',c';f,\mu')}^A P_{aa'e,b}^s}{(d_a d_{a'} d_c d_{c'} d_f^2)^{1/4} \text{Pr}(s)} \\ &\quad \times [(F_{a'c'}^{ac})^{-1}]_{(f,\mu,\mu')(e,\alpha,\beta)} [F_{a'c'}^{ac}]_{(e,\alpha,\beta)(f',\nu,\nu')} \\ &= \sum_{\substack{a,a',c,c',f,\mu,\mu' \\ (e,\alpha,\beta),(f',\nu,\nu')}} \frac{\rho_{(a,c;f,\mu),(a',c';f,\mu')}^A P_{aa'e,b}^s}{(d_f d_{f'})^{1/2} \text{Pr}(s)} [(F_{a',c'}^{a,c})^{-1}]_{(f,\mu,\mu')(e,\alpha,\beta)} \\ &\quad \times [F_{a',c'}^{a,c}]_{(e,\alpha,\beta)(f',\nu,\nu')} |a, c; f', \nu\rangle \langle a', c'; f', \nu'| \end{aligned} \quad (3.16)$$


where the probability of measurement outcome s is found by additionally taking the quantum trace of the target system, which projects onto the $e = 1$ components, giving

$$\text{Pr}(s) = \widetilde{\text{Tr}}[\rho \Pi_s] = \sum_{a,c,f,\mu} \rho_{(a,c;f,\mu),(a,c;f,\mu)}^A P_{aa1,b}^s. \quad (3.17)$$

We note that

$$p_{aa1,b}^\rightarrow = |t_1|^2 |r_2|^2 + |r_1|^2 |t_2|^2 + 2\text{Re} \{ t_1 r_1^* r_2^* t_2^* e^{i(\theta_1 - \theta_{II})} M_{ab} \} \quad (3.18)$$

$$p_{aa1,b}^\uparrow = |t_1|^2 |t_2|^2 + |r_1|^2 |r_2|^2 - 2\text{Re} \{ t_1 r_1^* r_2^* t_2^* e^{i(\theta_1 - \theta_{II})} M_{ab} \} \quad (3.19)$$

give a well-defined probability distribution (i.e. $0 \leq p_{aa1,b}^s \leq 1$ and $p_{aa1,b}^{\rightarrow} + p_{aa1,b}^{\uparrow} = 1$).

The quantity

$$t_1 r_1^* t_2^* r_2^* e^{i(\theta_I - \theta_{II})} \equiv T e^{i\theta} \quad (3.20)$$

determines the visibility of quantum interference in this experiment, where varying θ allows one to observe the interference term modulation. The amplitude $T = |t_1 r_1 t_2 r_2|$ is maximized by $|t_j| = |r_j| = 1/\sqrt{2}$. In realistic experiments, the experimental parameters t_j , r_j , θ_I , and θ_{II} will have some variance, even for a single probe, that gives rise to some degree of phase incoherence. Averaging over some distribution in θ , one finds that $e^{i\theta}$ in the interference terms should effectively be replaced by $\langle e^{i\theta} \rangle = Q e^{i\theta^*}$. In this expression, $e^{i\theta^*}$ is the resulting effective phase, and $Q \in [0, 1]$ is a suppression factor that reflects the interferometer's lack of coherence, and reduces the visibility of quantum interference. For the rest of the paper, we will ignore this issue and assume $Q = 1$, but it should always be kept in mind that success of any interferometry experiment is crucially dependent on Q being made as large as possible.

We can now obtain the result for general ρ^B by simply replacing $p_{aa'e,b}^s$ everywhere with

$$p_{aa'e,B}^s = \sum_b \Pr_B(b) p_{aa'e,b}^s \quad (3.21)$$

$$\Pr_B(b) = \sum_{d,h,\lambda} \rho_{(d,b_{\rightarrow};h,\lambda),(d,b_{\rightarrow};h,\lambda)}^B. \quad (3.22)$$

We will also use the notation $M_{aB} = \sum_b \Pr_B(b) M_{ab}$. That this replacement gives the appropriate results follows from the fact that we trace out the D anyon, and may

be seen from

$$\begin{aligned}
\widetilde{\text{Tr}}_D [\rho^B] &= \sum_{b,b',d,h,\lambda,\lambda'} \frac{\rho_{(d,b_{\rightarrow};h,\lambda),(d,b'_{\rightarrow};h,\lambda)}^B}{(d_d^2 d_b d_{b'} d_h^2)^{1/4}} \begin{array}{c} \text{---} d \text{---} \\ \text{---} h \text{---} \\ \text{---} d \text{---} \\ \text{---} \lambda \text{---} \\ \text{---} \lambda' \text{---} \\ \text{---} b_{\rightarrow} \text{---} \\ \text{---} b'_{\rightarrow} \text{---} \end{array} \\
&= \sum_{b,d,h,\lambda} \rho_{(d,b_{\rightarrow};h,\lambda),(d,b_{\rightarrow};h,\lambda)}^B \frac{1}{d_b} \begin{array}{c} | \\ b_{\rightarrow} \end{array} \\
&= \sum_{b,d,h,\lambda} \rho_{(d,b_{\rightarrow};h,\lambda),(d,b_{\rightarrow};h,\lambda)}^B \frac{1}{d_b} \begin{array}{c} \text{---} \bar{b} \text{---} \\ \text{---} b_{\rightarrow} \text{---} \\ \text{---} \bar{b} \text{---} \\ \text{---} b_{\rightarrow} \text{---} \end{array} \\
&= \sum_b \text{Pr}_B(b) \widetilde{\text{Tr}}_{\bar{b}} |\bar{b}, b_{\rightarrow}; 1\rangle \langle \bar{b}, b_{\rightarrow}; 1| \\
&= \widetilde{\text{Tr}}_{\bar{B}} \sum_b \text{Pr}_B(b) |\bar{b}, b_{\rightarrow}; 1\rangle \langle \bar{b}, b_{\rightarrow}; 1| \tag{3.23}
\end{aligned}$$

where we used Eq. (2.48) in the first step.

3.2 N Probes

The result for N (initially unentangled) identical probe particles sent through the interferometer may now be easily produced by iterating the single probe calculation. The string of measurement outcomes (s_1, \dots, s_N) occurs with probability

$$\text{Pr}(s_1, \dots, s_N) = \sum_{a,c,f,\mu} \rho_{(a,c;f,\mu),(a,c;f,\mu)}^A p_{aa1,B}^{s_1} \cdots p_{aa1,B}^{s_N} \tag{3.24}$$

and results in the measured target anyon reduced density matrix

$$\begin{aligned}
\rho^A(s_1, \dots, s_N) &= \sum_{\substack{a,a',c,c',f,\mu,\mu' \\ (e,\alpha,\beta),(f',\nu,\nu')}} \frac{\rho_{(a,c;f,\mu),(a',c';f',\mu')}^A}{(d_f d_{f'})^{1/2}} \frac{p_{aa'e,B}^{s_1} \cdots p_{aa'e,B}^{s_N}}{\text{Pr}(s_1, \dots, s_N)} \\
&\times [(F_{a'c'}^{ac})^{-1}]_{(f,\mu,\mu')(e,\alpha,\beta)} [F_{a'c'}^{ac}]_{(e,\alpha,\beta)(f',\nu,\nu')} |a, c; f', \nu\rangle \langle a', c'; f', \nu'|. \tag{3.25}
\end{aligned}$$

It is apparent that the specific order of the measurement outcomes is not important in the result, but that only the total number of outcomes of each type matters, hence leading to a binomial distribution. We denote the total number of $s_j \Rightarrow$ in the string of measurement outcomes as n , and cluster together all results with the same n . Defining (for arbitrary p and q)

$$W_N(n; p, q) = \frac{N!}{n!(N-n)!} p^n q^{N-n} \quad (3.26)$$

the probability of measuring n of the N probes at the horizontal detector is

$$\text{Pr}_N(n) = \sum_{a,c,f,\mu} \rho_{(a,c;f,\mu),(a,c;f,\mu)}^A W_N(n; p_{aa1,B}^{\rightarrow}, p_{aa1,B}^{\uparrow}) \quad (3.27)$$

and these measurements produce the target anyon reduced density matrix

$$\begin{aligned} \rho_N^A(n) &= \sum_{\substack{a,a',c,c',f,\mu,\mu' \\ (e,\alpha,\beta),(f',\nu,\nu')}} \frac{\rho_{(a,c;f,\mu),(a',c';f,\mu')}^A W_N(n; p_{aa'e,B}^{\rightarrow}, p_{aa'e,B}^{\uparrow})}{(d_f d_{f'})^{1/2} \text{Pr}_N(n)} \\ &\times [(F_{a'c'}^{ac})^{-1}]_{(f,\mu,\mu')(e,\alpha,\beta)} [F_{a'c'}^{ac}]_{(e,\alpha,\beta)(f',\nu,\nu')} |a, c; f', \nu\rangle \langle a', c'; f', \nu'|. \end{aligned} \quad (3.28)$$

In Ref. [102], we obtained the reduced density matrix that ignores the measurement outcomes and describes the decoherence (rather than the precise details of collapse) due to the probe measurements. We find this density matrix by averaging over n , giving us the result in Eq. (15c) of [102], though for more general target and probe systems

$$\begin{aligned} \rho_N^A &= \sum_{n=0}^N \text{Pr}_N(n) \rho_N^A(n) \\ &= \sum_{\substack{a,a',c,c',f,\mu,\mu' \\ (e,\alpha,\beta),(f',\nu,\nu')}} \frac{\rho_{(a,c;f,\mu),(a',c';f,\mu')}^A}{(d_f d_{f'})^{1/2}} (|t_1|^2 M_{eB} + |r_1|^2)^N \\ &\times [(F_{a'c'}^{ac})^{-1}]_{(f,\mu,\mu')(e,\alpha,\beta)} [F_{a'c'}^{ac}]_{(e,\alpha,\beta)(f',\nu,\nu')} |a, c; f', \nu\rangle \langle a', c'; f', \nu'| \end{aligned} \quad (3.29)$$

where we used

$$\begin{aligned} \sum_{n=0}^N W_N(n; p_{aa'e,B}^{\rightarrow}, p_{aa'e,B}^{\uparrow}) &= (p_{aa'e,B}^{\rightarrow} + p_{aa'e,B}^{\uparrow})^N \\ &= (|t_1|^2 M_{eB} + |r_1|^2)^N. \end{aligned} \quad (3.30)$$

The interferometry experiment distinguishes anyonic charges in the target by their values of $p_{aa1,B}^s$, which determine the possible measurement distributions. Different anyonic charges with the same probability distributions of probe outcomes are indistinguishable by such probes, and so should be grouped together into distinguishable subsets. We define \mathcal{C}_κ for $\kappa = 1, \dots, m \leq |\mathcal{C}|$ to be the maximal disjoint subsets of \mathcal{C} such that $p_{aa1,B}^{\rightarrow} = p_\kappa$ for all $a \in \mathcal{C}_\kappa$, i.e.

$$\begin{aligned} \mathcal{C}_\kappa &\equiv \{a \in \mathcal{C} : p_{aa1,B}^{\rightarrow} = p_\kappa\} \\ \mathcal{C}_\kappa \cap \mathcal{C}_{\kappa'} &= \emptyset \quad \text{for } \kappa \neq \kappa' \\ \bigcup_{\kappa} \mathcal{C}_\kappa &= \mathcal{C}. \end{aligned} \quad (3.31)$$

Note that $p_{aa1,B}^{\rightarrow} = p_{a'a'1,B}^{\rightarrow}$ (for two different charges a and a') iff

$$\text{Re} \{t_1 r_1^* r_2^* t_2^* e^{i(\theta_I - \theta_{II})} M_{aB}\} = \text{Re} \{t_1 r_1^* r_2^* t_2^* e^{i(\theta_I - \theta_{II})} M_{a'B}\} \quad (3.32)$$

which occurs either when:

- (i) at least one of t_1 , t_2 , r_1 , or r_2 is zero, or
- (ii) $|M_{aB}| \cos(\theta + \varphi_a) = |M_{a'B}| \cos(\theta + \varphi_{a'})$, where $\theta = \arg(t_1 r_1^* r_2^* t_2^* e^{i(\theta_I - \theta_{II})})$ and $\varphi_a = \arg(M_{aB})$.

If condition (i) is satisfied, then there is no interference and $\mathcal{C}_1 = \mathcal{C}$ (all target anyonic charges give the same probe measurement distribution). Condition (ii) is generically² only satisfied when $M_{aB} = M_{a'B}$, but is non-generically satisfied by

²The term ‘‘generic’’ is used in this paper only in reference to the collection of interferometer parameters t_j , r_j , θ_I , and θ_{II} .

setting $\theta = -\arg\{M_{aB} - M_{a'B}\} \pm \frac{\pi}{2}$. With this notation, we may write

$$\Pr_N(n) = \sum_{\kappa} \Pr_A(\kappa) W_N(n; p_{\kappa}, 1 - p_{\kappa}) \quad (3.33)$$

$$\Pr_A(\kappa) = \sum_{a \in \mathcal{C}_{\kappa, c, f, \mu}} \rho_{(a, c; f, \mu), (a, c; f, \mu)}^A. \quad (3.34)$$

We emphasize that if the parameters t_j, r_j and θ in the experiment are known and adjustable, then the measurements may be used to gather information regarding the quantities M_{ab} , which, through its relation to the topological S -matrix, may be used to properly identify the anyon model that describes an unknown system [105].

In Chapters 3.2.1 and 3.2.2, we show that, as $N \rightarrow \infty$, the fraction $r = n/N$ of measurement outcomes will be found to go to $r = p_{\kappa}$ with probability $\Pr_A(\kappa)$, and the target anyon density matrix will generically collapse onto the corresponding “fixed states” given by

$$\begin{aligned} \rho_{\kappa}^A &= \sum_{\substack{a, a', c, c', f, \mu, \mu' \\ (e, \alpha, \beta), (f', \nu, \nu')}} \frac{\rho_{(a, c; f, \mu), (a', c'; f, \mu')}^A}{(d_f d_{f'})^{1/2}} \Delta_{aa'e, B}(p_{\kappa}) \\ &\times [(F_{a'c'}^{ac})^{-1}]_{(f, \mu, \mu')(e, \alpha, \beta)} [F_{a'c'}^{ac}]_{(e, \alpha, \beta)(f', \nu, \nu')} |a, c; f', \nu\rangle \langle a', c'; f', \nu| \end{aligned} \quad (3.35)$$

where

$$\Delta_{aa'e, B}(p_{\kappa}) = \begin{cases} \frac{1}{\Pr_A(\kappa)} & \text{if } p_{aa'e, B}^{\rightarrow} = 1 - p_{aa'e, B}^{\uparrow} = p_{\kappa} \text{ and } a, a' \in C_{\kappa} \\ 0 & \text{otherwise} \end{cases}. \quad (3.36)$$

Fixed state density matrices are left unchanged by probe measurements. We also emphasize that the condition: $p_{aa'e, B}^{\rightarrow} = 1 - p_{aa'e, B}^{\uparrow} = p_{\kappa}$ and $a, a' \in C_{\kappa}$ is equivalent to $M_{eB} = 1$ (which also implies $M_{aB} = M_{a'B}$). This gives the interpretation that the probes have the effect of collapsing superpositions of anyonic charges a and a' in the target that they can distinguish by monodromy ($M_{aB} \neq M_{a'B}$), and removing any entanglement between the target anyon A and anyons C outside the central interferometry region corresponding to e -channels that they can “see” by monodromy ($M_{eB} \neq 1$). Non-generically, it is also possible to collapse onto “rogue states,” for

which the diagonal density matrix elements are all fixed and some of the off-diagonal elements have fixed magnitude, but phases that change depending on the measurement outcome (i.e. are “quasi-fixed”). Because rogue states occur only for specific, exactly precise experimental parameters, they will not actually survive realistic experiments. We note that if $M_{eB} = 1$ only for $e = 1$, then the probe distinguishes all charges, and the fixed states are given by

$$\rho_{\kappa_a}^A = \sum_{f, f' \in \{a \times c\}, \mu, \nu} \frac{\rho_{(a,c;f,\mu),(a,c;f,\mu)}^A}{d_a d_c} |a, c; f', \nu\rangle \langle a, c; f', \nu|, \quad (3.37)$$

for which the target anyon A has definite charge and no entanglement with C . We give examples of fixed state density matrices for several significant anyon models in Chapter 5.

In principle, one may also consider the “many-to-many” experiment described in Ref. [103], where the target anyon system is replaced with a fresh one (described by the same initial density matrix) after each probe measurement. For this type of experiment, the result for each probe is described by the single probe outcome probability, Eq. (3.17):

$$\Pr(s) = \sum_{a,c,f,\mu} \rho_{(a,c;f,\mu),(a,c;f,\mu)}^A P_{aa1,B}^s. \quad (3.38)$$

Thus, for N such probe measurements, the number of measurement outcomes n found at the horizontal detector will have the binomial distribution: $W_N(n; \Pr(\rightarrow), \Pr(\uparrow))$.

3.2.1 Large N

We would like to analyze the large N behavior of the measurements. This is essentially determined by $W_N(n; p_\kappa, 1 - p_\kappa)$ and $\frac{W_N(n; p_{aa'e,B}^\rightarrow, p_{aa'e,B}^\uparrow)}{\Pr_N(n)}$, so we now consider these in detail. Of course, $W_N(n; p_\kappa, 1 - p_\kappa)$ is just a familiar binomial distribution. Changing variables to the fraction $r = n/N$ of total probe measurement outcomes in

the horizontal detector, the distribution in r is given by

$$W_N(r; p_\kappa, 1 - p_\kappa) = W_N(rN; p_\kappa, 1 - p_\kappa) N \quad (3.39)$$

and has mean and variance

$$\bar{r} = p_\kappa \quad (3.40)$$

$$\Delta r = \sigma_\kappa \equiv \sqrt{p_\kappa(1 - p_\kappa)/N}. \quad (3.41)$$

Taking N large and using Stirling's formula, this may be approximated by a Gaussian distribution

$$W_N(r; p_\kappa, 1 - p_\kappa) \simeq \frac{1}{\sqrt{2\pi\sigma_\kappa^2}} e^{-\frac{(r-p_\kappa)^2}{2\sigma_\kappa^2}}. \quad (3.42)$$

Taking the limit $N \rightarrow \infty$ gives

$$\lim_{N \rightarrow \infty} W_N(r; p_\kappa, 1 - p_\kappa) = \delta(r - p_\kappa) \quad (3.43)$$

(defined such that $\int_0^1 \delta(r - p) dr = 1$, when $p = 0$ or 1), so the resulting probability distribution for the measurement outcomes is

$$\Pr(r) = \lim_{N \rightarrow \infty} \Pr_N(r) = \sum_{\kappa} \Pr_A(\kappa) \delta(r - p_\kappa) \quad (3.44)$$

Thus, as $N \rightarrow \infty$, we will find the fraction of measurement outcomes $r \rightarrow p_\kappa$ with probability $\Pr_A(\kappa)$.

Though the probability of obtaining the outcome r which is away from the closest p_κ vanishes as

$$W_N(r; p_\kappa, 1 - p_\kappa) \sim \sqrt{N} \left(\frac{p_\kappa^r (1 - p_\kappa)^{1-r}}{r^r (1 - r)^{1-r}} \right)^N \quad (3.45)$$

for large N , the resulting density matrix should still be well defined for all r (at least for large, but finite N). In particular, we will use positivity of density matrices, in the form of the Cauchy-Schwarz type inequality $\rho_{\mu\mu}\rho_{\nu\nu} \geq |\rho_{\mu\nu}|^2$, to evince their large

N behavior in terms of conditions on $p_{aa'e,B}^s$. From the quantity

$$\begin{aligned} \Delta_{N;aa'e,B}(r) &\equiv \frac{W_N(rN; p_{aa'e,B}^{\rightarrow}, p_{aa'e,B}^{\uparrow})}{\text{Pr}_N(rN)} \\ &= \left\{ \sum_{\kappa'} \text{Pr}_A(\kappa') \left[\left(\frac{p_{\kappa'}}{p_{aa'e,B}^{\rightarrow}} \right)^r \left(\frac{1-p_{\kappa'}}{p_{aa'e,B}^{\uparrow}} \right)^{1-r} \right]^N \right\}^{-1} \end{aligned} \quad (3.46)$$

we can see that as $N \rightarrow \infty$, the $e = 1$ terms (those that determine the “diagonal” elements) behave as:

- (i) $\Delta_{N;aa1,B}(r) \rightarrow \frac{1}{\text{Pr}_A(\kappa_1)}$ for $a \in \mathcal{C}_{\kappa_1}$, if $\text{Pr}_A(\kappa_1) \neq 0$ and $p_{\kappa_1}^r (1-p_{\kappa_1})^{1-r} > p_{\kappa}^r (1-p_{\kappa})^{1-r}$ for all $\kappa \neq \kappa_1$,
- (ii) $\Delta_{N;aa1,B}(r) \rightarrow \frac{1}{\text{Pr}_A(\kappa_1) + \text{Pr}_A(\kappa_2)}$ for $a \in \mathcal{C}_{\kappa_1} \cup \mathcal{C}_{\kappa_2}$, if $\text{Pr}_A(\kappa_1) + \text{Pr}_A(\kappa_2) \neq 0$ and $p_{\kappa_1}^r (1-p_{\kappa_1})^{1-r} = p_{\kappa_2}^r (1-p_{\kappa_2})^{1-r} > p_{\kappa}^r (1-p_{\kappa})^{1-r}$ for all $\kappa \neq \kappa_1, \kappa_2$, or
- (iii) $\Delta_{N;aa1,B}(r) \rightarrow 0$ for $a \in \mathcal{C}_{\kappa_1}$, if there is some κ with $\text{Pr}_A(\kappa) \neq 0$ and $p_{\kappa}^r (1-p_{\kappa})^{1-r} > p_{\kappa_1}^r (1-p_{\kappa_1})^{1-r}$.

If $a \in \mathcal{C}_{\kappa_1}$, where $p_{\kappa_1}^r (1-p_{\kappa_1})^{1-r} > p_{\kappa}^r (1-p_{\kappa})^{1-r}$ for all $\kappa \neq \kappa_1$, but $\text{Pr}_A(\kappa_1) = 0$, then $\Delta_{N;aa1,B}(r) \rightarrow \infty$. However, $\text{Pr}_A(\kappa_1) = 0$ also implies that the density matrix coefficients involving a are strictly zero, so we need not worry about this case.

We note that for each κ , the variable r has a closed interval I_{κ} , containing p_{κ} in its interior, such that $p_{\kappa}^r (1-p_{\kappa})^{1-r} \geq p_{\kappa'}^r (1-p_{\kappa'})^{1-r}$ for all $\kappa' \neq \kappa$ (i.e. I_{κ} satisfies (i) in its interior and (ii) at its endpoints). We say that r is congruous with \mathcal{C}_{κ} in this interval I_{κ} (and congruous to two different \mathcal{C}_{κ} at the intersecting endpoints of such intervals).

For arbitrary (in particular, the “off-diagonal”) terms, the positivity condition combined with Eq. (3.46) as $N \rightarrow \infty$ tells us that we must have $\Delta_{N;aa'e,B}(r) \rightarrow 0$, except when r is congruous with both a and a' , in which case $|\Delta_{N;aa'e,B}(r)| \leq \Delta_{N;aa1,B}(r)$, and $\Delta_{N;aa'e,B}(r) \rightarrow \infty$ should not be allowed (except when the density matrix elements involving a or a' are strictly zero, making it irrelevant). From this we find that either:

- (a) there is some κ (possibly even with a and/or a' in \mathcal{C}_{κ}) with $\text{Pr}_A(\kappa) \neq 0$ and $p_{\kappa}^r (1-p_{\kappa})^{1-r} > |p_{aa'e,B}^{\rightarrow}|^r |p_{aa'e,B}^{\uparrow}|^{1-r}$, in which case $\Delta_{N;aa'e,B}(r) \rightarrow 0$, or

(b) $|p_{aa'e,B}^{\rightarrow}|^r |p_{aa'e,B}^{\uparrow}|^{1-r} = (p_{aa1,B}^{\rightarrow})^r (p_{aa1,B}^{\uparrow})^{1-r} = (p_{a'a'1,B}^{\rightarrow})^r (p_{a'a'1,B}^{\uparrow})^{1-r}$ with r congruous with both a and a' , in which case $|\Delta_{N;aa'e,B}(r)| \rightarrow \Delta_{N;aa1,B}(r)$.

Case (b) deserves some further inspection. First, we note that we have

$$|p_{aa'e,B}^{\rightarrow}|^r |p_{aa'e,B}^{\uparrow}|^{1-r} \leq p_{\kappa}^r (1 - p_{\kappa})^{1-r} \quad (3.47)$$

on the entire interval I_{κ} congruous with $a \in \mathcal{C}_{\kappa}$. If there is some point r_* in the interior of I_{κ} for which

$$|p_{aa'e,B}^{\rightarrow}|^{r_*} |p_{aa'e,B}^{\uparrow}|^{1-r_*} = p_{\kappa}^{r_*} (1 - p_{\kappa})^{1-r_*}, \quad (3.48)$$

then in order not to violate the inequality when r is increased or decreased from r_* , we must have

$$\frac{|p_{aa'e,B}^{\rightarrow}|}{|p_{aa'e,B}^{\uparrow}|} = \frac{p_{\kappa}}{1 - p_{\kappa}}. \quad (3.49)$$

It follows that

$$|p_{aa'e,B}^{\rightarrow}|^r |p_{aa'e,B}^{\uparrow}|^{1-r} = p_{\kappa}^r (1 - p_{\kappa})^{1-r} \quad (3.50)$$

on the entire interval I_{κ} , and, more significantly, that

$$|p_{aa'e,B}^{\rightarrow}| = 1 - |p_{aa'e,B}^{\uparrow}| = p_{\kappa}. \quad (3.51)$$

The same argument holds with respect to a' instead of a , giving the additional condition $a, a' \in \mathcal{C}_{\kappa}$. Hence, even at exponentially suppressed r , superpositions of anyonic charges from different \mathcal{C}_{κ} do not survive measurement.

Pushing this a bit further, we note that for $r \in [0, 1]$ and fixed $p \in [0, 1]$

$$r^r (1 - r)^{1-r} \geq p^r (1 - p)^{1-r} \quad (3.52)$$

with equality at $r = p$. The positivity condition gave us (rewriting (a) and (b))

$$\max_{\kappa} \{p_{\kappa}^r (1 - p_{\kappa})^{1-r}\} \geq |p_{aa'e,B}^{\rightarrow}|^r |p_{aa'e,B}^{\uparrow}|^{1-r} \quad (3.53)$$

with equality for $r \in I_\kappa$ if $a, a' \in \mathcal{C}_\kappa$ and $|p_{aa'e,B}^\rightarrow| = 1 - |p_{aa'e,B}^\uparrow| = p_\kappa$. Combining these, we have

$$r^r (1-r)^{1-r} \geq |p_{aa'e,B}^\rightarrow|^r |p_{aa'e,B}^\uparrow|^{1-r} \quad (3.54)$$

for all r , with equality occurring at $r = |p_{aa'e,B}^\rightarrow|$ only when $p_a = p_{a'} = |p_{aa'e,B}^\rightarrow| = 1 - |p_{aa'e,B}^\uparrow|$. If $|p_{aa'e,B}^\rightarrow| + |p_{aa'e,B}^\uparrow| > 1$, then there is some r (e.g. $r = |p_{aa'e,B}^\rightarrow|$) for which $r^r (1-r)^{1-r} < |p_{aa'e,B}^\rightarrow|^r |p_{aa'e,B}^\uparrow|^{1-r}$, violating Eq. (3.54). If $|p_{aa'e,B}^\rightarrow| + |p_{aa'e,B}^\uparrow| = 1$, then $r^r (1-r)^{1-r} = |p_{aa'e,B}^\rightarrow|^r |p_{aa'e,B}^\uparrow|^{1-r}$ at $r = |p_{aa'e,B}^\rightarrow|$. Hence, we have

$$|p_{aa'e,B}^\rightarrow| + |p_{aa'e,B}^\uparrow| \leq 1 \quad (3.55)$$

with equality only if $p_a = p_{a'} = |p_{aa'e,B}^\rightarrow| = 1 - |p_{aa'e,B}^\uparrow|$. One should be able to show that this condition on $p_{aa'e,b}^s$ follows directly from the properties of anyon models, in which case these arguments could be made in the opposite direction, i.e. that positivity of the density matrix being preserved by these probe measurements follows from properties of anyon models; however, we have been unable to succeed in doing so.

For $p_{aa'e,B}^\rightarrow = p_\kappa e^{i\alpha_{aa'e,B}}$ and $p_{aa'e,B}^\uparrow = (1-p_\kappa) e^{i\beta_{aa'e,B}}$, we see that if $\alpha_{aa'e,B} = \beta_{aa'e,B}$, then

$$|t_1|^2 M_{eB} + |r_1|^2 = p_{aa'e,B}^\rightarrow + p_{aa'e,B}^\uparrow = e^{i\alpha_{aa'e,B}} \quad (3.56)$$

implies that either: (a) $r_1 = 0$ and $M_{eB} = e^{i\alpha_{aa'e,B}}$, or (b) $M_{eB} = 1$ and $\alpha_{aa'e,B} = \beta_{aa'e,B} = 0$.

One might also find it instructive to consider a large N expansion (using Stirling's formula) around p_κ to get

$$W_N(r; p_{aa'e,B}^\rightarrow, p_{aa'e,B}^\uparrow) \simeq W_N(r; p_\kappa, 1-p_\kappa) e^{-G_N(r; p_{aa'e,B}^\rightarrow, p_{aa'e,B}^\uparrow)} \quad (3.57)$$

$$\Delta_{N;aa'e,B}(r) \simeq \frac{1}{\text{Pr}_A(\kappa)} e^{-G_N(r; p_{aa'e,B}^\rightarrow, p_{aa'e,B}^\uparrow)} \quad (3.58)$$

$$\begin{aligned} G_N(r; p, q) &\approx N \left[p_\kappa \ln \left(\frac{p_\kappa}{p} \right) + (1-p_\kappa) \ln \left(\frac{1-p_\kappa}{q} \right) \right] \\ &\quad + N (r-p_\kappa) \ln \left(\frac{p_\kappa}{p} \frac{q}{(1-p_\kappa)} \right). \end{aligned} \quad (3.59)$$

Clearly, $e^{-G_N(r;p,q)}$ gives exponential suppression in N , unless $p = p_\kappa e^{i\alpha}$ and $q = (1 - p_\kappa) e^{i\beta}$, in which case

$$e^{-G_N(r;p,q)} = e^{i[\alpha p_\kappa + \beta(1-p_\kappa)]N} e^{i(\alpha-\beta)N(r-p_\kappa)} \quad (3.60)$$

(which is equal to 1, when $\alpha = \beta = 0$). We also note that integrating the quantity $W_N(r; p_{aa'e,B}^\rightarrow, p_{aa'e,B}^\uparrow)$ over r vanishes exponentially in N , unless $\alpha_{aa'e,B} = \beta_{aa'e,B} = 0$, which is why such quasi-fixed terms do not appear in Eq. (3.29), the density matrix obtained by ignoring measurement outcomes (except in the case when $r_1 = 0$).

To summarize, we found that, for large N , the quantity $\Delta_{N;aa'e,B}(r)$ vanishes exponentially unless r is congruous with $a, a' \in \mathcal{C}_\kappa$ and $|p_{aa'e,B}^\rightarrow| = 1 - |p_{aa'e,B}^\uparrow| = p_\kappa$. This means a measurement outcome fraction r exponentially collapses the density matrix onto one that has support only in \mathcal{C}_κ , and consequently will drive r toward p_κ . The resulting target anyon reduced density matrix

$$\begin{aligned} \rho^A(r) &= \sum_{\substack{a,a',c,c',f,\mu,\mu' \\ (e,\alpha,\beta),(f',\nu,\nu')}} \frac{\rho_{(a,c;f,\mu),(a',c';f',\mu')}^A}{(d_f d_{f'})^{1/2}} \Delta_{aa'e,B}(r) \\ &\times [(F_{a'c'}^{ac})^{-1}]_{(f,\mu,\mu')(e,\alpha,\beta)} [F_{a'c'}^{ac}]_{(e,\alpha,\beta)(f',\nu,\nu')} |a, c; f', \nu\rangle \langle a', c'; f', \nu'| \end{aligned} \quad (3.61)$$

$$\Delta_{aa'e,B}(r) = \lim_{N \rightarrow \infty} \Delta_{N;aa'e,B}(r) \quad (3.62)$$

is found with the probability distribution

$$\Pr(r) = \sum_{\kappa} \Pr_A(\kappa) \delta(r - p_\kappa). \quad (3.63)$$

The resulting density matrices are of two forms:

- (1) *fixed states*, for which all non-zero elements of the density matrix correspond to $p_{aa'e,B}^\rightarrow = 1 - p_{aa'e,B}^\uparrow = p_\kappa$, and
- (2) *rogues states* (or *quasi-fixed states*), for which all elements of the density matrix correspond to $|p_{aa'e,B}^\rightarrow| = 1 - |p_{aa'e,B}^\uparrow| = p_\kappa$, but for some of the ‘‘off-diagonal’’ elements ($e \neq 1$) with $p_{aa'e,B}^\rightarrow = p_\kappa e^{i\alpha_{aa'e,B}}$ and $p_{aa'e,B}^\uparrow = (1 - p_\kappa) e^{i\beta_{aa'e,B}}$, where $\alpha_{aa'e,B}$ and

$\beta_{aa'e,B}$ are non-zero (unless $r_1 = 0$).

Fixed states have the property that probe measurements leave their density matrix invariant. Rogue states have the property that probe measurements leave their “diagonal” elements and possibly some of their “off-diagonal” elements invariant, while some of their “off-diagonal” elements are unchanged in magnitude, but have a changing phase. We will see in Chapter 3.2.2 that satisfying the conditions for rogue states requires non-generic experimental parameters.

3.2.2 Minding our p’s

In Chapter 3.2.1, we have shown that performing many probe measurements collapses the target density matrix onto its elements which correspond to $p_{aa'e,B}^s$ satisfying

$$|p_{aa'e,B}^{\rightarrow}| = 1 - |p_{aa'e,B}^{\uparrow}| = p_{\kappa} \quad (3.64)$$

for $a, a' \in \mathcal{C}_{\kappa}$, so we would like to determine when this condition is satisfied.

For completeness, we first list the results for the trivial cases where there is no actual interferometry (for which $\mathcal{C}_1 = \mathcal{C}$):

- (i) When $t_1 = 0$, we have $p_{aa'e,B}^{\rightarrow} = |t_2|^2$ and $p_{aa'e,B}^{\uparrow} = |r_2|^2$, so all elements are fixed.
- (ii) When $r_1 = 0$, we have $p_{aa'e,B}^{\rightarrow} = |r_2|^2 M_{eB}$ and $p_{aa'e,B}^{\uparrow} = |t_2|^2 M_{eB}$, so elements with $M_{eB} = e^{i\varphi_{eB}}$ ($\varphi_{eB} \neq 0$) are quasi-fixed, and those with $M_{eB} = 1$ are fixed.
- (iii) When $t_2 = 0$ (and $t_1 \neq 0$), we have $p_{aa'e,B}^{\rightarrow} = |t_1|^2 M_{eB}$ and $p_{aa'e,B}^{\uparrow} = |r_1|^2$, so elements with $M_{eB} = e^{i\varphi_{eB}}$ ($\varphi_{eB} \neq 0$) are quasi-fixed, and those with $M_{eB} = 1$ are fixed.
- (iv) When $r_2 = 0$ (and $t_1 \neq 0$), we have $p_{aa'e,B}^{\rightarrow} = |r_1|^2$ and $p_{aa'e,B}^{\uparrow} = |t_1|^2 M_{eB}$, so elements with $M_{eB} = e^{i\varphi_{eB}}$ ($\varphi_{eB} \neq 0$) are quasi-fixed, and those with $M_{eB} = 1$ are fixed.

From here on, we assume that $|t_1 r_1 t_2 r_2| \neq 0$ (unless explicitly stated otherwise). We begin by considering the more stringent condition necessary for fixed elements. Using $p_{aa'e,b}^{\rightarrow} + p_{aa'e,b}^{\uparrow} = |t_1|^2 M_{eB} + |r_1|^2$, and Eq. (2.70), we have:

- (v) (When $t_1 \neq 0$) An element is fixed, with $p_{aa'e,b}^{\rightarrow} = 1 - p_{aa'e,b}^{\uparrow} = p_{\kappa}$, iff $M_{eB} = 1$,

and this implies $M_{aB} = M_{a'B}$ and $a, a' \in \mathcal{C}_\kappa$.

Thus, even without initially requiring $a, a' \in \mathcal{C}_\kappa$ (from positivity), we find that it is a necessary condition for fixed elements.

Now, we examine the conditions that give quasi-fixed elements. Such terms have $p_{aa'e,B}^\rightarrow = p_\kappa e^{i\alpha_{aa'e,B}}$ and $p_{aa'e,B}^\uparrow = (1 - p_\kappa) e^{i\beta_{aa'e,B}}$, with $\alpha_{aa'e,B} \neq \beta_{aa'e,B}$ and $a, a' \in \mathcal{C}_\kappa$. (Recall that if $\alpha_{aa'e,B} = \beta_{aa'e,B}$ and $r_1 \neq 0$, then $\alpha_{aa'e,B} = \beta_{aa'e,B} = 0$.) Examining these conditions for $M_{aB} = M_{a'B}$, we find

$$\begin{aligned} 0 &= |t_2|^2 \left(|p_{aa'e,B}^\rightarrow|^2 - p_\kappa^2 \right) + |r_2|^2 \left(|p_{aa'e,B}^\uparrow|^2 - (1 - p_\kappa)^2 \right) \\ &= |t_1|^4 |t_2|^2 |r_2|^2 (|M_{eB}|^2 - 1) + 2 |t_1|^2 |r_1|^2 |t_2|^2 |r_2|^2 (\operatorname{Re} \{M_{eB}\} - 1) \end{aligned} \quad (3.65)$$

which requires $M_{eB} = 1$ and, hence, gives us:

(vi) (When $|t_1 r_1 t_2 r_2| \neq 0$) There are no quasi-fixed elements for $p_{aa'e,B}^s$ with $M_{aB} = M_{a'B}$, only fixed ones. (In particular, this applies to $a = a'$.)

For $M_{aB} \neq M_{a'B}$, we can only have $a, a' \in \mathcal{C}_\kappa$ (i.e. $p_{aa1,B}^s = p_{a'a'1,B}^s$) when the experimental parameters are tuned to $\theta = -\arg \{M_{aB} - M_{a'B}\} \pm \frac{\pi}{2}$, so quasi-fixed elements only occur non-generically. From the conditions on $p_{aa'e,B}^s$, at these values of θ , we find

$$\begin{aligned} 0 &= |p_{aa'e,B}^\rightarrow|^2 - p_\kappa^2 - |p_{aa'e,B}^\uparrow|^2 + (1 - p_\kappa)^2 \\ &= |t_1|^4 (|t_2|^2 - |r_2|^2) (1 - |M_{eB}|^2) \\ &\quad - 2 |t_1|^2 (1 - \operatorname{Re} \{M_{eB}\}) 2 |t_1 r_1 t_2 r_2| \operatorname{Re} \{e^{i\theta} M_{aB}\} \\ &\quad + 2 |t_1|^2 \operatorname{Im} \{M_{eB}\} |t_1 r_1 t_2 r_2| \operatorname{Im} \{e^{i\theta} M_{aB} + e^{-i\theta} M_{a'B}^*\} \end{aligned} \quad (3.66)$$

and

$$\begin{aligned} 0 &= |t_2|^2 \left(|p_{aa'e,B}^\rightarrow|^2 - p_\kappa^2 \right) + |r_2|^2 \left(|p_{aa'e,B}^\uparrow|^2 - (1 - p_\kappa)^2 \right) \\ &= |t_1|^4 |t_2|^2 |r_2|^2 (|M_{eB}|^2 - 1) + 2 |t_1|^2 |r_1|^2 |t_2|^2 |r_2|^2 (\operatorname{Re} \{M_{eB}\} - 1) \\ &\quad + (|t_1 r_1 t_2 r_2| \operatorname{Im} \{e^{i\theta} M_{aB} + e^{-i\theta} M_{a'B}^*\})^2 \end{aligned} \quad (3.67)$$

which may be rewritten to give:

(vii) Quasi-fixed elements with $p_{aa'e,B}^s$ only occur non-generically, and the conditions (when $|t_1 r_1 t_2 r_2| \neq 0$) that must be satisfied for them to occur are:

$$\theta = -\arg \{M_{aB} - M_{a'B}\} \pm \frac{\pi}{2} \quad (3.68)$$

$$[\text{Im} \{e^{i\theta} M_{aB} + e^{-i\theta} M_{a'B}^*\}]^2 = \frac{|t_1|^2}{|r_1|^2} (1 - |M_{eB}|^2) + 2(1 - \text{Re} \{M_{eB}\}) \quad (3.69)$$

$$\begin{aligned} \text{Re} \{e^{i\theta} M_{aB}\} &= \left[\frac{|t_1|}{4|r_1|} \left(\frac{|t_2|}{|r_2|} - \frac{|r_2|}{|t_2|} \right) (1 - |M_{eB}|^2) \right. \\ &\left. + \frac{1}{2} \text{Im} \{M_{eB}\} \text{Im} \{e^{i\theta} M_{aB} + e^{-i\theta} M_{a'B}^*\} \right] (1 - \text{Re} \{M_{eB}\})^{-1}. \end{aligned} \quad (3.70)$$

To demonstrate that it is, in fact, sometimes possible to satisfy the conditions for quasi-fixed elements given in (vii), we present the following example:

Consider an anyon model which has at least two different Abelian anyons a and a' , and some anyon b for which $M_{ab} = e^{i\varphi_{ab}}$ and $M_{a'b} = e^{i\varphi_{a'b}}$ are not equal (for example, almost any \mathbb{Z}_N model, such as $\mathbb{Z}_2^{(1/2)}$ or $\mathbb{Z}_3^{(1)}$, is sufficient). The difference charge e is uniquely determined (since a and a' are Abelian) and has $M_{eb} = e^{i\varphi_{eb}} = e^{i(\varphi_{ab} - \varphi_{a'b})}$. Setting $\theta = -\frac{1}{2}(\varphi_{ab} + \varphi_{a'b}) + n\pi$ gives

$$p_{aa'e,b}^{\rightarrow} = \left(|t_1| |r_2| e^{i(\frac{\varphi_{eb}}{2} + n\pi)} + |r_1| |t_2| \right)^2 \quad (3.71)$$

$$p_{aa'e,b}^{\uparrow} = \left(-|t_1| |t_2| e^{i(\frac{\varphi_{eb}}{2} + n\pi)} + |r_1| |r_2| \right)^2 \quad (3.72)$$

$$\begin{aligned} p_{aa1,b}^{\rightarrow} &= p_{a'a'1,b}^{\rightarrow} = |p_{aa'e,b}^{\rightarrow}| = 1 - |p_{aa'e,b}^{\uparrow}| \\ &= |t_1|^2 |r_2|^2 + 2|t_1 r_1 t_2 r_2| \cos \left(\frac{\varphi_{eb}}{2} + n\pi \right) + |r_1|^2 |t_2|^2. \end{aligned} \quad (3.73)$$

In fact, it turns out this example is the only way to satisfy the conditions for quasi-fixed elements with $|M_{eB}| = 1$. Indeed, this can even be shown without initially requiring $a, a' \in \mathcal{C}_\kappa$ from positivity. It seems rather difficult to satisfy the conditions for quasi-fixed elements when $|M_{eB}| \neq 1$, and we suspect (but are unable to prove)

that it may, in general, actually be impossible. It is certainly not possible to have quasi-fixed elements with $|M_{eB}| \neq 1$ for arbitrary non-Abelian anyon models, as one can check that they do not exist for either the Ising or Fib anyon models, for example.

3.3 Distinguishability

We would like to know how many probe anyons should be used to establish a desired level of confidence in distinguishing between the various possible outcomes. For a confidence level $1 - \alpha$, the margin of error around p_κ is specified as

$$E_\kappa = z_{\alpha/2}^* \sigma_\kappa, \quad (3.74)$$

i.e. the interval $[p_\kappa - E_\kappa, p_\kappa + E_\kappa]$ contains c of the probability distribution, where $z_{\alpha/2}^*$ is defined by

$$1 - \alpha = \text{erf}\left(\frac{z_{\alpha/2}^*}{\sqrt{2}}\right). \quad (3.75)$$

To achieve this level of confidence in distinguishing two values, p_1 and p_2 , we pick N so that these intervals have no overlap

$$\begin{aligned} \Delta p &= |p_1 - p_2| \gtrsim E_1 + E_2 = z_{\alpha/2}^* (\sigma_1 + \sigma_2) \\ &= z_{\alpha/2}^* \left(\sqrt{\frac{p_1(1-p_1)}{N}} + \sqrt{\frac{p_2(1-p_2)}{N}} \right) \end{aligned} \quad (3.76)$$

which gives the estimated N needed

$$N \gtrsim \left(\frac{z_{\alpha/2}^* \left(\sqrt{p_1(1-p_1)} + \sqrt{p_2(1-p_2)} \right)}{\Delta p} \right)^2. \quad (3.77)$$

Since $p(1-p) \leq \frac{1}{4}$, we could conservatively estimate this for arbitrary p_j as

$$N \gtrsim \left(\frac{z_{\alpha/2}^*}{\Delta p} \right)^2. \quad (3.78)$$

On the other hand, if p_1 and p_2 are of order $|t_1|^2 \sim |t_2|^2 \sim t^2 \ll 1$, and Δp is of order $2t^2 \Delta M$, where $\Delta M = |M_{a_1 B} - M_{a_2 B}|$, (i.e. employing θ such that Δp is as large as it can be) then we can estimate

$$N \gtrsim \left(\frac{z_{\alpha/2}^*}{t \Delta M} \right)^2. \quad (3.79)$$

We note that for any two outcome probabilities, p_1 and p_2 , there are always two values of θ (i.e. non-generic conditions) that make $p_1 = p_2$, and hence indistinguishable. Here are the values of $z_{\alpha/2}^*$ for some typical levels of confidence

$1 - \alpha$.6827	.9545	.99	.999	.9999
$z_{\alpha/2}^*$	1	2	2.576	3.2905	3.89059

A special case of interest exists when $|t_1| = |t_2|$ and $|M_{a_1 B}| = 1$ for one of two probabilities that we wish to distinguish. In this case, using $\theta = \pi - \arg \{M_{a_1 B}\}$ gives $p_1 = 0$, so any measurement outcome $s \Rightarrow$ automatically tells us the target's anyonic charge is not in \mathcal{C}_1 . If the alternative outcome has $p_2 \neq 0, 1$, then \mathcal{C}_1 and \mathcal{C}_2 are said to be sometimes perfectly distinguishable, since a $s \Rightarrow$ outcomes tells us the target's anyonic charge is in \mathcal{C}_2 . If $M_{a_1 B} = -M_{a_2 B}$ and we also have $|t_j|^2 = 1/2$, then $p_2 = 1$, and \mathcal{C}_1 and \mathcal{C}_2 are always perfectly distinguishable, since any single probe measurement will indicate whether the target's anyonic charge is in \mathcal{C}_1 or in \mathcal{C}_2 .

3.4 Probe Generalizations

In this section, we examine the effects of using probe systems that are even more general than those used so far. We will first consider generalizing the input direction, so that probes may enter in arbitrary superpositions of the two input directions. Then we will consider the use of probes that are not identical, so that each probe system is described by a different density matrix. For both of these, the probe systems and target system are all still initially unentangled. One may also consider cases where there is nontrivial initial entanglement between these systems, or post-interferometer

charge projections, but these typically lead to qualitatively different behavior, and greatly increase the complexity of analysis, so we will not consider them here.

3.4.1 Generalized Input Directions

For probes that are allowed to enter the interferometer through either of the input legs, possibly even in superposition, the probe systems' density matrices take the form

$$\rho^B = \sum_{b,b',d,d',h,\lambda,\lambda',r,r'} \rho_{(d,b_r;h,\lambda),(d',b_{r'};h,\lambda')}^B \frac{1}{d_h} |d, b_r; h, \lambda\rangle \langle d', b_{r'}; h, \lambda'|. \quad (3.80)$$

Using this, we find the same result as before, except with the values of $p_{aa'e,B}^s$ instead given by

$$p_{aa'e,B}^s = \sum_{d,h,\lambda,b,r,r'} \rho_{(d,b_r;h,\lambda),(d,b_{r'};h,\lambda)}^B p_{aa'e,b,r,r'}^s \quad (3.81)$$

where

$$\begin{aligned} p_{aa'e,b,\rightarrow,\rightarrow}^{\rightarrow} &= |t_1|^2 |r_2|^2 M_{eb} + t_1 r_1^* t_2^* r_2^* e^{i(\theta_1 - \theta_{II})} M_{ab} \\ &\quad + t_1^* r_1 t_2 r_2 e^{-i(\theta_1 - \theta_{II})} M_{a'b}^* + |r_1|^2 |t_2|^2 \end{aligned} \quad (3.82)$$

$$\begin{aligned} p_{aa'e,b,\rightarrow,\uparrow}^{\rightarrow} &= t_1 r_1 |r_2|^2 M_{eb} - t_1 t_1^* t_2^* r_2^* e^{i(\theta_1 - \theta_{II})} M_{ab} \\ &\quad + r_1 r_1 t_2 r_2 e^{-i(\theta_1 - \theta_{II})} M_{a'b}^* - t_1 r_1 |t_2|^2 \end{aligned} \quad (3.83)$$

$$\begin{aligned} p_{aa'e,b,\uparrow,\rightarrow}^{\rightarrow} &= t_1^* r_1^* |r_2|^2 M_{eb} + r_1^* r_1^* t_2^* r_2^* e^{i(\theta_1 - \theta_{II})} M_{ab} \\ &\quad - t_1^* t_1^* t_2 r_2 e^{-i(\theta_1 - \theta_{II})} M_{a'b}^* - t_1^* r_1^* |t_2|^2 \end{aligned} \quad (3.84)$$

$$\begin{aligned} p_{aa'e,b,\uparrow,\uparrow}^{\rightarrow} &= |r_1|^2 |r_2|^2 M_{eb} - t_1 r_1^* t_2^* r_2^* e^{i(\theta_1 - \theta_{II})} M_{ab} \\ &\quad - t_1^* r_1 t_2 r_2 e^{-i(\theta_1 - \theta_{II})} M_{a'b}^* + |t_1|^2 |t_2|^2 \end{aligned} \quad (3.85)$$

and

$$\begin{aligned} p_{aa'e,b,\rightarrow,\rightarrow}^\dagger &= |t_1|^2 |t_2|^2 M_{eb} - t_1 r_1^* t_2^* r_2^* e^{i(\theta_1 - \theta_{II})} M_{ab} \\ &\quad - t_1^* r_1 t_2 r_2 e^{-i(\theta_1 - \theta_{II})} M_{a'b}^* + |r_1|^2 |r_2|^2 \end{aligned} \quad (3.86)$$

$$\begin{aligned} p_{aa'e,b,\rightarrow,\uparrow}^\dagger &= t_1 r_1 |t_2|^2 M_{eb} + t_1 t_1^* t_2^* r_2^* e^{i(\theta_1 - \theta_{II})} M_{ab} \\ &\quad - r_1 r_1 t_2 r_2 e^{-i(\theta_1 - \theta_{II})} M_{a'b}^* - t_1 r_1 |r_2|^2 \end{aligned} \quad (3.87)$$

$$\begin{aligned} p_{aa'e,b,\uparrow,\rightarrow}^\dagger &= t_1^* r_1^* |t_2|^2 M_{eb} - r_1^* r_1^* t_2^* r_2^* e^{i(\theta_1 - \theta_{II})} M_{ab} \\ &\quad + t_1^* t_1^* t_2 r_2 e^{-i(\theta_1 - \theta_{II})} M_{a'b}^* - t_1^* r_1^* |r_2|^2 \end{aligned} \quad (3.88)$$

$$\begin{aligned} p_{aa'e,b,\uparrow,\uparrow}^\dagger &= |r_1|^2 |t_2|^2 M_{eb} + t_1 r_1^* t_2^* r_2^* e^{i(\theta_1 - \theta_{II})} M_{ab} \\ &\quad + t_1^* r_1 t_2 r_2 e^{-i(\theta_1 - \theta_{II})} M_{a'b}^* + |t_1|^2 |r_2|^2. \end{aligned} \quad (3.89)$$

It is straightforward to check that

$$p_{aa1,B}^{\rightarrow} + p_{aa1,B}^{\uparrow} = \sum_{d,h,\lambda,b,r} \rho_{(d,b_r;h,\lambda),(d,b_r;h,\lambda)}^B = 1, \quad (3.90)$$

and one can see that, generically, the only terms in the target anyons' density matrix that will survive many probe measurements are those in e -channels with

$$M_{eB} = \sum_{d,h,\lambda,b,r} \rho_{(d,b_r;h,\lambda),(d,b_r;h,\lambda)}^B M_{eb} = 1. \quad (3.91)$$

3.4.2 Non-Identical Probes

When the probes B_1, \dots, B_N are described by different density matrices ρ^{B_j} (though are all still unentangled with each other and with the target system), we must use

$$p_{aa'e,B_j}^s = \sum_b \Pr_{B_j}(b) p_{aa'e,b}^s \quad (3.92)$$

$$\Pr_{B_j}(b) = \sum_{d,h,\lambda} \rho_{(d,b_{\rightarrow};h,\lambda),(d,b_{\rightarrow};h,\lambda)}^{B_j} \quad (3.93)$$

for each probe. This gives us the probability for the string of measurement outcomes (s_1, \dots, s_N) to occur as

$$\Pr(s_1, \dots, s_N) = \sum_{a,c,f,\mu} \rho_{(a,c;f,\mu),(a,c;f,\mu)}^A p_{aa_1, B_1}^{s_1} \cdots p_{aa_1, B_N}^{s_N}, \quad (3.94)$$

with the resulting target anyon density matrix

$$\begin{aligned} \rho^A(s_1, \dots, s_N) &= \sum_{\substack{a,a',c,c',f,\mu,\mu' \\ (e,\alpha,\beta),(f',\nu,\nu')}} \frac{\rho_{(a,c;f,\mu),(a',c';f',\mu')}^A p_{aa'e, B_1}^{s_1} \cdots p_{aa'e, B_N}^{s_N}}{(d_f d_{f'})^{1/2} \Pr(s_1, \dots, s_N)} \\ &\times [(F_{a'c'}^{ac})^{-1}]_{(f,\mu,\mu')(e,\alpha,\beta)} [F_{a'c'}^{ac}]_{(e,\alpha,\beta)(f',\nu,\nu')} |a, c; f', \nu\rangle \langle a', c'; f', \nu'|. \end{aligned} \quad (3.95)$$

With this generalization, we find that the order of measurement outcomes does, in fact, matter. This is obstructive to providing a quantitative description of the large N behavior; however, the qualitative behavior should be transparent after the analysis in previous sections for the identical probes. Each probe measurement will execute some amount of projection, to some extent collapsing superpositions of anyonic charges that the probe is able to distinguish by monodromy.

Chapter 4 Fractional Quantum Hall Two Point-Contact Interferometer

After enduring the detailed analysis of Chapter 3, one hopes that it has application in physical systems, and not just to the abstract idealizations that exist in our minds. In pursuing this hope, we turn our attention to fractional quantum Hall systems, since they represent the most likely candidates for possessing anyons and realizing braiding statistics (either Abelian or non-Abelian).

Indeed, a setup that is rather similar to the Mach-Zehnder interferometer described in Chapter 3 has been experimentally realized in a quantum Hall system [106]. This interferometer has, so far, only achieved functionality in the integer quantum Hall regime (though, even there, the physical observations are not completely understood [107, 108]), but it should be able, in principle, to detect the presence of braiding statistics [109, 110, 111], and even discern whether a system possesses non-Abelian statistics [112]. Unfortunately however, there is a crucial and debilitating difference between the FQH Mach-Zehnder interferometer of [106] and the Mach-Zehnder interferometer described in Chapter 3: because of the chiral nature of FQH edge currents, one of the detectors and its drain are unavoidably situated *inside* the central interferometry region. As a result, probe anyons accumulate in this region, effectively altering the target anyon's charge. This effect renders the interferometer incapable of measuring a target charge, and hence, useless for qubit readout in topological quantum computation.

Fortunately, there is another type of interferometer that can be constructed in quantum Hall systems which *is* capable of measuring a target charge: the two point-contact interferometer. Moreover, such interferometers, which are of the Fabry-Pérot type [113], involving higher orders of interference, have already achieved experimental functionality in the fractional quantum Hall regime. The two point-contact interfer-

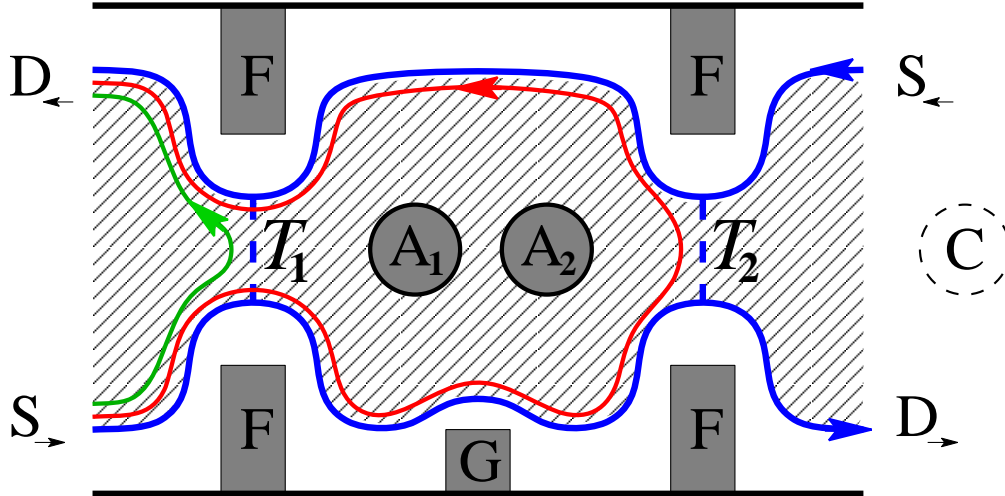


Figure 4.1: A two point-contact interferometer for measuring braiding statistics in fractional quantum Hall systems. The hatched region contains an incompressible FQH liquid. S_s and D_s indicate the “sources” and “detectors” of edge currents. The front gates (F) are used to bring the opposite edge currents (indicated by arrows) close to each other to form two tunneling junctions. Applying voltage to the central gate creates an antidot in the middle and controls the number n of quasipoles contained there. An additional side gate (G) can be used to change the shape and the length of one of the paths in the interferometer.

ometer was first proposed for use in FQH systems in Ref. [114], where it was analyzed for the Abelian states. It was analyzed for the Moore–Read state [47], the most likely physical realization of non-Abelian statistics, expected to occur at $\nu = 5/2$ and $7/2$ filling fractions, in Refs. [115, 86, 116, 117]. See also [118, 119, 120, 121] for related matters. It was further analyzed for arbitrary anyon models, and specifically for the Read–Rezayi state [53] expected to occur at $\nu = 12/5$ filling fraction, in Ref. [105] (and subsequently analyzed for the $\nu = 12/5$ Read–Rezayi state with homoplastic techniques in Refs. [122, 123]). In all of these previous analyses for non-Abelian states, the results were given to lowest order in the tunneling amplitude, and only for target anyons that were assumed to be in a state of definite anyonic charge (i.e. already collapsed). In what follows, we provide expressions including all orders of tunneling, both to explicitly display the unitarity of the quantum evolution and to account for potentially measurable corrections. Furthermore, we allow the target to be in a superposition of different anyonic charges, and relate the results to the

analysis of Chapter 3, so that we now have a proper description of the measurement collapse behavior for these interferometers. Experimental efforts in realization of the two point-contact interferometer have been carried out for Abelian FQH states [42, 43, 44, 45, 46]. Whether or not these experiments have conclusively demonstrated fractional statistics of excitations in the Abelian FQHE regime remains a topic of some debate [124, 125]¹.

The two point-contact interferometer consists of a quantum Hall bar with two constrictions (point-contacts) and (at least) two antidots, A_1 and A_2 , in between them, as depicted in Fig. 4.1. The constrictions are created by applying voltage to the front gates (F) on top of the Hall bar; by adjusting this voltage, one may control the tunneling amplitudes t_1 and t_2 . In the absence of inter-edge tunneling, the gapped bulk of the FQH liquid gives rise to a quantized Hall conductance: $G_{xy} = I/(V_{D_{\leftarrow}} - V_{S_{\leftarrow}}) = \nu e^2/h$, where the current through the Hall bar is $I = (I_{D_{\leftarrow}} - I_{S_{\leftarrow}})$. At the same time, the diagonal resistance vanishes: $R_{xx} = (V_{D_{\leftarrow}} - V_{S_{\leftarrow}})/I = 0$. Tunneling current between the opposite edges leads to a deviation of G_{xy} from its quantized value, or equivalently, to the appearance of $G_{xx} \propto R_{xx} \neq 0$. By measuring the diagonal conductance G_{xx} , one effectively measures the interference between the two tunneling paths around the antidot. The tunneling amplitudes t_1 and t_2 must be kept small, to ensure that the tunneling current is completely due to quasiholes rather than composite excitations. Treating tunneling as a perturbation, one can use renormalization group (RG) methods to compare various contributions to the overall current. Such analysis shows that in the weak tunneling regime, the tunneling current has the dependence $I \propto V^{4s-1}$ where s is the scaling dimension/spin of the corresponding fields/anyons [127, 120, 121]. It follows that the dominant contribution in this regime is from the field with lowest scaling dimension, which, in FQH systems, is the quasihole. It should be noted that the quasihole tunneling is actually relevant

¹One of the reasons for the uncertainty in interpreting the results of the experiments testing the Abelian statistics in the FQH regime is the fact that the statistical angle and the conventional Aharonov–Bohm phase acquired by a charged quasiparticle in a magnetic field are not easy to tell apart (this point is discussed in Refs. [126, 114]). From this perspective, a non-Abelian FQH state might have an advantage, being that its effect from braiding statistics dramatically differs from the charge-background field contribution.

in the RG sense, which, in more physical terms, translates into the tendency of these point contacts to become effectively pinched off in the limit of zero temperature and zero bias. On a more mundane level, the quantum Hall liquid can be broken into separate puddles by the introduction of a constriction due to purely electrostatic effects (such as edges not being sufficiently sharp). In this regard, the recent experimental evidence [128], indicating that it is possible to construct a point contact for which the $\nu = 5/2$ state persists in the tunneling region, is reassuring.

The two antidots are used to store two clusters of non-Abelian quasiparticles, A_1 and A_2 respectively, whose combined anyonic charge is being probed. The reason for two antidots, rather than just one (as has been previously suggested in [114, 115, 116, 117, 105]), is to allow for the combined target to maintain a coherent superposition of anyonic charges without decoherence from energetics that become important at short range. In particular, the energy splitting between the states of different anyonic charge on an antidot is expected to scale as L^{-1} (where L is the linear size of the dot) due to both kinetic (different angular momentum) and potential (different Coulomb energy) effects [117]. On the other hand, for two separated antidots, this energy difference should vanish exponentially with the distance between them, with suppression determined by the gap [86].

In order to appropriately examine the resulting interference patterns, we envision several experimentally variable parameters: (i) the central gate voltages allowing one to control the number of quasiholes on the antidots, (ii) the perpendicular magnetic field, (iii) the back gate voltage controlling the uniform electron density, and (iv) a side gate (G) that can be used to modify the shape of the edge (and, hence, total area and background flux within) the central interferometry region. The reason for proposing all these different controls is to be able to separately vary the Abelian Aharonov-Bohm phase and the number of quasiholes on the antidots. In fact, having all these different controls may turn out to be redundant, but they may prove beneficial for experimental success.

The target anyon A , is the combination of the anyons A_1 , A_2 , and all others (including strays) situated inside the central interferometry region. In general, any

edge excitation qualifies as a probe anyon, but since tunneling is dominated by the fundamental quasiholes, we can effectively allow the probes to have definite charge b given by the quasihole's anyonic charge label. Letting $(1, 0)$ and $(0, 1)$ correspond to the top and bottom edge, respectively (also denoted as $s = \leftarrow, \rightarrow$, respectively), the unitary evolution operator for a probe anyon B entering the system along the edge is given by

$$U = \begin{bmatrix} r_1^* r_2^* e^{i\theta_I} R_{AB} W_{AB} R_{CB} & \frac{1}{t_1^*} (1 - |r_1|^2 W_{BA}) \\ R_{BC} \frac{1}{t_2} (-1 + |r_2|^2 W_{AB}) R_{CB} & r_1 r_2 e^{i\theta_{II}} R_{BC} R_{BA} W_{BA} \end{bmatrix}, \quad (4.1)$$

when the C anyons (those outside the central interferometry region that are entangled with A) are in the region to the right of central, where we have defined

$$\begin{aligned} W_{AB} &= \sum_{n=0}^{\infty} (-t_1^* t_2 e^{i(\theta_I + \theta_{II})} R_{BA} R_{AB})^n \\ &= [1 + t_1^* t_2 e^{i(\theta_I + \theta_{II})} R_{BA} R_{AB}]^{-1} \end{aligned} \quad (4.2)$$

$$\begin{aligned} W_{BA} &= \sum_{n=0}^{\infty} (-t_1^* t_2 e^{i(\theta_I + \theta_{II})} R_{AB} R_{BA})^n \\ &= [1 + t_1^* t_2 e^{i(\theta_I + \theta_{II})} R_{AB} R_{BA}]^{-1}. \end{aligned} \quad (4.3)$$

The phases θ_I and θ_{II} are respectively picked up from traveling counter-clockwise along the top and bottom edge around the central interferometry region, and include the contribution from the enclosed background magnetic field. We note that when higher order terms are significant, it might also be the case that tunneling contributions from excitations other than the fundamental quasiholes (which have different tunneling amplitudes) are also important, but nevertheless proceed with considering all orders of tunneling in this manner. The tunneling matrices are

$$T_j = \begin{bmatrix} r_j^* & t_j \\ -t_j^* & r_j \end{bmatrix} \quad (4.4)$$

with $j = 1, 2$ for the left and right point contacts, respectively. We can perform

a similar density matrix calculation as for the Mach-Zehnder interferometer, except with more complicated diagrams in this case. Sending a single probe particle in from the bottom edge ($s \Rightarrow$) (which is effectively done by applying a bias voltage across the edges), and detecting it coming out at the bottom or top edge gives the same form for the resulting density matrix as in Eq. (3.28), except with more complicated $p_{aa'e,b}^s$ that are determined by using U of Eq. (4.1) for VU in Eqs. (3.9–3.11). To order $|t|^2$ (for $|t_1| \sim |t_2|$ small), we find

$$\begin{aligned} p_{aa'e,b}^{\rightarrow} &\simeq |r_1|^2 |r_2|^2 (1 - t_1^* t_2 e^{i(\theta_1 + \theta_{II})} M_{ab} - t_1 t_2^* e^{-i(\theta_1 + \theta_{II})} M_{a'b}^*) \\ &\simeq 1 - |t_1|^2 - |t_2|^2 - |t_1 t_2| (e^{i\beta} M_{ab} + e^{-i\beta} M_{a'b}^*) \end{aligned} \quad (4.5)$$

and

$$\begin{aligned} p_{aa'e,b}^{\leftarrow} &\simeq |t_1|^2 + |r_1|^2 t_1^* t_2 e^{i(\theta_1 + \theta_{II})} M_{ab} \\ &\quad + |r_1|^2 t_1 t_2^* e^{-i(\theta_1 + \theta_{II})} M_{a'b}^* + |r_1|^4 |t_2|^2 M_{eb} \\ &\simeq |t_1|^2 + |t_1 t_2| (e^{i\beta} M_{ab} + e^{-i\beta} M_{a'b}^*) + |t_2|^2 M_{eb} \end{aligned} \quad (4.6)$$

where we have defined $\beta = \arg \{t_1^* t_2 e^{i(\theta_1 + \theta_{II})}\}$. We see that

$$p_{aa'e,b}^{\rightarrow} + p_{aa'e,b}^{\leftarrow} \simeq |t_2|^2 M_{eb} + |r_2|^2 \quad (4.7)$$

(where here we have $|t_2|^2$ as the probability of the probe B passing between anyons A and C , rather than $|t_1|^2$). The values for the two outcome probabilities (i.e. the $e = 1$ terms) to all orders are

$$\begin{aligned} p_{aa1,b}^{\rightarrow} &= \sum_c N_{ab}^c \frac{d_c}{d_a d_b} \frac{|r_1|^2 |r_2|^2}{|1 + t_1^* t_2 e^{i(\theta_1 + \theta_{II})} e^{i2\pi(s_c - s_a - s_b)}|^2} \\ &= \sum_c N_{ab}^c \frac{d_c}{d_a d_b} \frac{|r_1|^2 |r_2|^2}{1 + |t_1|^2 |t_2|^2 + 2 |t_1 t_2| \cos[\beta + 2\pi(s_c - s_a - s_b)]} \end{aligned} \quad (4.8)$$

$$\simeq 1 - |t_1|^2 - |t_2|^2 - 2 |t_1 t_2| \operatorname{Re} \{e^{i\beta} M_{ab}\} \quad (4.9)$$

$$p_{aa1,b}^{\leftarrow} = 1 - p_{aa1,b}^{\rightarrow} \quad (4.10)$$

These are also the values of $p_{aa'e,b}^s$ to all orders when $M_{eb} = 1$, but in general $p_{aa'e,b}^s$ does not have such a nice form. As before, the target system collapses onto states with common values of $p_{aa1,b}^{\rightarrow}$, generically producing a density matrix with non-zero elements that correspond to difference charges e with $M_{eb} = 1$ (and $M_{ab} = M_{a'b}$). To first order, the behavior is essentially identical to that of the Mach-Zehnder interferometer which we previously obtained, but the higher order terms may require more stringent conditions for superpositions to survive measurement collapse than just indistinguishability of monodromy scalar components (since this only guarantees proper matching to first order). Specifically, for superpositions of a and a' to survive, they must have

$$\sum_c N_{ab}^c \frac{d_c}{d_a} \left(\frac{\theta_c}{\theta_a} \right)^n = \sum_c N_{a'b}^c \frac{d_c}{d_{a'}} \left(\frac{\theta_c}{\theta_{a'}} \right)^n \quad (4.11)$$

for all n , and some much more cumbersome condition for the survival of coherent superpositions corresponding to difference charge e . However, it seems that this condition is often equivalent to indistinguishability of monodromy scalar components for models of interest. In order to have $p_{aa1,b}^{\leftarrow} = 0$, i.e. producing sometimes perfect distinguishability², we require $|t_1| = |t_2|$ and $\cos[\beta + 2\pi(s_c - s_a - s_b)] = -1$ for all $N_{ab}^c \neq 0$. Using Eq. (3.79), we estimate the number of tunneling events (approximately $N|t|^2$) needed to collapse a superposition of two anyonic charges in the target is on the order of $(\Delta M)^{-2}$.

From the above results, we find that when the target is in a state of definite charge a (or, more exactly, fully collapsed by probe measurements), the longitudinal conductance will be proportional to the probability of the probe injected along the bottom edge to be “detected” exiting along the top edge:

$$G_{xx} \propto p_{aa1,b}^{\leftarrow} \simeq |t_1|^2 + |t_2|^2 + 2|t_1 t_2| \operatorname{Re} \{ e^{i\beta} M_{ab} \} \quad (4.12)$$

which is exactly Eq. (7) in Ref. [105]. This is a readily measurable quantity, found by measuring the voltage between S_{\rightarrow} and D_{\leftarrow} . Using the side gate (G), one can vary

²One can never have *always* perfect distinguishability for this interferometer, since it must be in the weak tunneling limit, which prevents ever having $|t_j|^2 = 1/2$.

β and, from the resulting modulation in the conductance, determine the amplitude of M_{ab} .

Though this interferometer has been examined for the Moore-Read state in previous papers, we will re-examine it here, now also providing the higher order terms, which may be of interest. The anyon model $RR_{2,1}$ describing this state is given in Eq. (5.53). We begin by letting the probe anyon be the fundamental quasihole, which has electric charge $\frac{e}{4}$ and anyon charge $b = (\sigma, [1]_8)$. If the target anyon is composed of an even (possibly negative) number n of such quasiholes, its total anyonic charge will be in some superposition of $a = (I, [n]_8)$ and $(\psi, [n]_8)$. Defining $N_\psi = 0, 1$ depending on whether the Ising charge is I or ψ , respectively, for n even, these give rise to

$$p_{aa1,b}^{\leftarrow} = 1 - \frac{|r_1|^2 |r_2|^2}{\left|1 + (-1)^{N_\psi} |t_1 t_2| e^{i(\beta + n\frac{\pi}{4})}\right|^2} \quad (4.13)$$

$$\simeq |t_1|^2 + |t_2|^2 + (-1)^{N_\psi} 2 |t_1 t_2| \cos\left(\beta + n\frac{\pi}{4}\right). \quad (4.14)$$

The Ising charges I and ψ are in different charge classes when probed by σ , so interferometry will collapse any superposition of them in the target onto a definite charge state of one or the other. If the target anyon is a composite of an odd number n of quasiholes, then its total anyonic charge is $a = (\sigma, [n]_8)$, which gives

$$p_{aa1,b}^{\leftarrow} = 1 - \frac{|r_1|^2 |r_2|^2 (1 + |t_1 t_2|^2)}{\left|1 - (-1)^{\frac{n-1}{2}} |t_1 t_2|^2 e^{i2\beta}\right|^2} \quad (4.15)$$

$$\simeq |t_1|^2 + |t_2|^2 - 2 |t_1 t_2|^2 \left[1 + (-1)^{\frac{n-1}{2}} \cos(2\beta)\right]. \quad (4.16)$$

Of specific note is that for n odd, the interference is suppressed, giving rise to modulations in 2β that are fourth order in t . In fact, higher order harmonics enter as modulations in $2m\beta$ that are $4m^{\text{th}}$ order in t .

If we had sufficiently good precision and control over the experimental variables to set them exactly to $|t_1| = |t_2|$ and $\cos(\beta + n\frac{\pi}{4}) = (-1)^{N_\psi+1}$ for n even, then we would find $p_{aa1,b}^{\leftarrow} = 0$ to all orders (these settings would give $p_{aa1,b}^{\leftarrow} = \frac{4|t_1|^2}{(1+|t_1|^2)^2}$ for the target with the other N_ψ). In this way (or perhaps some other) one may effectively

suppress the tunneling of fundamental quasiholes, and then the next most dominant contribution to tunneling comes from excitations with anyonic charge $b = (I, [2]_8)$, which are Abelian, and give (with different values of T_j)

$$p_{aa1,b}^{\leftarrow} = 1 - \frac{|r_1|^2 |r_2|^2}{\left|1 + |t_1 t_2| e^{i(\beta + n\frac{\pi}{2})}\right|^2} \quad (4.17)$$

$$\simeq |t_1|^2 + |t_2|^2 + 2|t_1 t_2| \cos\left(\beta + n\frac{\pi}{2}\right), \quad (4.18)$$

which is actually the value for these b probes for any n . The Ising charges are obviously indistinguishable when probed by I , so superpositions of I and ψ will not be affected by these probes.

From the anyon model description in Eq. (5.51), we reproduce the results of Ref. [105] for the Read–Rezayi states $\overline{\text{RR}}_{k,M}$ (for FQH states, M should be odd to give a fermionic system), which occur at filling fraction $\nu = \frac{k}{kM+2}$, most likely in the second Landau level. We take the probes to be the fundamental quasiholes, which have electric charge $\frac{e}{kM+2}$ and anyonic charge $b = (\Phi_1^1, [1]_N)$. If the target is composed of n such quasiholes, its total anyonic charge will be in some superposition of the charges $a = (\Phi_n^{\Lambda_n}, [n]_N)$, where $[\Lambda_n + n]_2 = 0$. To leading order, these give rise to

$$p_{aa1,b}^{\leftarrow} \simeq |t_1|^2 + |t_2|^2 + 2|t_1 t_2| \frac{\cos\left(\frac{(\Lambda_n+1)\pi}{k+2}\right)}{\cos\left(\frac{\pi}{k+2}\right)} \cos\left(\beta - n\frac{M\pi}{kM+2}\right). \quad (4.19)$$

Finally, the Read–Rezayi state $\overline{\text{RR}}_{3,1}$ is expected to describe the observed $\nu = \frac{12}{5}$ FQH plateau, so we give its details more explicitly. Its anyon model may be described neatly by a direct product as in Eq. (5.54). The probes are fundamental quasiholes, which have electric charge $\frac{e}{5}$ and anyonic charge $b = (\varepsilon, [1]_{10})$. If the target is composed of n such quasiholes, its total anyonic charge will be in some superposition of the charges $a = (I, [n]_{10})$ and $a = (\varepsilon, [n]_{10})$. Defining $N_\varepsilon = 0, 1$ to indicate whether the $\overline{\text{Fib}}$ charge is I or ε , respectively, to leading order, these give

$$p_{aa1,b}^{\leftarrow} \simeq |t_1|^2 + |t_2|^2 + 2|t_1 t_2| (-\phi^{-2})^{N_\varepsilon} \cos\left(\beta - n\frac{4\pi}{5}\right). \quad (4.20)$$

The $\overline{\text{Fib}}$ charges I and ε are in different charge classes when probed by ε , so interferometry will collapse any superposition of them in the target onto a definite anyonic charge state. By varying β , one can distinguish whether the $\overline{\text{Fib}}$ charge of a target anyon is I or ε , without needing to know the precise value of the phase involved, because the interference fringe amplitude is suppressed by a factor of $\phi^{-2} \approx .38$ for ε . We emphasize that this provides the $\overline{\text{RR}}_{3,1}$ state with a distinct advantage over the Moore-Read state with respect to being able to distinguish the non-Abelian anyonic charges that would be used in these systems as the computational basis states for topological qubits (i.e. I and ψ for $\text{RR}_{2,1}$ vs. I and ε for $\overline{\text{RR}}_{3,1}$).

Chapter 5 Examples

In this chapter, we consider some important examples of anyon models. All of these will have $N_{ab}^c = 0, 1$, so we will drop the fusion/splitting spaces' basis labels (greek indices), with the understanding that any symbol involving a prohibited fusion vertex is set to zero. Also, for these particular models, it is more convenient to label the vacuum charge by 0, (so, we let $1 = 0$). Anyon models are completely specified by their F -symbols and R -symbols, so we will provide these, as well as list some additional important quantities that can be derived from them, for convenience. To relate these examples to interferometry experiments, we also give the corresponding fixed state probabilities p_κ and density matrices ρ_κ^A , as described in Chapter 3.2.

5.1 \mathbb{Z}_N

The (Abelian) \mathbb{Z}_N anyon models [25] have the anyonic charges $\mathcal{C} = \{0, 1, \dots, N - 1\}$, and defining $[a]_N \in \mathcal{C}$ as the least residue of $a \bmod N$, they are described (only writing the bracket $[\]_N$ when the distinction is significant) by:

$\mathbb{Z}_N^{(n)}$ for all N and $n = 0, 1, \dots, N - 1$:

$[a]_N \times [b]_N = [a + b]_N$	
$\left[F_{a+b+c}^{a,b,c} \right]_{a+b,b+c} = 1$	$R_{a+b}^{a,b} = e^{i\frac{2\pi n}{N}ab}$
$S_{a,b} = \frac{1}{\sqrt{N}} e^{i\frac{4\pi n}{N}ab}$	$M_{a,b} = e^{i\frac{4\pi n}{N}ab}$
$d_a = 1$	$\theta_a = e^{i2\pi\frac{n}{N}a^2}$
$c_N^{((N-1)/2)} = N - 1$ (N odd)	$\mathcal{D} = \sqrt{N}$

and

$\mathbb{Z}_N^{(n+\frac{1}{2})}$ for N even, $n = 0, 1, \dots, N-1$:

$[a]_N \times [b]_N = [a+b]_N$	
$\left[F_{a+b+c}^{a,b,c} \right]_{a+b,b+c} = e^{i\frac{\pi}{N}a([b]_N+[c]_N-[b+c]_N)}$	$R_{a+b}^{a,b} = e^{i\frac{2\pi}{N}(n+\frac{1}{2})[a]_N[b]_N}$
$S_{a,b} = \frac{1}{\sqrt{N}} e^{i\frac{4\pi}{N}(n+\frac{1}{2})ab}$	$M_{a,b} = e^{i\frac{4\pi}{N}(n+\frac{1}{2})ab}$
$d_a = 1$	$\theta_a = e^{i2\pi\frac{(2n+1)}{2N}[a]_N^2}$
$c_N^{(N-1)/2} = N-1, \quad c_N^{(1/2)} = 1$	$\mathcal{D} = \sqrt{N}$

In these tables, we have given the central charge $c_N^{(n)}$ only for the values of n which correspond to the $SU(N)_1$ and the $U(1)_{N/2}$ CFTs. For $SU(N)_1$ the corresponding anyon models are $\mathbb{Z}_N^{((N-1)/2)}$ for N odd and $\mathbb{Z}_N^{(N/2-1)}$ for N even. For $U(1)_{N/2}$ it is $\mathbb{Z}_N^{(1/2)}$, with N necessarily even. In general, the central charges of \mathbb{Z}_N theories are integers whenever they are defined (i.e. when the theory is modular). More information on the central charges of theories of type \mathbb{Z}_N may be found in Ref. [25].

Of course, for Abelian anyon models such as these, each physical quasiparticle excitation has a specific anyonic charge and all fusion channels are uniquely determined, so superpositions of anyonic charge are not actually possible, but one may still perform interferometry experiments to determine the charge of a target anyon. Also, such models might occur as a subset of a non-Abelian anyon model, in which case superpositions of these charges could potentially occur. For $\mathbb{Z}_N^{(w)}$ with $w = n$ or $n + \frac{1}{2}$ ¹, using b probes, we have:

$$p_a = p_{aa0,b}^{\rightarrow} = |t_1|^2 |r_2|^2 + 2 |t_1 r_1 t_2 r_2| \cos \left(\theta + \frac{4\pi w}{N} ab \right) + |r_1|^2 |t_2|^2 \quad (5.1)$$

and

$$\text{Pr}_A(\kappa) = \sum_{a \in C_{\kappa}, f} \rho_{(a,f-a;f), (a,f-a;f)} \quad (5.2)$$

$$\rho_{\kappa}^A = \sum_{a, a' \in C_{\kappa}, f} \rho_{(a,f-a;f), (a',f-a';f)} |a, f-a; f\rangle \langle a', f-a'; f| \quad (5.3)$$

¹If we write $w = n$ or $n + \frac{1}{2}$ for $n \notin \{0, 1, \dots, N-1\}$, it should be understood that we really mean $[n]_N$ instead of n .

For $\mathbb{Z}_N^{(n)}$ with N odd and $\gcd(n, N) = 1$ and for $\mathbb{Z}_N^{(n+\frac{1}{2})}$ with N even and $\gcd(2n+1, N) = 1$ (i.e. the modular \mathbb{Z}_N models), the charge classes are singletons $\mathcal{C}_a = \{a\}$, so $a = a'$ in the fixed state density matrices.

5.2 $\mathbf{D}(\mathbb{Z}_N)$

The Abelian anyon models derived from the quantum double $\mathbf{D}(\mathbb{Z}_N)$ of $\mathbb{Z}_N^{(0)}$ describe certain orbifold CFTs [129, 130], topological \mathbb{Z}_N gauge theories [131], and also Kitaev's toric code [62] based on the group \mathbb{Z}_N . These models have the anyonic charges $a \equiv (a_1, a_2)$, with $a_1, a_2 \in \mathbb{Z}_N$. We can think of a_1 and a_2 as \mathbb{Z}_N charge and flux quantum numbers.

$\mathbf{D}(\mathbb{Z}_N)$ for all N

$[a_1, a_2]_N \times [b_1, b_2]_N = [a_1 + b_1, a_2 + b_2]_N$	
$\left[F_{a+b+c}^{a,b,c} \right]_{a+b, b+c} = 1$	$R_{a+b}^{a,b} = e^{i\frac{2\pi}{N}a_1b_2}$
$S_{a,b} = \frac{1}{N}e^{i\frac{2\pi}{N}(a_1b_2+a_2b_1)}$	$M_{a,b} = e^{i\frac{2\pi}{N}(a_1b_2+a_2b_1)}$
$d_a = 1$	$\theta_a = e^{i2\pi\frac{a_1a_2}{N}}$
$c = 0$	$\mathcal{D} = N$

Using b probes, we have:

$$p_a = p_{aa0,b}^{\vec{}} = |t_1|^2 |r_2|^2 + 2 |t_1 r_1 t_2 r_2| \cos \left(\theta + \frac{2\pi}{N}(a_1 b_2 + a_2 b_1) \right) + |r_1|^2 |t_2|^2 \quad (5.4)$$

and

$$\Pr_A(\kappa) = \sum_{a \in \mathcal{C}_{\kappa, f}} \rho_{(a, f-a; f), (a, f-a; f)} \quad (5.5)$$

$$\rho_{\kappa}^A = \sum_{a, a' \in \mathcal{C}_{\kappa, f}} \rho_{(a, f-a; f), (a', f-a'; f)} |a, f-a; f\rangle \langle a', f-a'; f|. \quad (5.6)$$

For these quantum double theories, the charge classes \mathcal{C}_{κ} for any probe b always contain multiple charges a . For example, $M_{a,b} = M_{a',b}$ for $a' = (a_1 + b_1, a_2 - b_2)$. On

the other hand all $D(\mathbb{Z}_N)$ theories are modular, so by using multiple types of probe particles, one may always completely determine the charge of the target.

5.3 $D'(\mathbb{Z}_2)$

The $D'(\mathbb{Z}_2)$ model occurs in the description of the non-Abelian quantum Hall states proposed in Ref. [61]. It is an Abelian anyon model which, like $D(\mathbb{Z}_2)$ has anyonic charges labeled by elements of $\mathbb{Z}_2 \times \mathbb{Z}_2$ and fusion rules given by $\mathbb{Z}_2 \times \mathbb{Z}_2$ group multiplication. It also has the same S -matrix as $D(\mathbb{Z}_2)$.

$D'(\mathbb{Z}_2)$

$[a_1, a_2]_2 \times [b_1, b_2]_2 = [a_1 + b_1, a_2 + b_2]_2$	
$\left[F_{a+b+c}^{a,b,c} \right]_{a+b,b+c} = 1$	$R_{(0,0)}^{(1,0),(1,0)} = R_{(0,0)}^{(0,1),(0,1)} = R_{(0,0)}^{(1,1),(1,1)} = -1,$ $R_{(1,1)}^{(1,0),(0,1)} = R_{(1,0)}^{(0,1),(1,1)} = R_{(0,1)}^{(1,1),(1,0)} = 1$ $R_{(1,1)}^{(0,1),(1,0)} = R_{(1,0)}^{(1,1),(0,1)} = R_{(0,1)}^{(1,0),(1,1)} = -1$
$S_{a,b} = \frac{1}{2} e^{i\pi(a_1 b_2 + a_2 b_1)}$	$M_{a,b} = e^{i\pi(a_1 b_2 + a_2 b_1)}$
$d_a = 1$	$\theta_{(1,0)} = \theta_{(0,1)} = \theta_{(1,1)} = -1$
$c = 4$	$\mathcal{D} = 2$

Using b probes, we have:

$$p_a = p_{aa0,b}^{\rightarrow} = |t_1|^2 |r_2|^2 + 2 |t_1 r_1 t_2 r_2| \cos(\theta + \pi(a_1 b_2 + a_2 b_1)) + |r_1|^2 |t_2|^2 \quad (5.7)$$

and

$$\text{Pr}_A(\kappa) = \sum_{a \in \mathcal{C}_{\kappa,f}} \rho_{(a,f-a;f),(a,f-a;f)} \quad (5.8)$$

$$\rho_{\kappa}^A = \sum_{a,a' \in \mathcal{C}_{\kappa,f}} \rho_{(a,f-a;f),(a',f-a';f)} |a, f-a; f\rangle \langle a', f-a'; f|. \quad (5.9)$$

For this model, the charge classes \mathcal{C}_{κ} for any nontrivial probe b contain two charges. Specifically, given b , $M_{a,b} = M_{a',b}$ for $a' = (a_1 + b_1, a_2 - b_2)$. However, one may

always completely determine the charge of the target using any two different types of nontrivial probes.

5.4 $SU(2)_k$

The $SU(2)_k$ anyon models (for k an integer) are “ q -deformed” versions of the usual $SU(2)$ for $q = e^{i\frac{2\pi}{k+2}}$, which, roughly speaking, means integers n are replaced by $[n]_q \equiv \frac{q^{n/2} - q^{-n/2}}{q^{1/2} - q^{-1/2}}$. These describe $SU(2)_k$ Chern-Simons theories [26] and WZW CFTs [132, 133], and give rise to the Jones polynomials of knot theory [134]. They have the anyonic charges $\mathcal{C} = \{0, \frac{1}{2}, \dots, \frac{k}{2}\}$, and are described by:

$j_1 \times j_2 = \sum_{j= j_1-j_2 }^{\min\{j_1+j_2, k-j_1-j_2\}} j$	
$[F_j^{j_1, j_2, j_3}]_{j_{12}, j_{23}} = (-1)^{j_1+j_2+j_3+j} \sqrt{[2j_{12}+1]_q [2j_{23}+1]_q} \left\{ \begin{matrix} j_1 & j_2 & j_{12} \\ j_3 & j & j_{23} \end{matrix} \right\}_q,$	
$\left\{ \begin{matrix} j_1 & j_2 & j_{12} \\ j_3 & j & j_{23} \end{matrix} \right\}_q = \Delta(j_1, j_2, j_{12}) \Delta(j_{12}, j_3, j) \Delta(j_2, j_3, j_{23}) \Delta(j_1, j_{23}, j)$ $\times \sum_z \left\{ \frac{(-1)^z [z+1]_q!}{[z-j_1-j_2-j_{12}]_q! [z-j_{12}-j_3-j]_q! [z-j_2-j_3-j_{23}]_q! [z-j_1-j_{23}-j]_q!} \right.$ $\left. \times \frac{1}{[j_1+j_2+j_3+j-z]_q! [j_1+j_{12}+j_3+j_{23}-z]_q! [j_2+j_{12}+j+j_{23}-z]_q!} \right\},$	
$\Delta(j_1, j_2, j_3) = \sqrt{\frac{[-j_1+j_2+j_3]_q! [j_1-j_2+j_3]_q! [j_1+j_2-j_3]_q!}{[j_1+j_2+j_3+1]_q!}}, \quad [n]_q! = \prod_{m=1}^n [m]_q$	
$R_j^{j_1, j_2} = (-1)^{j-j_1-j_2} q^{\frac{1}{2}(j(j+1)-j_1(j_1+1)-j_2(j_2+1))}$	
$S_{j_1, j_2} = \sqrt{\frac{2}{k+2}} \sin\left(\frac{(2j_1+1)(2j_2+1)\pi}{k+2}\right)$	$M_{j_1, j_2} = \frac{\sin\left(\frac{(2j_1+1)(2j_2+1)\pi}{k+2}\right) \sin\left(\frac{\pi}{k+2}\right)}{\sin\left(\frac{(2j_1+1)\pi}{k+2}\right) \sin\left(\frac{(2j_2+1)\pi}{k+2}\right)}$
$d_j = \frac{\sin\left(\frac{(2j+1)\pi}{k+2}\right)}{\sin\left(\frac{\pi}{k+2}\right)}$	$\theta_j = e^{i2\pi \frac{j(j+1)}{k+2}}$
$c = \frac{3k}{k+2}$	$\mathcal{D} = \frac{\sqrt{k+2}}{2 \sin\left(\frac{\pi}{k+2}\right)}$

where $\left\{ \begin{matrix} \\ \end{matrix} \right\}_q$ is a “ q -deformed” version of the usual $SU(2)$ $6j$ -symbols. Notice that for k even, the S -matrix always has vanishing elements, e.g. $S_{\frac{1}{2}, \frac{k}{4}} = 0$. Using $b = 1/2$ probes, each anyonic charge is distinguishable by monodromy, forming the singletons

$\mathcal{C}_{2j} = \{j\}$, and so we have

$$p_{2j} = p_{jj0, \frac{1}{2}}^{\rightarrow} = |t_1|^2 |r_2|^2 + 2 |t_1 r_1 t_2 r_2| \frac{\cos\left(\frac{(2j+1)\pi}{k+2}\right)}{\cos\left(\frac{\pi}{k+2}\right)} \cos \theta + |r_1|^2 |t_2|^2 \quad (5.10)$$

$$\Pr_A(2j) = \sum_{f \in \overset{c}{\{j \times c\}}} \rho_{(j,c;f),(j,c;f)} \quad (5.11)$$

$$\rho_{\kappa}^A = \sum_{f, f' \in \overset{c}{\{j \times c\}}} \frac{\rho_{(j,c;f),(j,c;f')}}{\Pr_A(2j) d_j d_c} |j, c; f'\rangle \langle j, c; f| \quad (5.12)$$

5.5 Fib

The Fibonacci (Fib) anyon model (also known as $\text{SO}(3)_3$, since it may be obtained from the $\text{SU}(2)_3$ anyon model by restricting to integer j)² is known to be universal for topological quantum computation [135, 136]. It has two charges $\mathcal{C} = \{0, 1\}$ (these are also often denoted as I and ε , respectively) and is described by (listing only the non-trivial F -symbols and R -symbols, i.e. those not listed are equal to one if their vertices are permitted by fusion, and equal to zero if they are not permitted):

$0 \times 0 = 0, \quad 0 \times 1 = 1, \quad 1 \times 1 = 0 + 1$	
$[F_1^{1,1,1}]_{e,f} = \begin{bmatrix} \phi^{-1} & \phi^{-1/2} \\ \phi^{-1/2} & -\phi^{-1} \end{bmatrix}_{e,f}$	$R_0^{1,1} = e^{-i4\pi/5}, \quad R_1^{1,1} = e^{i3\pi/5}$
$S = \frac{1}{\sqrt{\phi+2}} \begin{bmatrix} 1 & \phi \\ \phi & -1 \end{bmatrix}$	$M = \begin{bmatrix} 1 & 1 \\ 1 & -\phi^{-2} \end{bmatrix}$
$d_0 = 1, \quad d_1 = \phi$	$\theta_0 = 1, \quad \theta_1 = e^{i\frac{4\pi}{5}}$
$c = \frac{14}{5}$	$\mathcal{D} = \sqrt{1 + 2\phi}$

where $\phi = \frac{1+\sqrt{5}}{2}$ is the Golden ratio.

²As a Chern-Simons or WZW theory, this is properly denoted as $(G_2)_1$, since $\text{SO}(3)_k$ is only allowed for $k = 0 \pmod{4}$.

For $b = 1$ probes, we have $\mathcal{C}_1 = \{0\}$, $\mathcal{C}_2 = \{1\}$ and

$$p_1 = p_{000,1}^{\vec{}} = |t_1|^2 |r_2|^2 + 2\text{Re} \{t_1 r_1^* r_2^* t_2^* e^{i(\theta_I - \theta_{II})}\} + |r_1|^2 |t_2|^2 \quad (5.13)$$

$$p_2 = p_{110,1}^{\vec{}} = |t_1|^2 |r_2|^2 - 2\phi^{-2} \text{Re} \{t_1 r_1^* r_2^* t_2^* e^{i(\theta_I - \theta_{II})}\} + |r_1|^2 |t_2|^2 \quad (5.14)$$

$$\text{Pr}_A(1) = \sum_c \rho_{(0,c;c),(0,c;c)} \quad (5.15)$$

$$\rho_1^A = \sum_c \frac{\rho_{(0,c;c),(0,c;c)}}{\text{Pr}_A(1)} |0, c; c\rangle \langle 0, c; c| \quad (5.16)$$

$$= \frac{1}{\text{Pr}_A(1)} \left\{ \rho_{(0,0;0),(0,0;0)} |0, 0; 0\rangle \langle 0, 0; 0| \right. \\ \left. + \phi^{-1} \rho_{(0,1;1),(0,1;1)} |0, 1; 1\rangle \langle 0, 1; 1| \right\} \quad (5.17)$$

$$\text{Pr}_A(2) = \sum_{c,f} \rho_{(1,c;f),(1,c;f)} = \rho_{(1,0;1),(1,0;1)} + \rho_{(1,1;0),(1,1;0)} + \rho_{(1,1;1),(1,1;1)} \quad (5.18)$$

$$\rho_2^A = \sum_{c,f,f'} \frac{\rho_{(1,c;f),(1,c;f)}}{\text{Pr}_A(2)} |1, c; f'\rangle \langle 1, c; f'| \quad (5.19)$$

$$= \frac{1}{\text{Pr}_A(2)} \left\{ \phi^{-1} \rho_{(1,0;1),(1,0;1)} |1, 0; 1\rangle \langle 1, 0; 1| \right. \\ \left. + \phi^{-2} (\rho_{(1,1;0),(1,1;0)} + \rho_{(1,1;1),(1,1;1)}) \right. \\ \left. \times [|1, 1; 0\rangle \langle 1, 1; 0| + |1, 1; 1\rangle \langle 1, 1; 1|] \right\} \quad (5.20)$$

We note that one can sometimes (approximately 69% of the time, when the target charge is not vacuum) perfectly distinguish the charges 0 and 1 with a single $b = 1$ probe measurement by setting the experimental parameters to: $|t_1|^2 = |t_2|^2 = 1/2$ and $\theta = \pi$, which give $p_1 = 0$ and $p_2 = 1 - \frac{1}{2\phi} \simeq .69$.

5.6 Ising

The Ising anyon model, which is derived from the CFT that describes the Ising model at criticality [25], is closely related to $\text{SU}(2)_2$, so we use the charge labels 0, $\frac{1}{2}$, and 1 (which are respectively I , σ , and ψ in the conventional Ising model notation). It is

described by (listing only the non-trivial F s and R s):

$0 \times a = a, \quad \frac{1}{2} \times \frac{1}{2} = 0 + 1, \quad \frac{1}{2} \times 1 = \frac{1}{2}, \quad 1 \times 1 = 0$	
$\left[F_{\frac{1}{2}}^{\frac{1}{2}, \frac{1}{2}, \frac{1}{2}} \right]_{e,f} = \begin{bmatrix} \frac{1}{\sqrt{2}} & \frac{1}{\sqrt{2}} \\ \frac{1}{\sqrt{2}} & -\frac{1}{\sqrt{2}} \end{bmatrix}_{e,f}$	$R_0^{\frac{1}{2}, \frac{1}{2}} = e^{-i\frac{\pi}{8}}, \quad R_1^{\frac{1}{2}, \frac{1}{2}} = e^{i\frac{3\pi}{8}}$
$\left[F_1^{\frac{1}{2}, 1, \frac{1}{2}} \right]_{\frac{1}{2}, \frac{1}{2}} = \left[F_{\frac{1}{2}}^{1, \frac{1}{2}, 1} \right]_{\frac{1}{2}, \frac{1}{2}} = -1$	$R_{\frac{1}{2}}^{\frac{1}{2}, 1} = R_{\frac{1}{2}}^{1, \frac{1}{2}} = e^{-i\frac{\pi}{2}}, \quad R_0^{1, 1} = -1$
$S = \frac{1}{2} \begin{bmatrix} 1 & \sqrt{2} & 1 \\ \sqrt{2} & 0 & -\sqrt{2} \\ 1 & -\sqrt{2} & 1 \end{bmatrix}$	$M = \begin{bmatrix} 1 & 1 & 1 \\ 1 & 0 & -1 \\ 1 & -1 & 1 \end{bmatrix}$
$d_0 = d_1 = 1, \quad d_{\frac{1}{2}} = \sqrt{2}$	$\theta_0 = 1, \quad \theta_{\frac{1}{2}} = e^{i\frac{\pi}{8}}, \quad \theta_1 = -1$
$c = \frac{1}{2}$	$\mathcal{D} = 2$

where $e, f \in \{0, 1\}$.

For $b = 1$ probes, we have $\mathcal{C}_1 = \{0, 1\}$, $\mathcal{C}_2 = \{\frac{1}{2}\}$, and define $\mathcal{C}_\Delta = (\mathcal{C}_1 \times \mathcal{C}_1) \cup (\mathcal{C}_2 \times \mathcal{C}_2)$, to give us

$$\begin{aligned} p_1 &= p_{000,1}^{\vec{}} = p_{110,1}^{\vec{}} = p_{011,1}^{\vec{}} = p_{101,1}^{\vec{}} \\ &= |t_1|^2 |r_2|^2 + 2 |t_1 r_1 r_2 t_2| \cos \theta + |r_1|^2 |t_2|^2 \end{aligned} \quad (5.21)$$

$$p_2 = p_{\frac{1}{2}\frac{1}{2}0,1}^{\vec{}} = p_{\frac{1}{2}\frac{1}{2}1,1}^{\vec{}} = |t_1|^2 |r_2|^2 - 2 |t_1 r_1 r_2 t_2| \cos \theta + |r_1|^2 |t_2|^2 \quad (5.22)$$

$$\Pr_A(1) = \sum_c [\rho_{(0,c;c),(0,c;c)} + \rho_{(1,c;1-c),(1,c;1-c)}] \quad (5.23)$$

$$\rho_1^A = \sum_{\substack{a, a' \in \mathcal{C}_1 \\ (c, c') \in \mathcal{C}_\Delta \\ f \in \{a \times c\}}} \frac{\rho_{(a,c;f),(a',c';f)}}{\Pr_A(1) d_f} |a, c; f\rangle \langle a', c'; f| \quad (5.24)$$

$$\text{Pr}_A(2) = \sum_{\substack{c \\ f \in \{\frac{1}{2} \times c\}}} \rho_{(\frac{1}{2}, c; f), (\frac{1}{2}, c; f)} \quad (5.25)$$

$$\rho_2^A = \sum_{\substack{(c, c') \in \mathcal{C}_\Delta \\ f \in \{\frac{1}{2} \times c\}}} \frac{\rho_{(\frac{1}{2}, c; f), (\frac{1}{2}, c'; f)}}{\text{Pr}_A(2) d_f} \left| \frac{1}{2}, c; f \right\rangle \left\langle \frac{1}{2}, c'; f \right| \quad (5.26)$$

For $b = \frac{1}{2}$ probes, we have $\mathcal{C}_1 = \{0\}$, $\mathcal{C}_2 = \{\frac{1}{2}\}$, $\mathcal{C}_3 = \{1\}$, and

$$p_1 = p_{000, \frac{1}{2}}^{\vec{}} = |t_1|^2 |r_2|^2 + 2 |t_1 r_1 r_2 t_2| \cos \theta + |r_1|^2 |t_2|^2 \quad (5.27)$$

$$p_2 = p_{\frac{1}{2} \frac{1}{2} 0, \frac{1}{2}}^{\vec{}} = |t_1|^2 |r_2|^2 + |r_1|^2 |t_2|^2 \quad (5.28)$$

$$p_3 = p_{110, \frac{1}{2}}^{\vec{}} = |t_1|^2 |r_2|^2 - 2 |t_1 r_1 r_2 t_2| \cos \theta + |r_1|^2 |t_2|^2 \quad (5.29)$$

$$\text{Pr}_A(1) = \sum_c \rho_{(0, c; c), (0, c; c)} \quad (5.30)$$

$$\rho_1^A = \sum_c \frac{\rho_{(0, c; c), (0, c; c)}}{\text{Pr}_A(1) d_c} |0, c; c\rangle \langle 0, c; c| \quad (5.31)$$

$$\text{Pr}_A(2) = \sum_{\substack{c \\ f \in \{\frac{1}{2} \times c\}}} \rho_{(\frac{1}{2}, c; f), (\frac{1}{2}, c; f)} \quad (5.32)$$

$$\rho_2^A = \sum_{\substack{c \\ f, f' \in \{\frac{1}{2} \times c\}}} \frac{\rho_{(\frac{1}{2}, c; f), (\frac{1}{2}, c; f')}}{\text{Pr}_A(2) d_{\frac{1}{2}} d_c} \left| \frac{1}{2}, c; f' \right\rangle \left\langle \frac{1}{2}, c; f \right| \quad (5.33)$$

$$\begin{aligned} &= \frac{1}{\text{Pr}_A(2)} \left\{ \frac{1}{\sqrt{2}} \rho_{(\frac{1}{2}, 0; \frac{1}{2}), (\frac{1}{2}, 0; \frac{1}{2})} \left| \frac{1}{2}, 0; \frac{1}{2} \right\rangle \left\langle \frac{1}{2}, 0; \frac{1}{2} \right| \right. \\ &\quad + \frac{1}{\sqrt{2}} \rho_{(\frac{1}{2}, 1; \frac{1}{2}), (\frac{1}{2}, 1; \frac{1}{2})} \left| \frac{1}{2}, 1; \frac{1}{2} \right\rangle \left\langle \frac{1}{2}, 1; \frac{1}{2} \right| \\ &\quad + \frac{1}{2} \left(\rho_{(\frac{1}{2}, \frac{1}{2}; 0), (\frac{1}{2}, \frac{1}{2}; 0)} + \rho_{(\frac{1}{2}, \frac{1}{2}; 1), (\frac{1}{2}, \frac{1}{2}; 1)} \right) \\ &\quad \left. \times \left[\left| \frac{1}{2}, \frac{1}{2}; 0 \right\rangle \left\langle \frac{1}{2}, \frac{1}{2}; 0 \right| + \left| \frac{1}{2}, \frac{1}{2}; 1 \right\rangle \left\langle \frac{1}{2}, \frac{1}{2}; 1 \right| \right] \right\} \quad (5.34) \end{aligned}$$

$$\Pr_A(3) = \sum_c \rho_{(1,c;1-c),(1,c;1-c)} \quad (5.35)$$

$$\rho_3^A = \sum_c \frac{\rho_{(1,c;1-c),(1,c;1-c)}}{\Pr_A(3) d_c} |1, c; 1 - c\rangle \langle 1, c; 1 - c| \quad (5.36)$$

We note that one can always perfectly distinguish the charges 0 and 1 with a single $b = \frac{1}{2}$ probe measurement by setting the experimental parameters such that $|t_1|^2 = |t_2|^2 = 1/2$ and $\theta = \pi$, which give $p_1 = 0$ and $p_3 = 1$.

5.7 Constructing New Models from Old

Given some known anyon models \mathcal{A} , \mathcal{A}_1 , and \mathcal{A}_2 , there are several ways to construct new anyon models from them. We will briefly describe a few of these here:

(i) By applying charge conjugation C to \mathcal{A} , we obtain the theory \mathcal{A}^C defined by making the replacements

$$[F_d^{abc}]_{(e,\alpha,\beta)(f,\mu,\nu)}^C = [F_{\bar{d}}^{\bar{a}\bar{b}\bar{c}}]_{(\bar{e},\alpha,\beta)(\bar{f},\mu,\nu)} \quad (5.37)$$

$$[R_c^{ab}]_{\mu\nu}^C = [R_{\bar{c}}^{\bar{a}\bar{b}}]_{\mu\nu}. \quad (5.38)$$

(ii) By applying parity P to \mathcal{A} , we obtain the theory \mathcal{A}^P defined by making the replacements

$$[R_c^{ab}]_{\mu\nu}^P = [(R_c^{ba})^{-1}]_{\mu\nu}. \quad (5.39)$$

(iii) By applying time reversal T to \mathcal{A} , we obtain the theory \mathcal{A}^T (often denoted in the literature as \mathcal{A}^{-1} or $\overline{\mathcal{A}}$) defined by making the replacements

$$[F_d^{abc}]_{(e,\alpha,\beta)(f,\mu,\nu)}^T = [(F_d^{abc})^{-1}]_{(f,\mu,\nu)(e,\alpha,\beta)} \quad (5.40)$$

$$[R_c^{ab}]_{\mu\nu}^T = [(R_c^{ab})^{-1}]_{\nu\mu}. \quad (5.41)$$

We note that this also gives $M_{ab}^T = M_{ab}^*$.

Note: The models obtained by applying constructions (i), (ii), and (iii) are not necessarily distinct from each other, and in fact sometimes not even distinct from the

original anyon model. In particular, it is often true that the F -symbols are real and $R_c^{ab} = R_c^{ba}$ (at least in some preferred gauge) for examples of interest, e.g. Chern-Simons theories and all the examples given above, except $D(\mathbb{Z}_N)$ and $D'(\mathbb{Z}_2)$, in which case $\mathcal{A}^P = \mathcal{A}^T$ and the model is invariant under PT .

(iv) If the label set \mathcal{C} of \mathcal{A} has a proper subset \mathcal{C}' that gives a closed fusion subalgebra, then the restriction $\mathcal{A}|_{\mathcal{C}'}$ to this subset of charges is a subcategory of \mathcal{A} , and, hence, also an anyon model. We note that M_{ab} of $\mathcal{A}|_{\mathcal{C}'}$ is simply given by M_{ab} of \mathcal{A} restricted to the charges \mathcal{C}' .

(v) A direct product $\mathcal{A}_1 \times \mathcal{A}_2$ of anyon models is an anyon model, defined, with charge and basis labels $a = (a_1, a_2)$ and $\mu = (\mu_1, \mu_2)$, by

$$N_{ab}^c = N_{a_1 b_1}^{c_1} N_{a_2 b_2}^{c_2} \quad (5.42)$$

$$[F_d^{abc}]_{(e, \alpha, \beta)(f, \mu, \nu)} = [F_{d_1}^{a_1 b_1 c_1}]_{(e_1, \alpha_1, \beta_1)(f_1, \mu_1, \nu_1)} [F_{d_2}^{a_2 b_2 c_2}]_{(e_2, \alpha_2, \beta_2)(f_2, \mu_2, \nu_2)} \quad (5.43)$$

$$[R_c^{ab}]_{\mu\nu} = [R_{c_1}^{a_1 b_1}]_{\mu_1 \nu_1} [R_{c_2}^{a_2 b_2}]_{\mu_2 \nu_2} . \quad (5.44)$$

We note that $M_{ab} = M_{a_1 b_1} M_{a_2 b_2}$.

(vi) If an anyon model \mathcal{A} has an Abelian subcategory \mathcal{Z} (the “extending fields” in CFT) such that

$$\begin{aligned} [F_d^{abc}]_{(e, \alpha, \beta)(f, \mu, \nu)} &= [F_{(d \times z)}^{(a \times z)bc}]_{((e \times z), \alpha, \beta)(f, \mu, \nu)} \\ &= [F_{(d \times z)}^{a(b \times z)c}]_{((e \times z), \alpha, \beta)((f \times z), \mu, \nu)} = [F_{(d \times z)}^{ab(c \times z)}]_{(e, \alpha, \beta)((f \times z), \mu, \nu)} \end{aligned} \quad (5.45)$$

and

$$[R_c^{ab}]_{\mu\nu} = [R_{(c \times z)}^{(a \times z)b}]_{\mu\nu} = [R_{(c \times z)}^{a(b \times z)}]_{\mu\nu} \quad (5.46)$$

for all $z \in \mathcal{C}_{\mathcal{Z}}$, and all $a, b, c, d, e, f \in \mathcal{C}$ (this also requires a cooperative choice of gauge to work), then identifying charges into the equivalence classes $\langle a \rangle = \{a \times z : z \in \mathcal{C}_{\mathcal{Z}}\}$

and defining

$$N_{\langle a \rangle \langle b \rangle}^{\langle c \rangle} \equiv N_{ab}^c \quad (5.47)$$

$$\left[F_{\langle d \rangle}^{\langle a \rangle \langle b \rangle \langle c \rangle} \right]_{((e), \alpha, \beta) \langle f \rangle, \mu, \nu} \equiv \left[F_d^{abc} \right]_{(e, \alpha, \beta) \langle f \rangle, \mu, \nu} \quad (5.48)$$

$$\left[R_{\langle c \rangle}^{\langle a \rangle \langle b \rangle} \right]_{\mu\nu} \equiv \left[R_c^{ab} \right]_{\mu\nu} \quad (5.49)$$

for representative charges on the right hand sides that give non-zero symbols if such exist (otherwise the symbol is defined to be zero) defines a reduced anyon model $\langle \mathcal{A} \rangle$. We note that $M_{ab} = M_{\langle a \rangle \langle b \rangle}$.

For many coset conformal field theories, one may describe the associated anyon model by application of identification to a subset of a product theory [i.e. using (iv), (v), and (vi)] [137, 138]. For a G/H coset, one first forms the product $\mathcal{A} \times \mathcal{B}^{-1}$, where \mathcal{A} and \mathcal{B} are anyon models corresponding to the G and H WZW-theories. Then, one takes a subset of this product to implement the branching rules of the coset. Finally, one identifies modulo some simple currents (the ‘‘identification currents’’) that may exist and this should take care of the field identifications of the coset. This procedure does not work for all cosets (e.g. it fails for conformal embeddings and maverick cosets), but it works for the ones we will consider.

Here are some interesting and/or useful examples of relations that employ these constructions:

(a) $\mathbb{Z}_N^{(w)T} = \mathbb{Z}_N^{(-w)}$ for $w = n$ or $n + \frac{1}{2}$.

(b) $\mathbb{Z}_{2m}^{(n)} = \mathbb{Z}_m^{(2n)} \times \mathbb{Z}_2^{(n)}$ and $\mathbb{Z}_{2m}^{(n+\frac{1}{2})} = \mathbb{Z}_m^{(2n+1)} \times \mathbb{Z}_2^{(i^{(2n+1)m-1}/2)}$ for m odd, via the isomorphism:

$$[a]_{2m} \mapsto \left(\left[\frac{a + m [a]_2}{2} \right]_m, [a]_2 \right)$$

(a change of gauge is needed to see this from the description of $\mathbb{Z}_{2m}^{(n+\frac{1}{2})}$ given in Chapter 5.1).

(c) $\mathbb{Z}_m^{(2n)} = \mathbb{Z}_m^{((m+n)/2)}$ for m and n odd, via the isomorphism: $[a]_m \mapsto [2a]_m$.

(d) $\text{SO}(3)_k = \text{SU}(2)_k|_{\mathcal{C}'}$ where $\mathcal{C}' = \{0, 1, \dots, \lfloor \frac{k}{2} \rfloor\}$.

(e) $SU(2)_k = SO(3)_k \times \mathbb{Z}_2^{(i^{k-1}/2)}$ for k odd, via the isomorphism:

$$j \mapsto \begin{cases} (j, [0]_2) & \text{for } 2j \text{ even} \\ (\frac{k}{2} - j, [1]_2) & \text{for } 2j \text{ odd} \end{cases}$$

(a change of gauge is needed to see this from the description of $SU(2)_k$ given in Chapter 5.4; in particular, the gauge transformation specified by: $u_{\frac{k}{2}-j_1, j_2}^{\frac{k}{2}-j_1, j_2} = (-i)^{j_1-j} (-1)^{j_2}$, $u_{\frac{k}{2}-j}^{j_1, \frac{k}{2}-j_2} = i^{j_2-j} (-1)^{j_1}$, and $u_j^{\frac{k}{2}-j_1, \frac{k}{2}-j_2} = i^{j_1-j_2} (-1)^j$, for integer j_1, j_2 , and j makes this property manifest).

(f) The \mathbb{Z}_k -Parafermion model [139, 140] is a CFT described by the coset $SU(2)_k/U(1)_k$. The corresponding anyon model is

$$\begin{aligned} \text{Pf}_k &= \left\langle SU(2)_k \times \mathbb{Z}_{2k}^{(-1/2)} \Big|_{\mathcal{C}'} \right\rangle \\ \mathcal{C}' &= \{(j, [m]_{2k}) : [2j + m]_2 = 0\} \\ \mathcal{C}_{\mathcal{Z}} &= \left\{ (0, [0]_{2k}), \left(\frac{k}{2}, [k]_{2k} \right) \right\} \end{aligned} \quad (5.50)$$

(i.e. $\mathcal{Z} = \mathbb{Z}_2^{(0)}$). The Pf_k fields are conventionally written as Φ_λ^Λ where $\Lambda = 2j$ and $\lambda = m$ (and thus have the restriction $[\Lambda + \lambda]_2 = 0$ and field identifications $\Phi_\lambda^\Lambda = \Phi_{\lambda+2k}^\Lambda = \Phi_{\lambda+k}^{k-\Lambda}$). The previously alluded to relation between Ising and $SU(2)_2$ is precisely given by $\text{Pf}_2 = \text{Ising}$. For k odd, one can show [141], using (b) and (e), that this results in the direct product $\text{Pf}_k = SO(3)_k \times \mathbb{Z}_k^{(-1)}$.

5.8 Anyon Models in the Physical World

The best hope for finding anyons in physical systems lies in the fractional quantum Hall effect; therefore, in this section, we describe the anyon models corresponding to the leading candidates states for experimentally observed filling fractions. However, before proceeding, we would like to say a few things about the \mathbb{Z}_N models and their relation to $U(1)$ Chern-Simons theory and CFT. For N an integer, the $U(1)_N$ Chern-Simons theory [142, 143, 144, 26] is related to a chiral CFT which is called the

“rational torus”. This is a CFT with one scalar field φ which takes its values on a circle of radius $\sqrt{2N}$. This theory has $2N$ primary fields V_a ($a = 0, \dots, 2N - 1$) with conformal weights $h_a = \frac{a^2}{4N}$, given by $V_a = e^{i2\pi a\varphi/\sqrt{2N}}$. The anyon model corresponding to this theory is $\mathbb{Z}_{2N}^{(1/2)}$. If we were to forget about taking the least residue mod $2N$ in these models, we would find the charge $a = 2N$ which is a boson (i.e. $R^{aa} = 1$) and which (in an appropriately chosen gauge) has trivial monodromy with all other fields, so we could perform an identification with $\mathcal{Z} = \{2mN : m \in \mathbb{Z}\}$ to reobtain $\mathbb{Z}_{2N}^{(1/2)}$. For $N = m/2$ with m odd, one can still have a $U(1)_N$ theory, however, there is some additional subtlety. The “extending field” $a = 2N = m$ that one would normally identify with the vacuum in this case is a fermion, so to describe it by a \mathbb{Z}_m anyon model, one must introduce spin structures on the spacetime manifold and augment the chiral current algebra to a \mathbb{Z}_2 -graded chiral current superalgebra [145] (in CFT, the fermion becomes a descendant field in the vacuum sector). However, since these fermions can actually be created and manipulated in manners that expose their fermionic nature, it is more accurate to describe $U(1)_N$ for $N = m/2$ with m odd by the anyon model $\mathbb{Z}_{2m}^{(1)} = \mathbb{Z}_m^{(2)} \times \mathbb{Z}_2^{(1)}$, which is not modular. More generally, for systems with fermions that have trivial monodromy with all other anyons (e.g. any fractional quantum Hall system), there will always be a similar sort of \mathbb{Z}_2 -grading. However, it does not always manifest as the anyon model simply being a product of some anyon model with a $\mathbb{Z}_2^{(1)}$, and, in fact, it is sometimes not even possible to produce an anyon model for the fusion rule where the fermion (electron) has been identified with the vacuum, as we will show in Appendix A.1.25.

The Abelian fractional quantum Hall states can all be constructed from \mathbb{Z}_N models. The general formulation in terms of K matrices may be found in Ref. [146], but we will describe the Laughlin and hierarchy states [48, 147, 148, 149] that occur at filling fractions $\nu = \frac{n}{m}$ (m odd and $n < m$). As shown in Ref. [47], the statistical factor of the quasihole in these states is $\theta = \frac{\pi p}{m}$ where p is odd and $np \equiv 1 \pmod{m}$ (which uniquely defines p modulo $2m$). It follows that these states are described by $\mathbb{Z}_{2m}^{(p)} = \mathbb{Z}_m^{(2p)} \times \mathbb{Z}_2^{(1)}$, where a fundamental quasihole has anyonic charge $[1]_{2m}$ and electric charge $\frac{e}{m}$, and an electron has anyonic charge $[m]_{2m}$ (and electric charge $-e$).

Apart from these fractional quantum Hall states described by Abelian anyon models, there are also believed to be a number of quantum Hall plateaus which host non-Abelian anyons. These are more interesting from the point of view of measurement theory and also for possible applications to quantum computing, since they would allow for superpositions of different overall anyonic charges on clusters of quasiholes. There is an important point to keep in mind when considering such superpositions for non-Abelian FQH states, which is that the anyonic charge is coupled to the electric charge, and consequently some superpositions of anyonic charge may be prohibited by superselection of electric charge.

The Read-Rezayi states [53] (which include the Moore-Read state) for filling fraction $\nu = \frac{k}{kM+2}$ are the most prominent series of Hall states with non-Abelian anyons (for FQH, M should be odd to give a fermionic system). They are formed by combining Pf_k with $U(1)_{k(kM+2)/2}$ in the following manner

$$\begin{aligned} \text{RR}_{k,M} &= \left\langle \text{Pf}_k \times \mathbb{Z}_N^{(1/2)} \Big|_{\mathcal{C}'} \right\rangle \\ \mathcal{C}' &= \{(\Phi_\lambda^\Lambda, [\lambda]_N) : [\Lambda + \lambda]_2 = 0\} \\ \mathcal{Z} &= \{(\Phi_0^0, [0]_N), (\Phi_4^0, [2(kM+2)]_N)\} \end{aligned} \quad (5.51)$$

where $N = 2k(kM+2)$ if k and M are odd, and $N = k(kM+2)$ otherwise. The fundamental quasihole has anyonic charge $(\Phi_1^1, [1]_N)$ and electric charge $\frac{e}{kM+2}$. The electron has anyonic charge $(\Phi_{kM+2}^k, [kM+2]_N)$. When k and M are odd, one can show [141], using (b) and (f) from Chapter 5.7, that this results in the direct product

$$\begin{aligned} \text{RR}_{k,M} &= \text{SO}(3)_k \times \mathbb{Z}_{2(kM+2)}^{((k(kM+2)-M)/2)} \\ &= \text{SO}(3)_k \times \mathbb{Z}_{kM+2}^{(k(kM+2)-M)} \times \mathbb{Z}_2^{(1)}. \end{aligned} \quad (5.52)$$

In addition to the Read-Rezayi states there are a number of other proposed series of non-Abelian quantum Hall states. This includes the non-Abelian spin singlet (NASS) states for filling fractions $\nu = \frac{2k}{2kM+3}$, proposed in Ref. [61]. These states are based on the parafermionic CFTs constructed as $SU(3)_k/(U(1) \times U(1))$ cosets [150]. To generate

the FQH states, these cosets are then combined with two $U(1)$ factors that respectively account for the electric charge and spin quantum numbers of the quasiholes.

We now focus more on three specific proposed non-Abelian FQH states, since they correspond to observed filling fractions. The Moore-Read state ($MR = RR_{2,1}$) [47] is the expected description for the plateaus at $\nu = \frac{5}{2}$ and $\frac{7}{2}$, and currently represents the best hope for discovering non-Abelian statistics. Its corresponding anyon model is

$$\begin{aligned} RR_{2,1} &= \text{Ising} \times \mathbb{Z}_8^{(1/2)} \Big|_{\mathcal{C}'} \\ \mathcal{C}' &= \{(I, [2n]_8), (\sigma, [2n+1]_8), (\psi, [2n]_8)\} \end{aligned} \quad (5.53)$$

(for $n \in \mathbb{Z}$). The fundamental quasihole has anyonic charge $(\sigma, [1]_8)$ and electric charge $\frac{e}{4}$. The electron has anyonic charge $(\psi, [4]_8)$.

The Read-Rezayi state expected to describe the $\nu = \frac{12}{5}$ plateau is $\overline{RR}_{3,1}$, the particle-hole conjugate (i.e. parity or time reversal) of

$$RR_{3,1} = \text{Fib} \times \mathbb{Z}_{10}^{(7)} = \text{Fib} \times \mathbb{Z}_5^{(1)} \times \mathbb{Z}_2^{(1)}. \quad (5.54)$$

The fundamental quasihole has anyonic charge $(\varepsilon, [1]_{10})$ and electric charge $\frac{e}{5}$. The electron has anyonic charge $(I, [5]_{10})$. Being a direct product of Fib and an Abelian theory, universal topological quantum computation could be achieved through braiding quasiholes of this system.

The first fermionic non-Abelian state ($k = 2, M = 1$) in the NASS series is a candidate for the FQH plateau observed at $\nu = \frac{4}{7}$. For $k = 2$, the parafermionic coset $SU(3)_k / (U(1) \times U(1))$ is equal to $\text{Fib}^{-1} \times D'(\mathbb{Z}_2)$. Hence, the anyon model that describes the resulting NASS state is a subcategory of $\text{Fib}^{-1} \times D'(\mathbb{Z}_2) \times \mathbb{Z}_{28}^{(1/2)} \times \mathbb{Z}_4^{(1/2)}$ (the \mathbb{Z}_{28} factor is for the electric charge and the \mathbb{Z}_4 factor for the spin). The electrons in this state have anyonic charges $(I, ([1]_2, [0]_2), [7]_{28}, [1]_4)$ and $(I, ([0]_2, [1]_2), [7]_{28}, [-1]_4)$ for those with spin up and spin down, respectively. The two quasiholes with minimal electric charge $\frac{e}{7}$ form a spin doublet, and their anyonic charges are $(\varepsilon, ([0]_2, [1]_2), [1]_{28}, [1]_4)$

for spin up, and $(\varepsilon, ([1]_2, [0]_2), [1]_{28}, [-1]_4)$ for spin down. The quasihole with minimal scaling dimension (which dominates weak tunneling currents) is spinless and has anyonic charge $(\varepsilon, ([1]_2, [1]_2), [2]_{28}, [0]_4)$ and electric charge $\frac{2\varepsilon}{7}$. It may be formed by combining a spin up and a spin down quasihole. Though we will not write them explicitly, the restricted charge set \mathcal{C}' is that generated by the minimal charge quasiholes, and the identification set \mathcal{C}_Z is given by the anyonic charges of all pairs of electrons. Since the quasiholes of this anyon model carry a nontrivial Fib charge, this state also would allow for universal topological quantum computation by braiding quasiholes.

Appendix A Tabulating Anyon Models

A.1 Key to the Tables

In this appendix, we tabulate a number of gauge invariant quantities for a list of anyon models (UBTCs)¹ that we have found using the Pentagon and Hexagon solving program described in Chapter 2.5. This list includes:

(i) All multiplicity-free anyon models with 4, or fewer, particle types. In particular, these include all modular anyon models with up to 4 particle types (and arbitrary fusion multiplicities), as indicated by the TQFT “periodic table” of Ref. [151].

(ii) All multiplicity-free anyon models with 5 and 6 particle types with fusion rules that permit modular solutions and have no fusions with more than 4 channels. These fusion rules are contained in the list given in Ref. [152] of fusion rules with up to 6 particle types (and limited fusion multiplicity) that can give rise to modular tensor categories.

(iii) Anyon models for several additional fusion rules that are relevant for proposed non-Abelian quantum Hall states.

While we have calculated full solutions to the Pentagon and Hexagon solutions for the anyon models listed, we will not tabulate their F -symbols and R -symbols, since most of these are not gauge invariant and they would take excessive space. Instead, we have used them to calculate a number of characteristic and physically interesting gauge invariant quantities for these anyon models. In particular, for every theory we give the central charge c , total quantum dimension \mathcal{D} and a CFT or Chern-Simons theory that realizes that theory or its image under parity reversal. For each particle type ψ in these models, we give the quantum dimension d_ψ , the topological spin θ_ψ and the Frobenius-Schur indicator κ_ψ . In most cases, we also give the topological S -matrix

¹In a forthcoming paper [141], we will also include non-unitary braided tensor categories that are modular. We caution the reader that some of the formulae in this section are only true for unitary theories.

(though it can always be calculated from the other data). Since we already gave the analytic expressions of these quantities (as well as the F -symbols and R -symbols) for the \mathbb{Z}_N , $D(\mathbb{Z}_N)$, $D'(\mathbb{Z}_2)$, $SU(2)_N$, Fib, and Ising anyon models in Chapter 5, when these appear we will refrain from giving full tables and instead refer back their analytic expressions. The list of anyon models are ordered by the number of particles types, and then by their fusion rules. We now give some details on how the data in the tables are calculated from the F -symbols and R -symbols, and on the conventions used in the tables.

From the F -symbols alone we can calculate the quantum dimensions of the particles and their Frobenius-Schur indicators. We have

$$d_\psi = \frac{1}{\sqrt{\left[F_\psi^{\psi\bar{\psi}\psi} \right]_{1,1} \left[F_{\bar{\psi}}^{\bar{\psi}\psi\bar{\psi}} \right]_{1,1}}} \quad (\text{A.1})$$

$$\kappa_\psi = \begin{cases} \left[F_\psi^{\psi\psi\psi} \right]_{1,1} d_\psi & (\psi = \bar{\psi}) \\ 0 & (\psi \neq \bar{\psi}) \end{cases} \quad (\text{A.2})$$

The Frobenius-Schur indicator only has a gauge invariant meaning for self dual particles, and it is conventional to set it to zero for other particles. When $\psi = \bar{\psi}$, we have $\kappa_\psi = \varkappa_\psi = \pm 1$, where \varkappa_ψ is the phase introduced in Eq. (2.23). Given the quantum dimensions of the particle types, we can also calculate the total quantum dimension

$$\mathcal{D} = \sqrt{\sum_i d_i^2}. \quad (\text{A.3})$$

More exotic quantities that we can calculate from the F -symbols are the Frobenius-Schur indicators for a vertices. If $\bar{\psi} \in \{\psi \times \psi\}$, then there is a map from the corresponding splitting vertex space to itself given by clockwise $2\pi/3$ rotation, i.e. by bending the top right leg down to the right and the bottom leg up to the left. The eigenvalue $\kappa_{\bar{\psi}}^{\psi\psi}$ of this map is a third root of unity called the Frobenius-Schur indicator

of the trivalent vertex, and it is given by

$$\kappa_{\psi}^{\psi\psi} = \frac{\left[F_{\psi}^{\psi\psi\bar{\psi}} \right]_{\bar{\psi},1} \left[F_{\psi}^{\bar{\psi}\psi\psi} \right]_{1,\bar{\psi}}}{\left[F_{\bar{\psi}}^{\bar{\psi}\psi\bar{\psi}} \right]_{1,1}} \quad (\text{A.4})$$

We will mention $\kappa_{\psi}^{\psi\psi}$ only when it does not equal 1, which rarely happens. If it does happen, then the anyon model \mathcal{A} in question has the property that $\mathcal{A}^P \neq \mathcal{A}^T$; in other words, it is not PT -invariant (or, given CPT -invariance, not C -invariant). None of the other quantities listed in the tables signal the lack of PT -invariance, because T conjugates the F -symbols, whereas P does not, and none of the other quantities listed actually depend on the phase of the F -symbols.

Using R -symbols in addition to F -symbols, we may calculate the topological spins of the particles. We have

$$\theta_{\psi} = \frac{1}{d_{\psi}} \sum_a N_{\psi\psi}^a R_a^{\psi\psi} d_a. \quad (\text{A.5})$$

This also gives us the central charge modulo 8, by the formula

$$e^{\frac{2\pi i}{8}c} = \frac{1}{\mathcal{D}} \sum_a d_a^2 \theta_a \quad (\text{A.6})$$

and the S -matrix

$$S_{ab} = \frac{1}{\mathcal{D}} \sum_c N_{ab}^c \frac{\theta_c}{\theta_a \theta_b} d_c. \quad (\text{A.7})$$

In the tables, we will actually give the quantities $s_{\psi} \in \mathbb{R}/\mathbb{Z}$ defined by

$$\theta_{\psi} = e^{2\pi i s_{\psi}}, \quad (\text{A.8})$$

which give the fractional parts of the conformal weights of the fields in a CFT realization of the anyon model.

In the following sections, we will often refer to “mirror pairs” of anyon models, by which we mean an anyon model \mathcal{A} and its image under parity \mathcal{A}^P .

A.1.1 \mathbb{Z}_2

For the \mathbb{Z}_2 fusion algebra, we find 2 solutions to the Pentagon equations, each of which gives rise to 2 solutions to the Hexagon equations, for 4 solutions in total. These are precisely the $\mathbb{Z}_2^{(w)}$ theories with $w \in \{0, \frac{1}{2}, 1, \frac{3}{2}\}$ (cf. Chapter 5.1). Only $\mathbb{Z}_2^{(1/2)}$ and $\mathbb{Z}_2^{(3/2)}$ are modular, and these correspond to the $SU(2)_1$ CFT and its image under parity. The modular theories have $\kappa_{\psi_1} = -1$, the non-modular theories have $\kappa_{\psi_1} = 1$.

A.1.2 Fib, or $SO(3)_3$

For the $SO(3)_3$ fusion algebra, we find one unitary solution to the Pentagon equations, which gives rise to a mirror pair of modular Hexagon solutions. These solutions are just the parity orbit of the Fib theory, which corresponds to the $(G_2)_1$ CFT. See Chapter 5.5 for details.

A.1.3 \mathbb{Z}_3

For the \mathbb{Z}_3 fusion algebra, we find 3 solutions to the Pentagon equations. Only one of these, the trivial solution (all F-symbols equal 1), allows for solutions to the Hexagon equations. The other two Pentagon solutions have nontrivial Frobenius-Schur indicators for the (ψ_1, ψ_1, ψ_2) and (ψ_2, ψ_2, ψ_1) vertices. The indicators for these vertices are both $e^{\frac{2\pi i}{3}}$ for one theory and both $e^{\frac{4\pi i}{3}}$ for the other. This shows that these solutions correspond to non-isomorphic fusion theories which are each other's image under T . The trivial Pentagon solution allows for 3 Hexagon solutions, giving three unitary anyon models. These are just the $\mathbb{Z}_3^{(n)}$ models with $n \in \{0, 1, 2\}$ (see Chapter 5.1). Only $\mathbb{Z}_3^{(1)}$ and $\mathbb{Z}_3^{(2)}$ are modular and they correspond to the $SU(3)_1$ CFT and its image under parity.

A.1.4 $SU(2)_2$

$$\begin{array}{|c|c|c|} \hline \psi_0 & \psi_1 & \psi_2 \\ \hline \psi_1 & \psi_0 + \psi_2 & \psi_1 \\ \hline \psi_2 & \psi_1 & \psi_0 \\ \hline \end{array} \quad (\text{A.9})$$

For the $SU(2)_2$ fusion rules, we find 4 solutions to the Pentagon equations. Two of these allow for solutions to the Hexagon equations, giving 4 Pentagon/Hexagon solutions (in two mirror pairs) for each solution to the Pentagon. Out of the 4 mirror pairs, 2 are the Ising and $SU(2)_2$ theories and their images under parity. Details for these are given in Chapters 5.6 and 5.4. We tabulate one theory from each of the other two pairs.

$c = \frac{5}{2}$	$\mathcal{D} = 2$	$SO(5)_1$																	
<table border="1" style="margin: auto; border-collapse: collapse;"> <tr> <td style="width: 5%;"></td> <td style="width: 15%;">ψ_0</td> <td style="width: 15%;">ψ_1</td> <td style="width: 15%;">ψ_2</td> </tr> <tr> <td style="width: 5%;">d</td> <td style="text-align: center;">1</td> <td style="text-align: center;">$\sqrt{2}$</td> <td style="text-align: center;">1</td> </tr> <tr> <td style="width: 5%;">s</td> <td style="text-align: center;">0</td> <td style="text-align: center;">$\frac{5}{16}$</td> <td style="text-align: center;">$\frac{1}{2}$</td> </tr> <tr> <td style="width: 5%;">κ</td> <td style="text-align: center;">1</td> <td style="text-align: center;">-1</td> <td style="text-align: center;">1</td> </tr> </table>		ψ_0	ψ_1	ψ_2	d	1	$\sqrt{2}$	1	s	0	$\frac{5}{16}$	$\frac{1}{2}$	κ	1	-1	1	$\mathcal{DS} = \begin{pmatrix} 1 & \sqrt{2} & 1 \\ \sqrt{2} & 0 & -\sqrt{2} \\ 1 & -\sqrt{2} & 1 \end{pmatrix}$		(A.10)
	ψ_0	ψ_1	ψ_2																
d	1	$\sqrt{2}$	1																
s	0	$\frac{5}{16}$	$\frac{1}{2}$																
κ	1	-1	1																

$c = \frac{7}{2}$	$\mathcal{D} = 2$	$SO(7)_1$																	
<table border="1" style="margin: auto; border-collapse: collapse;"> <tr> <td style="width: 5%;"></td> <td style="width: 15%;">ψ_0</td> <td style="width: 15%;">ψ_1</td> <td style="width: 15%;">ψ_2</td> </tr> <tr> <td style="width: 5%;">d</td> <td style="text-align: center;">1</td> <td style="text-align: center;">$\sqrt{2}$</td> <td style="text-align: center;">1</td> </tr> <tr> <td style="width: 5%;">s</td> <td style="text-align: center;">0</td> <td style="text-align: center;">$\frac{7}{16}$</td> <td style="text-align: center;">$\frac{1}{2}$</td> </tr> <tr> <td style="width: 5%;">κ</td> <td style="text-align: center;">1</td> <td style="text-align: center;">1</td> <td style="text-align: center;">1</td> </tr> </table>		ψ_0	ψ_1	ψ_2	d	1	$\sqrt{2}$	1	s	0	$\frac{7}{16}$	$\frac{1}{2}$	κ	1	1	1	$\mathcal{DS} = \begin{pmatrix} 1 & \sqrt{2} & 1 \\ \sqrt{2} & 0 & -\sqrt{2} \\ 1 & -\sqrt{2} & 1 \end{pmatrix}$		(A.11)
	ψ_0	ψ_1	ψ_2																
d	1	$\sqrt{2}$	1																
s	0	$\frac{7}{16}$	$\frac{1}{2}$																
κ	1	1	1																

The $SO(5)_1$ model is based on the same Pentagon solution as $SU(2)_2$ while $SO(7)_1$ model is based on the same Pentagon solution as the Ising model.

A.1.5 $\text{SO}(3)_4$

ψ_0	ψ_2	ψ_4
ψ_2	$\psi_0 + \psi_2 + \psi_4$	ψ_2
ψ_4	ψ_2	ψ_0

(A.12)

This is the only multiplicity-free fusion rules with three particle types that does not occur on the list in [152]. It has three solutions to the Pentagon equations. These all have $\left[F_{\psi_2}^{\psi_2\psi_2\psi_2} \right]_{\psi_2\psi_2} = 0$. One of these allows for 3 solutions to the Hexagons, which come as one parity invariant solution (tabulated below), and a mirror pair, which is the (non-modular) $\text{SO}(3)_4$ model given by the restriction of $\text{SU}(2)_4$ tabulated in Chapter 5.4, and its image under parity. The other two pentagon solutions are not braided, but have nontrivial Frobenius-Schur indicators for the (ψ_2, ψ_2, ψ_2) vertex (they are each other's parity conjugates).

not modular	$\mathcal{D} = \sqrt{6}$																
<table border="1" style="border-collapse: collapse; margin: 5px auto;"> <tr> <td style="padding: 5px;"></td> <td style="padding: 5px;">ψ_0</td> <td style="padding: 5px;">ψ_2</td> <td style="padding: 5px;">ψ_4</td> </tr> <tr> <td style="padding: 5px;">d</td> <td style="padding: 5px;">1</td> <td style="padding: 5px;">2</td> <td style="padding: 5px;">1</td> </tr> <tr> <td style="padding: 5px;">s</td> <td style="padding: 5px;">0</td> <td style="padding: 5px;">0</td> <td style="padding: 5px;">0</td> </tr> <tr> <td style="padding: 5px;">κ</td> <td style="padding: 5px;">1</td> <td style="padding: 5px;">1</td> <td style="padding: 5px;">1</td> </tr> </table>		ψ_0	ψ_2	ψ_4	d	1	2	1	s	0	0	0	κ	1	1	1	$\mathcal{DS} = \begin{pmatrix} 1 & 2 & 1 \\ 2 & 4 & 2 \\ 1 & 2 & 1 \end{pmatrix}$
	ψ_0	ψ_2	ψ_4														
d	1	2	1														
s	0	0	0														
κ	1	1	1														

(A.13)

A.1.6 $\text{SO}(3)_5$

For the $\text{SO}(3)_5$ fusion algebra, we find one unitary solution to the Pentagon equation and one mirror pair of unitary, modular solutions to the Hexagons. This is the $\text{SO}(3)_5$ model obtained from restriction of the $\text{SU}(2)_5$ model given in Chapter 5.4, and its image under parity.

A.1.7 \mathbb{Z}_4

For the \mathbb{Z}_4 fusion algebra, there are 4 solutions to the Pentagon and 2 of these allow for solutions to the Hexagon, with 4 solutions each. This gives 8 total solutions to the Pentagon and Hexagon equations, precisely the eight $\mathbb{Z}_4^{(w)}$ models given in Chapter 5.1. The modular theories are $\mathbb{Z}_4^{(1/2)}$ and $\mathbb{Z}_4^{(3/2)}$ and their parity images $\mathbb{Z}_4^{(7/2)}$ and $\mathbb{Z}_4^{(5/2)}$. Conformal field theory realizations are $U(1)_2$ for $\mathbb{Z}_4^{(1/2)}$ and $SU(4)_1$ for $\mathbb{Z}_4^{(3/2)}$. All Frobenius-Schur indicators for self dual particles equal 1 in all 8 anyon models.

A.1.8 $\mathbb{Z}_2 \times \mathbb{Z}_2$

For the $\mathbb{Z}_2 \times \mathbb{Z}_2$ product fusion algebra, we find 8 solutions to the Pentagon equation, in 4 different classes up to permutations of the nontrivial particles. Of the 8 solutions, 2 are invariant under such permutations and the other 6 split up into two orbits of 3 solutions each (this may be read off from the Frobenius-Schur indicators). Of the 8 solutions to the Pentagon equations, 4 give rise to solutions of the Hexagon, so there are 8 solutions to the Hexagon for each Pentagon solution. The Pentagon solutions which allow for Hexagon solutions all have an even number of particles with nontrivial Frobenius-Schur indicator, while the ones which don't all have an odd number of such particles.

The 32 solutions of Pentagon/Hexagon form 10 distinct classes up to permutations of the particles. Of these 10 classes, 4 are paired up into 2 mirror pairs and 8 can be obtained as products of two \mathbb{Z}_2 theories. The product theories are modular only if they are the product of two modular theories. The two theories which cannot be obtained as products are the modular $D(\mathbb{Z}_2)$ and $D'(\mathbb{Z}_2)$ theories, with central charges $c = 0$ and $c = 4$ (modulo 8). The 10 classes of theories are listed below.

- 4 bosons. $\mathbb{Z}_2^{(0)} \times \mathbb{Z}_2^{(0)}$.
- 3 bosons, 1 fermion, obtained in 3 ways. Not a product of \mathbb{Z}_2 theories. $D(\mathbb{Z}_2)$.
- 2 bosons, 2 fermions, obtained in 3 ways. $\mathbb{Z}_2^{(0)} \times \mathbb{Z}_2^{(1)}$ or $\mathbb{Z}_2^{(1)} \times \mathbb{Z}_2^{(1)}$.

- 2 bosons, 2 semions of weight $\frac{1}{4}$, obtained in 3 ways. $\mathbb{Z}_2^{(0)} \times \mathbb{Z}_2^{(1/2)}$.
- 2 bosons, 2 semions of weight $-\frac{1}{4}$, obtained in 3 ways (parity image of the previous). $\mathbb{Z}_2^{(0)} \times \mathbb{Z}_2^{(3/2)}$.
- 2 bosons, 2 semions of weights $\frac{1}{4}$ and $-\frac{1}{4}$, obtained in 6 ways. Modular. $\mathbb{Z}_2^{(1/2)} \times \mathbb{Z}_2^{(3/2)}$.
- 1 bosons, 3 fermions. Not a product of \mathbb{Z}_2 theories, quantum double of the non-braided \mathbb{Z}_2 fusion model. Modular. We denote it $D'(\mathbb{Z}_2)$.
- 1 boson, 2 semions of weight $\frac{1}{4}$, 1 fermion, obtained in 3 ways. Modular. $\mathbb{Z}_2^{(1/2)} \times \mathbb{Z}_2^{(1/2)}$.
- 1 boson, 2 semions of weight $-\frac{1}{4}$, 1 fermion, obtained in 3 ways (parity image of the previous). Modular. $\mathbb{Z}_2^{(3/2)} \times \mathbb{Z}_2^{(3/2)}$.
- 1 boson, 2 semions of weights $\frac{1}{4}$ and $-\frac{1}{4}$, 1 fermion, obtained in 6 ways. $\mathbb{Z}_2^{(1)} \times \mathbb{Z}_2^{(1/2)}$ or $\mathbb{Z}_2^{(1)} \times \mathbb{Z}_2^{(3/2)}$.

The data for the product theories can simply be obtained from the various \mathbb{Z}_2 data and we have given the data for $D(\mathbb{Z}_2)$ and $D'(\mathbb{Z}_2)$ in Chapters 5.2 and 5.3, respectively.

A.1.9 $SU(2)_3$, or $\text{Fib} \times \mathbb{Z}_2$

The $SU(2)_3$ fusion algebra is the product of those of Fib and \mathbb{Z}_2 . From them, we find 2 unitary solutions to the Pentagon equations. These are just the products of the 2 solutions of the \mathbb{Z}_2 theory with the solution of the Fibonacci theory. Each solution of the Pentagon gives rise to 4 solutions of the Hexagons. The 8 solutions we find in this way are again precisely the products of the 2 Fibonacci solutions with the 4 \mathbb{Z}_2 solutions. Modularity is inherited from the parent theories (if they are both modular, then the product will be modular). The 8 theories occur in 4 mirror pairs. The anyon model for the $SU(2)_3$ CFT (see Chapter 5.4) corresponds to the product $\text{Fib} \times \mathbb{Z}_2^{(3/2)}$. The other modular theories are its parity image and the mirror pair represented by $\text{Fib} \times \mathbb{Z}_2^{(1/2)} \equiv (G_2)_1 \times SU(2)_1$.

A.1.10 D_5

ψ_0	ψ_1	ψ_2	ψ_3
ψ_1	ψ_0	ψ_2	ψ_3
ψ_2	ψ_2	$\psi_0 + \psi_1 + \psi_3$	$\psi_2 + \psi_3$
ψ_3	ψ_3	$\psi_2 + \psi_3$	$\psi_0 + \psi_1 + \psi_2$

(A.14)

This fusion algebra describe the tensor product decomposition of the representations of the 10 element dihedral group D_5 (i.e. the symmetry group of a regular pentagon). Because of this, there is at least one solution to the Pentagon and Hexagon equations that just describes exchange of the tensor factors in the products of D_5 representations. However, it turns out that there are additional solutions. There are 5 solutions to the Pentagon equations. Of these, only one allows for solutions to the Hexagon equations (necessarily the one which corresponds to the representation theory of D_5). This Pentagon solution has the following 6 F -symbols equal to zero: $\left[F_{\psi_2}^{\psi_2\psi_2\psi_2} \right]_{\psi_3\psi_3}$, $\left[F_{\psi_3}^{\psi_2\psi_3\psi_2} \right]_{\psi_2\psi_2}$, $\left[F_{\psi_3}^{\psi_2\psi_3\psi_2} \right]_{\psi_3\psi_3}$, $\left[F_{\psi_2}^{\psi_3\psi_2\psi_3} \right]_{\psi_2\psi_2}$, $\left[F_{\psi_2}^{\psi_3\psi_2\psi_3} \right]_{\psi_3\psi_3}$, and $\left[F_{\psi_3}^{\psi_3\psi_3\psi_3} \right]_{\psi_2\psi_2}$. It gives 5 Hexagon solutions (tabulated below), one from the D_5 representation theory and 2 mirror pairs. These 2 mirror pairs of solutions may be obtained as charge spectrum restrictions of the 2 mirror pairs of solutions of the $SO(5)_2$ fusion algebra given in Appendix A.1.19. It would be interesting to determine whether their braiding is universal for topological quantum computation.

not modular					$\mathcal{D} = \sqrt{10}$
	ψ_0	ψ_1	ψ_2	ψ_3	
d	1	1	2	2	$\mathcal{D}S = \begin{pmatrix} 1 & 1 & 2 & 2 \\ 1 & 1 & 2 & 2 \\ 2 & 2 & 4 & 4 \\ 2 & 2 & 4 & 4 \end{pmatrix}$
s	0	0	0	0	
κ	1	1	1	1	

(A.15)

not modular					$\mathcal{D} = \sqrt{10}$																					
<table border="1" style="border-collapse: collapse; width: 100%;"> <tr> <td style="width: 5%;"></td> <td style="width: 15%;">ψ_0</td> <td style="width: 15%;">ψ_1</td> <td style="width: 15%;">ψ_2</td> <td style="width: 15%;">ψ_3</td> </tr> <tr> <td>d</td> <td>1</td> <td>1</td> <td>2</td> <td>2</td> </tr> <tr> <td>s</td> <td>0</td> <td>0</td> <td>$\frac{2}{5}$</td> <td>$-\frac{2}{5}$</td> </tr> <tr> <td>κ</td> <td>1</td> <td>1</td> <td>1</td> <td>1</td> </tr> </table>						ψ_0	ψ_1	ψ_2	ψ_3	d	1	1	2	2	s	0	0	$\frac{2}{5}$	$-\frac{2}{5}$	κ	1	1	1	1	$\mathcal{DS} = \begin{pmatrix} 1 & 1 & 2 & 2 \\ 1 & 1 & 2 & 2 \\ 2 & 2 & 2/\phi & -2\phi \\ 2 & 2 & -2\phi & 2/\phi \end{pmatrix}$	(A.16)
	ψ_0	ψ_1	ψ_2	ψ_3																						
d	1	1	2	2																						
s	0	0	$\frac{2}{5}$	$-\frac{2}{5}$																						
κ	1	1	1	1																						

not modular					$\mathcal{D} = \sqrt{10}$																					
<table border="1" style="border-collapse: collapse; width: 100%;"> <tr> <td style="width: 5%;"></td> <td style="width: 15%;">ψ_0</td> <td style="width: 15%;">ψ_1</td> <td style="width: 15%;">ψ_2</td> <td style="width: 15%;">ψ_3</td> </tr> <tr> <td>d</td> <td>1</td> <td>1</td> <td>2</td> <td>2</td> </tr> <tr> <td>s</td> <td>0</td> <td>0</td> <td>$\frac{1}{5}$</td> <td>$-\frac{1}{5}$</td> </tr> <tr> <td>κ</td> <td>1</td> <td>1</td> <td>1</td> <td>1</td> </tr> </table>						ψ_0	ψ_1	ψ_2	ψ_3	d	1	1	2	2	s	0	0	$\frac{1}{5}$	$-\frac{1}{5}$	κ	1	1	1	1	$\mathcal{DS} = \begin{pmatrix} 1 & 1 & 2 & 2 \\ 1 & 1 & 2 & 2 \\ 2 & 2 & -2\phi & 2/\phi \\ 2 & 2 & 2/\phi & -2\phi \end{pmatrix}$	(A.17)
	ψ_0	ψ_1	ψ_2	ψ_3																						
d	1	1	2	2																						
s	0	0	$\frac{1}{5}$	$-\frac{1}{5}$																						
κ	1	1	1	1																						

A.1.11 $\text{Fib} \times \text{Fib}$

For the $\text{Fib} \times \text{Fib}$ product fusion algebra, there is 1 solution to the Pentagon equations, which is just the product of the solution for Fib with itself. There are 4 solutions to the Hexagon, in two mirror pairs. These solutions are again just products of the 2 solutions to the Pentagon/Hexagon that we found for Fib . All solutions are modular.

A.1.12 $\text{SO}(3)_6$

The $\text{SO}(3)_6$ fusion algebra has 2 solutions to the Pentagon equations. Each gives rise to a mirror pair of Hexagon solutions, neither of which is modular. One of the mirror pairs is unitary, and is just the (non-modular) $\text{SO}(3)_6$ model given by the restriction of $\text{SU}(2)_6$ tabulated in Chapter 5.4, and its image under parity.

A.1.13 $\text{SO}(3)_7$

The $\text{SO}(3)_7$ fusion algebra has one unitary solution to the Pentagon equations and this gives rise to one mirror pair of unitary, modular solutions to the Hexagon equations. These are just the $\text{SO}(3)_7$ model given by restriction of the $\text{SU}(2)_7$ model tabulated in Chapter 5.4, and its image under parity.

A.1.14 \mathbb{Z}_5

The \mathbb{Z}_5 fusion algebra is invariant under relabelings of the particles that correspond to a new choice of canonical generator for \mathbb{Z}_5 (instead of $[1]_5$). In particular, sending $[a]_5$ to $[2a]_5$ leaves the fusion rules invariant. As a result of this permutation symmetry, different solutions to the Pentagon and Hexagon can correspond to isomorphic (braided) tensor categories.

There are 5 solutions to the Pentagon equation. Only 1 of these (the trivial one) allows for solutions to the Hexagon equations, 5 in total, which are just the $\mathbb{Z}_5^{(n)}$ models with $n \in \{0, 1, 2, 3, 4\}$. The 5 Pentagon/Hexagon solutions fall into 3 classes under permutations, giving three anyon models. One of these is just the non-modular $\mathbb{Z}_5^{(0)}$ theory with 5 bosons, the other two are modular. We have $\mathbb{Z}_5^1 \equiv \mathbb{Z}_5^4$ with central charge $c = 0$ (modulo 8) and $\mathbb{Z}_5^2 \equiv \mathbb{Z}_5^3$ with $c = 4$ (modulo 8). The $c = 4$ theory is realized by the $\text{SU}(5)_1$ CFT.

A.1.15 $\text{SU}(2)_4$

$$\begin{array}{ccccc}
 \psi_0 & \psi_1 & \psi_2 & \psi_3 & \psi_4 \\
 \psi_1 & \psi_0 + \psi_2 & \psi_1 + \psi_3 & \psi_2 + \psi_4 & \psi_3 \\
 \psi_2 & \psi_1 + \psi_3 & \psi_0 + \psi_2 + \psi_4 & \psi_1 + \psi_3 & \psi_2 \\
 \psi_3 & \psi_2 + \psi_4 & \psi_1 + \psi_3 & \psi_0 + \psi_2 & \psi_1 \\
 \psi_4 & \psi_3 & \psi_2 & \psi_1 & \psi_0
 \end{array} \tag{A.18}$$

This fusion algebra has 2 solutions to the Pentagon equations. These both have $\left[F_{\psi_2}^{\psi_2 \psi_2 \psi_2} \right]_{\psi_2 \psi_2} = 0$. Each solution leads to 4 Hexagon solutions in 2 mirror pairs. However, the fusion rules are symmetric under the exchange of ψ_1 and ψ_3 and the

two pairs are sent into each other under this exchange, so that they correspond to isomorphic anyon models. Hence, we find two pairs of anyon models with these fusion rules, both of which are modular. One of these is the $SU(2)_4$ theory given in Chapter 5.4 and its parity image. A representative of the other pair is tabulated below. Note that all theories with these fusion rules occur at $c = \pm 2$ (modulo 8).

$c = 2$	$\mathcal{D} = 2\sqrt{3}$																								
<table border="1" style="border-collapse: collapse; width: 100%;"> <tr> <td style="padding: 2px 5px;"></td> <td style="padding: 2px 5px;">ψ_0</td> <td style="padding: 2px 5px;">ψ_1</td> <td style="padding: 2px 5px;">ψ_2</td> <td style="padding: 2px 5px;">ψ_3</td> <td style="padding: 2px 5px;">ψ_4</td> </tr> <tr> <td style="padding: 2px 5px;">d</td> <td style="padding: 2px 5px;">1</td> <td style="padding: 2px 5px;">$\sqrt{3}$</td> <td style="padding: 2px 5px;">2</td> <td style="padding: 2px 5px;">$\sqrt{3}$</td> <td style="padding: 2px 5px;">1</td> </tr> <tr> <td style="padding: 2px 5px;">s</td> <td style="padding: 2px 5px;">0</td> <td style="padding: 2px 5px;">$-\frac{1}{8}$</td> <td style="padding: 2px 5px;">$\frac{1}{3}$</td> <td style="padding: 2px 5px;">$\frac{3}{8}$</td> <td style="padding: 2px 5px;">0</td> </tr> <tr> <td style="padding: 2px 5px;">κ</td> <td style="padding: 2px 5px;">1</td> <td style="padding: 2px 5px;">1</td> <td style="padding: 2px 5px;">1</td> <td style="padding: 2px 5px;">1</td> <td style="padding: 2px 5px;">1</td> </tr> </table>		ψ_0	ψ_1	ψ_2	ψ_3	ψ_4	d	1	$\sqrt{3}$	2	$\sqrt{3}$	1	s	0	$-\frac{1}{8}$	$\frac{1}{3}$	$\frac{3}{8}$	0	κ	1	1	1	1	1	$\mathcal{DS} = \begin{pmatrix} 1 & \sqrt{3} & 2 & \sqrt{3} & 1 \\ \sqrt{3} & -\sqrt{3} & 0 & \sqrt{3} & -\sqrt{3} \\ 2 & 0 & -2 & 0 & 2 \\ \sqrt{3} & \sqrt{3} & 0 & -\sqrt{3} & -\sqrt{3} \\ 1 & -\sqrt{3} & 2 & -\sqrt{3} & 1 \end{pmatrix} \quad (\text{A.19})$
	ψ_0	ψ_1	ψ_2	ψ_3	ψ_4																				
d	1	$\sqrt{3}$	2	$\sqrt{3}$	1																				
s	0	$-\frac{1}{8}$	$\frac{1}{3}$	$\frac{3}{8}$	0																				
κ	1	1	1	1	1																				

A.1.16 $SO(3)_8$

The $SO(3)_8$ fusion algebra has 2 solutions to the Pentagon equations. Each of these has a mirror pair of non-modular solutions to the Hexagon equations. One of the mirror pairs is unitary, and is just the $SO(3)_8$ model given by restriction of $SU(2)_8$ tabulated in Chapter 5.4, and its image under parity.

A.1.17 \mathbb{Z}_6

The \mathbb{Z}_6 fusion algebra has 6 solutions to the Pentagon equations and 2 of these allow for solutions to the Hexagons, 6 solutions each, giving precisely the 12 $\mathbb{Z}_6^{(w)}$ solutions tabulated in Chapter 5.1. These are also precisely the products of the 4 $\mathbb{Z}_2^{(w)}$ models with the 3 $\mathbb{Z}_3^{(n)}$ models. For $\mathbb{Z}_6^{(n+\frac{1}{2})}$, we have $\kappa_{[3]_6} = -1$. There are 4 modular theories (2 mirror pairs), corresponding to the $SU(6)_1$ and $U(1)_3$ CFTs and their parity images. We have $SU(6)_1 \equiv \mathbb{Z}_6^{(5/2)} \cong \mathbb{Z}_2^{(1/2)} \times \mathbb{Z}_3^{(2)}$ and $U(1)_3 \equiv \mathbb{Z}_6^{(1/2)} \cong \mathbb{Z}_2^{(3/2)} \times \mathbb{Z}_3^{(1)}$.

A.1.18 $SU(2)_2 \times \mathbb{Z}_2$

The $SU(2)_2 \times \mathbb{Z}_2$ product fusion algebra is invariant under the exchange of $(\frac{1}{2}, [0]_2)$ with $(\frac{1}{2}, [1]_2)$. Hence, the $SU(2)_2$ in this product may be thought of as corresponding to either the charges $\{(0, [0]_2), (\frac{1}{2}, [0]_2), (1, [0]_2)\}$, or $\{(0, [0]_2), (\frac{1}{2}, [1]_2), (1, [0]_2)\}$. When investigating solutions to Pentagon or Hexagon to see if they are product solutions, we must consider both of these factorizations. There are 16 solutions to the Pentagon equations. These are precisely twice the 8 products of the 4 solutions for $SU(2)_2$ with the 2 solutions for \mathbb{Z}_2 fusion rules, each product occurring for both factorizations. These 16 Pentagon solutions each give rise to 4 Hexagon solutions and the resulting 64 Hexagon solutions are just the products of the eight $SU(2)_2$ anyon models with the four \mathbb{Z}_2 anyon models, each occurring in two ways, according to the two different factorizations of the fusion rules. Of course, the solutions corresponding to the different factorizations give isomorphic anyon models, so the number of anyon models for these fusion rules up to isomorphism is 32 and all of these are products of theories tabulated before.

A.1.19 $SO(5)_2$

ψ_0	ψ_1		ψ_2		ψ_3		ψ_4		ψ_5
ψ_1	ψ_0		ψ_5		ψ_3		ψ_4		ψ_2
ψ_2	ψ_5	$\psi_0 + \psi_3 + \psi_4$		$\psi_2 + \psi_5$		$\psi_2 + \psi_5$		$\psi_1 + \psi_3 + \psi_4$	
ψ_3	ψ_3	$\psi_2 + \psi_5$	$\psi_0 + \psi_1 + \psi_4$		$\psi_3 + \psi_4$		$\psi_2 + \psi_5$		
ψ_4	ψ_4	$\psi_2 + \psi_5$	$\psi_3 + \psi_4$	$\psi_0 + \psi_1 + \psi_3$		$\psi_2 + \psi_5$		$\psi_2 + \psi_5$	
ψ_5	ψ_2	$\psi_1 + \psi_3 + \psi_4$		$\psi_2 + \psi_5$		$\psi_2 + \psi_5$		$\psi_0 + \psi_3 + \psi_4$	

(A.20)

This fusion algebra has 4 solutions to the Pentagon equation. In all of these the following 6 F -symbols are equal to zero: $\left[F_{\psi_3}^{\psi_3\psi_3\psi_3} \right]_{\psi_4\psi_4}$, $\left[F_{\psi_4}^{\psi_3\psi_4\psi_3} \right]_{\psi_3\psi_3}$, $\left[F_{\psi_4}^{\psi_3\psi_4\psi_3} \right]_{\psi_4\psi_4}$, $\left[F_{\psi_3}^{\psi_4\psi_3\psi_4} \right]_{\psi_3\psi_3}$, $\left[F_{\psi_3}^{\psi_4\psi_3\psi_4} \right]_{\psi_4\psi_4}$, and $\left[F_{\psi_4}^{\psi_4\psi_4\psi_4} \right]_{\psi_3\psi_3}$. Each Pentagon solution allows for 4 solutions to the Hexagon equations, in 2 mirror pairs. However, these solutions are related to each other by the automorphism of the fusion rules that exchanges ψ_2 with ψ_5 and/or ψ_3 with ψ_4 . As a result, there are only 4 mirror pairs of solutions,

giving 8 anyon models in total, all of which are modular. Note that we have two more examples of unitary theories with $c = 0 \pmod{8}$ here. It would be interesting to find a CFT or Chern-Simons description of these. We also note that restricting to particles types $\mathcal{C}' = \{\psi_0, \psi_1, \psi_3, \psi_4\}$ gives the four nontrivial D_5 theories.

$c = 0$	$\mathcal{D} = 2\sqrt{3}$																													
<table border="1" style="width: 100%; border-collapse: collapse; margin-top: 10px;"> <thead> <tr> <th style="width: 5%;"></th> <th style="width: 10%;">ψ_0</th> <th style="width: 10%;">ψ_1</th> <th style="width: 10%;">ψ_2</th> <th style="width: 10%;">ψ_3</th> <th style="width: 10%;">ψ_4</th> <th style="width: 10%;">ψ_5</th> </tr> </thead> <tbody> <tr> <td>d</td> <td>1</td> <td>1</td> <td>$\sqrt{5}$</td> <td>2</td> <td>2</td> <td>$\sqrt{5}$</td> </tr> <tr> <td>s</td> <td>0</td> <td>0</td> <td>$\frac{1}{4}$</td> <td>$\frac{1}{5}$</td> <td>$-\frac{1}{5}$</td> <td>$-\frac{1}{4}$</td> </tr> <tr> <td>κ</td> <td>1</td> <td>1</td> <td>1</td> <td>1</td> <td>1</td> <td>1</td> </tr> </tbody> </table>		ψ_0	ψ_1	ψ_2	ψ_3	ψ_4	ψ_5	d	1	1	$\sqrt{5}$	2	2	$\sqrt{5}$	s	0	0	$\frac{1}{4}$	$\frac{1}{5}$	$-\frac{1}{5}$	$-\frac{1}{4}$	κ	1	1	1	1	1	1	$\mathcal{DS} = \begin{pmatrix} 1 & 1 & \sqrt{5} & 2 & 2 & \sqrt{5} \\ 1 & 1 & -\sqrt{5} & 2 & 2 & -\sqrt{5} \\ \sqrt{5} & -\sqrt{5} & -\sqrt{5} & 0 & 0 & \sqrt{5} \\ 2 & 2 & 0 & -2\phi & 2/\phi & 0 \\ 2 & 2 & 0 & 2/\phi & -2\phi & 0 \\ \sqrt{5} & -\sqrt{5} & \sqrt{5} & 0 & 0 & -\sqrt{5} \end{pmatrix}$	(A.21)
	ψ_0	ψ_1	ψ_2	ψ_3	ψ_4	ψ_5																								
d	1	1	$\sqrt{5}$	2	2	$\sqrt{5}$																								
s	0	0	$\frac{1}{4}$	$\frac{1}{5}$	$-\frac{1}{5}$	$-\frac{1}{4}$																								
κ	1	1	1	1	1	1																								

$c = 4$	$\mathcal{D} = 2\sqrt{3}$																													
<table border="1" style="width: 100%; border-collapse: collapse; margin-top: 10px;"> <thead> <tr> <th style="width: 5%;"></th> <th style="width: 10%;">ψ_0</th> <th style="width: 10%;">ψ_1</th> <th style="width: 10%;">ψ_2</th> <th style="width: 10%;">ψ_3</th> <th style="width: 10%;">ψ_4</th> <th style="width: 10%;">ψ_5</th> </tr> </thead> <tbody> <tr> <td>d</td> <td>1</td> <td>1</td> <td>$\sqrt{5}$</td> <td>2</td> <td>2</td> <td>$\sqrt{5}$</td> </tr> <tr> <td>s</td> <td>0</td> <td>0</td> <td>0</td> <td>$\frac{2}{5}$</td> <td>$-\frac{2}{5}$</td> <td>$\frac{1}{2}$</td> </tr> <tr> <td>κ</td> <td>1</td> <td>1</td> <td>1</td> <td>1</td> <td>1</td> <td>1</td> </tr> </tbody> </table>		ψ_0	ψ_1	ψ_2	ψ_3	ψ_4	ψ_5	d	1	1	$\sqrt{5}$	2	2	$\sqrt{5}$	s	0	0	0	$\frac{2}{5}$	$-\frac{2}{5}$	$\frac{1}{2}$	κ	1	1	1	1	1	1	$\mathcal{DS} = \begin{pmatrix} 1 & 1 & \sqrt{5} & 2 & 2 & \sqrt{5} \\ 1 & 1 & -\sqrt{5} & 2 & 2 & -\sqrt{5} \\ \sqrt{5} & -\sqrt{5} & -\sqrt{5} & 0 & 0 & \sqrt{5} \\ 2 & 2 & 0 & 2/\phi & -2\phi & 0 \\ 2 & 2 & 0 & -2\phi & 2/\phi & 0 \\ \sqrt{5} & -\sqrt{5} & \sqrt{5} & 0 & 0 & -\sqrt{5} \end{pmatrix}$	(A.22)
	ψ_0	ψ_1	ψ_2	ψ_3	ψ_4	ψ_5																								
d	1	1	$\sqrt{5}$	2	2	$\sqrt{5}$																								
s	0	0	0	$\frac{2}{5}$	$-\frac{2}{5}$	$\frac{1}{2}$																								
κ	1	1	1	1	1	1																								

$c = 0$	$\mathcal{D} = 2\sqrt{3}$																													
<table border="1" style="width: 100%; border-collapse: collapse; margin-top: 10px;"> <thead> <tr> <th style="width: 5%;"></th> <th style="width: 10%;">ψ_0</th> <th style="width: 10%;">ψ_1</th> <th style="width: 10%;">ψ_2</th> <th style="width: 10%;">ψ_3</th> <th style="width: 10%;">ψ_4</th> <th style="width: 10%;">ψ_5</th> </tr> </thead> <tbody> <tr> <td>d</td> <td>1</td> <td>1</td> <td>$\sqrt{5}$</td> <td>2</td> <td>2</td> <td>$\sqrt{5}$</td> </tr> <tr> <td>s</td> <td>0</td> <td>0</td> <td>0</td> <td>$\frac{1}{5}$</td> <td>$-\frac{1}{5}$</td> <td>$\frac{1}{2}$</td> </tr> <tr> <td>κ</td> <td>1</td> <td>1</td> <td>-1</td> <td>1</td> <td>1</td> <td>-1</td> </tr> </tbody> </table>		ψ_0	ψ_1	ψ_2	ψ_3	ψ_4	ψ_5	d	1	1	$\sqrt{5}$	2	2	$\sqrt{5}$	s	0	0	0	$\frac{1}{5}$	$-\frac{1}{5}$	$\frac{1}{2}$	κ	1	1	-1	1	1	-1	$\mathcal{DS} = \begin{pmatrix} 1 & 1 & \sqrt{5} & 2 & 2 & \sqrt{5} \\ 1 & 1 & -\sqrt{5} & 2 & 2 & -\sqrt{5} \\ \sqrt{5} & -\sqrt{5} & \sqrt{5} & 0 & 0 & -\sqrt{5} \\ 2 & 2 & 0 & -2\phi & 2/\phi & 0 \\ 2 & 2 & 0 & 2/\phi & -2\phi & 0 \\ \sqrt{5} & -\sqrt{5} & -\sqrt{5} & 0 & 0 & \sqrt{5} \end{pmatrix}$	(A.23)
	ψ_0	ψ_1	ψ_2	ψ_3	ψ_4	ψ_5																								
d	1	1	$\sqrt{5}$	2	2	$\sqrt{5}$																								
s	0	0	0	$\frac{1}{5}$	$-\frac{1}{5}$	$\frac{1}{2}$																								
κ	1	1	-1	1	1	-1																								

$c = 4$							$\mathcal{D} = 2\sqrt{3}$																																	
							$\mathcal{DS} = \begin{pmatrix} 1 & 1 & \sqrt{5} & 2 & 2 & \sqrt{5} \\ 1 & 1 & -\sqrt{5} & 2 & 2 & -\sqrt{5} \\ \sqrt{5} & -\sqrt{5} & \sqrt{5} & 0 & 0 & -\sqrt{5} \\ 2 & 2 & 0 & 2/\phi & -2\phi & 0 \\ 2 & 2 & 0 & -2\phi & 2/\phi & 0 \\ \sqrt{5} & -\sqrt{5} & -\sqrt{5} & 0 & 0 & \sqrt{5} \end{pmatrix}$																																	
	<table border="1" style="border-collapse: collapse; width: 100%; text-align: center;"> <tr> <td style="border: none;"></td> <td>ψ_0</td> <td>ψ_1</td> <td>ψ_2</td> <td>ψ_3</td> <td>ψ_4</td> <td>ψ_5</td> </tr> <tr> <td style="border: none;">d</td> <td>1</td> <td>1</td> <td>$\sqrt{5}$</td> <td>2</td> <td>2</td> <td>$\sqrt{5}$</td> </tr> <tr> <td style="border: none;">s</td> <td>0</td> <td>0</td> <td>$\frac{1}{4}$</td> <td>$\frac{2}{5}$</td> <td>$-\frac{2}{5}$</td> <td>$-\frac{1}{4}$</td> </tr> <tr> <td style="border: none;">κ</td> <td>1</td> <td>1</td> <td>-1</td> <td>1</td> <td>1</td> <td>-1</td> </tr> </table>							ψ_0	ψ_1	ψ_2	ψ_3	ψ_4	ψ_5	d	1	1	$\sqrt{5}$	2	2	$\sqrt{5}$	s	0	0	$\frac{1}{4}$	$\frac{2}{5}$	$-\frac{2}{5}$	$-\frac{1}{4}$	κ	1	1	-1	1	1	-1						
	ψ_0	ψ_1	ψ_2	ψ_3	ψ_4	ψ_5																																		
d	1	1	$\sqrt{5}$	2	2	$\sqrt{5}$																																		
s	0	0	$\frac{1}{4}$	$\frac{2}{5}$	$-\frac{2}{5}$	$-\frac{1}{4}$																																		
κ	1	1	-1	1	1	-1																																		

(A.24)

A.1.20 $\text{SU}(2)_5$, or $\text{SO}(3)_5 \times \mathbb{Z}_2$

The $\text{SU}(2)_5$ fusion algebra is the product of the $\text{SO}(3)_5$ and \mathbb{Z}_2 fusion algebras. We find 2 unitary solutions to the Pentagon and 8 unitary solutions to the Hexagon, 4 for each Pentagon solution. These solutions are all products of the $\text{SO}(3)_5$ and \mathbb{Z}_2 type solutions tabulated before. Products of two modular theories are modular, giving 4 modular theories in 2 mirror pairs. The anyon model for the $\text{SU}(2)_5$ Chern-Simons theory, which we tabulated in Chapter 5.4, corresponds to $\text{SO}(3)_5 \times \mathbb{Z}_2^{(1/2)}$.

A.1.21 $\text{Fib} \times \text{SU}(2)_2$

For the $\text{Fib} \times \text{SU}(2)_2$ fusion algebra, there are 4 unitary solutions to the Pentagon equations. These are precisely the products of the 4 solutions for $\text{SU}(2)_2$ with the solution for the Fib fusion rules. Out of these 4 solutions, 2 allow for solutions to the Hexagon equations, giving 8 each, for a total of 16 Pentagon/Hexagon solutions in 8 mirror pairs. These are precisely the products of the 2 unitary Fib models with the 8 solutions we got for $\text{SU}(2)_2$ fusion rules.

A.1.22 \mathbb{Z}_3 -Parafermions, or $\mathbb{Z}_3 \times \text{Fib}$

ψ_0	ψ_1	ψ_2	ϵ_0	ϵ_1	ϵ_2
ψ_1	ψ_2	ψ_0	ϵ_1	ϵ_2	ϵ_0
ψ_2	ψ_0	ψ_1	ϵ_2	ϵ_0	ϵ_1
ϵ_0	ϵ_1	ϵ_2	$\epsilon_0 + \psi_0$	$\epsilon_1 + \psi_1$	$\epsilon_2 + \psi_2$
ϵ_1	ϵ_2	ϵ_0	$\epsilon_1 + \psi_1$	$\epsilon_2 + \psi_2$	$\epsilon_0 + \psi_0$
ϵ_2	ϵ_0	ϵ_1	$\epsilon_2 + \psi_2$	$\epsilon_0 + \psi_0$	$\epsilon_1 + \psi_1$

(A.25)

The fusion algebra is the product of those for Fib and \mathbb{Z}_3 , and it turns out that this product structure also holds for the F -symbols and R -symbols. We find 3 unitary solutions to the Pentagon, which are the products of the Fib solution with the 3 solutions for \mathbb{Z}_3 fusion rules. One of these allows for Hexagon solutions: namely, the solution which has trivial F -symbols for the \mathbb{Z}_3 factor. This yields 6 unitary solutions to the Hexagon equations, in 3 mirror pairs. These 6 solutions are gauge equivalent to products of the pair of Pentagon/Hexagon solutions for Fib with the 3 Pentagon/Hexagon solutions for \mathbb{Z}_3 . There are 4 modular solutions, which come from the 2 modular \mathbb{Z}_3 solutions. The anyon model for the \mathbb{Z}_3 -Parafermionic CFT is $\text{Fib} \times \mathbb{Z}_3^{(2)}$. Because of its interest in the description of the Read-Rezayi state for the $\nu = \frac{12}{5}$ quantum Hall plateau, we tabulate this anyon model explicitly.

$c = \frac{4}{5}$	$\mathcal{D} = \sqrt{3(\phi + 2)}$																												
<table border="1" style="border-collapse: collapse; margin: auto;"> <tr> <td></td><td>ψ_0</td><td>ψ_1</td><td>ψ_2</td><td>ϵ_0</td><td>ϵ_1</td><td>ϵ_2</td></tr> <tr> <td>d</td><td>1</td><td>1</td><td>1</td><td>ϕ</td><td>ϕ</td><td>ϕ</td></tr> <tr> <td>s</td><td>0</td><td>$-\frac{1}{3}$</td><td>$-\frac{1}{3}$</td><td>$\frac{2}{5}$</td><td>$\frac{1}{15}$</td><td>$\frac{1}{15}$</td></tr> <tr> <td>κ</td><td>1</td><td>0</td><td>0</td><td>1</td><td>0</td><td>0</td></tr> </table>		ψ_0	ψ_1	ψ_2	ϵ_0	ϵ_1	ϵ_2	d	1	1	1	ϕ	ϕ	ϕ	s	0	$-\frac{1}{3}$	$-\frac{1}{3}$	$\frac{2}{5}$	$\frac{1}{15}$	$\frac{1}{15}$	κ	1	0	0	1	0	0	$\mathcal{DS} = \begin{pmatrix} 1 & 1 & 1 & \phi & \phi & \phi \\ 1 & \omega^2 & \omega & \phi & \omega^2\phi & \omega\phi \\ 1 & \omega & \omega^2 & \phi & \omega\phi & \omega^2\phi \\ \phi & \phi & \phi & -1 & -1 & -1 \\ \phi & \omega^2\phi & \omega\phi & -1 & -\omega^2 & -\omega \\ \phi & \omega\phi & \omega^2\phi & -1 & -\omega & -\omega^2 \end{pmatrix}$
	ψ_0	ψ_1	ψ_2	ϵ_0	ϵ_1	ϵ_2																							
d	1	1	1	ϕ	ϕ	ϕ																							
s	0	$-\frac{1}{3}$	$-\frac{1}{3}$	$\frac{2}{5}$	$\frac{1}{15}$	$\frac{1}{15}$																							
κ	1	0	0	1	0	0																							

(A.26)

A.1.23 The (10 particle) $k = 3, M = 1$ Read-Rezayi State, or $\mathbb{Z}_5 \times \mathbf{Fib}$

ψ_0	ψ_1	ψ_2	ψ_3	ψ_4	ϵ_0	ϵ_1	ϵ_2	ϵ_3	ϵ_4
ψ_1	ψ_2	ψ_3	ψ_4	ψ_0	ϵ_1	ϵ_2	ϵ_3	ϵ_4	ϵ_0
ψ_2	ψ_3	ψ_4	ψ_0	ψ_1	ϵ_2	ϵ_3	ϵ_4	ϵ_0	ϵ_1
ψ_3	ψ_4	ψ_0	ψ_1	ψ_2	ϵ_3	ϵ_4	ϵ_0	ϵ_1	ϵ_2
ψ_4	ψ_0	ψ_1	ψ_2	ψ_3	ϵ_4	ϵ_0	ϵ_1	ϵ_2	ϵ_3
ϵ_0	ϵ_1	ϵ_2	ϵ_3	ϵ_4	$\epsilon_0 + \psi_0$	$\epsilon_1 + \psi_1$	$\epsilon_2 + \psi_2$	$\epsilon_3 + \psi_3$	$\epsilon_4 + \psi_4$
ϵ_1	ϵ_2	ϵ_3	ϵ_4	ϵ_0	$\epsilon_1 + \psi_1$	$\epsilon_2 + \psi_2$	$\epsilon_3 + \psi_3$	$\epsilon_4 + \psi_4$	$\epsilon_0 + \psi_0$
ϵ_2	ϵ_3	ϵ_4	ϵ_0	ϵ_1	$\epsilon_2 + \psi_2$	$\epsilon_3 + \psi_3$	$\epsilon_4 + \psi_4$	$\epsilon_0 + \psi_0$	$\epsilon_1 + \psi_1$
ϵ_3	ϵ_4	ϵ_0	ϵ_1	ϵ_2	$\epsilon_3 + \psi_3$	$\epsilon_4 + \psi_4$	$\epsilon_0 + \psi_0$	$\epsilon_1 + \psi_1$	$\epsilon_2 + \psi_2$
ϵ_4	ϵ_0	ϵ_1	ϵ_2	ϵ_3	$\epsilon_4 + \psi_4$	$\epsilon_0 + \psi_0$	$\epsilon_1 + \psi_1$	$\epsilon_2 + \psi_2$	$\epsilon_3 + \psi_3$

(A.27)

This is the fusion algebra for the anyonic charge sectors of the $k = 3, M = 1$ Read-Rezayi state, if we identify the sector containing the electron with the vacuum sector. There are 5 unitary solutions to the Pentagon equations, corresponding to the products of the 5 solutions for \mathbb{Z}_5 with the Fib solution. Of these Pentagon solutions, only 1 allows for solutions to the Hexagon equations, giving a total of 10 unitary anyon models with these fusion rules, in 5 mirror pairs. These 10 models are precisely the tensor products of the 5 \mathbb{Z}_5 theories with the 2 Fib theories. Modular products are modular, so we have 8 modular solutions. The model that describes the $k = 3$ Read-Rezayi state is $\mathbf{Fib} \times \mathbb{Z}_5^{(1)}$. Identifying the electron's anyonic charge with the trivial anyonic charge is a bit suspect because the electron is a fermion and, hence, has nontrivial (topological) exchange interactions. If we do not identify the electron's anyonic charge sector with the vacuum sector, but instead declare the anyonic charge of pairs of electrons (which, of course, form bosons) to be equivalent to the trivial charge, then we obtain an anyon model for the Read-Rezayi state which has one extra $\mathbb{Z}_2^{(1)}$ factor, namely $\mathbf{Fib} \times \mathbb{Z}_5^{(1)} \times \mathbb{Z}_2^{(1)}$. This simple way of taking the fermionic nature of the electron into account will only work for the RR-states with odd k , since the even k states are not products and, in fact, we will show that there is no anyon model

for the $k = 2$ RR-state with the electron identified with the vacuum. We give the quantum dimensions, spins and Frobenius-Schur indicators for $\text{Fib} \times \mathbb{Z}_5^{(1)}$ explicitly.

$c = \frac{14}{5}$	$\mathcal{D} = \sqrt{5}(\phi + 2)$										
	ψ_0	ψ_1	ψ_2	ψ_3	ψ_4	ϵ_0	ϵ_1	ϵ_2	ϵ_3	ϵ_4	
d	1	1	1	1	1	ϕ	ϕ	ϕ	ϕ	ϕ	(A.28)
s	0	$\frac{1}{5}$	$-\frac{1}{5}$	$-\frac{1}{5}$	$\frac{1}{5}$	$\frac{2}{5}$	$-\frac{2}{5}$	$\frac{1}{5}$	$\frac{1}{5}$	$-\frac{2}{5}$	
κ	1	0	0	0	0	1	0	0	0	0	

A.1.24 The (12 particle) Moore-Read State

$\psi_{0,0}$	$\psi_{0,2}$	$\psi_{0,4}$	$\psi_{0,6}$	$\psi_{1,1}$	$\psi_{1,3}$	$\psi_{1,5}$	$\psi_{1,7}$	$\psi_{2,0}$	$\psi_{2,2}$	$\psi_{2,4}$	$\psi_{2,6}$
$\psi_{0,2}$	$\psi_{0,4}$	$\psi_{0,6}$	$\psi_{0,0}$	$\psi_{1,3}$	$\psi_{1,5}$	$\psi_{1,7}$	$\psi_{1,1}$	$\psi_{2,2}$	$\psi_{2,4}$	$\psi_{2,6}$	$\psi_{2,0}$
$\psi_{0,4}$	$\psi_{0,6}$	$\psi_{0,0}$	$\psi_{0,2}$	$\psi_{1,5}$	$\psi_{1,7}$	$\psi_{1,1}$	$\psi_{1,3}$	$\psi_{2,4}$	$\psi_{2,6}$	$\psi_{2,0}$	$\psi_{2,2}$
$\psi_{0,6}$	$\psi_{0,0}$	$\psi_{0,2}$	$\psi_{0,4}$	$\psi_{1,7}$	$\psi_{1,1}$	$\psi_{1,3}$	$\psi_{1,5}$	$\psi_{2,6}$	$\psi_{2,0}$	$\psi_{2,2}$	$\psi_{2,4}$
$\psi_{1,1}$	$\psi_{1,3}$	$\psi_{1,5}$	$\psi_{1,7}$	$\psi_{0,2} + \psi_{2,2}$	$\psi_{0,4} + \psi_{2,4}$	$\psi_{0,6} + \psi_{2,6}$	$\psi_{0,0} + \psi_{2,0}$	$\psi_{1,1}$	$\psi_{1,3}$	$\psi_{1,5}$	$\psi_{1,7}$
$\psi_{1,3}$	$\psi_{1,5}$	$\psi_{1,7}$	$\psi_{1,1}$	$\psi_{0,4} + \psi_{2,4}$	$\psi_{0,6} + \psi_{2,6}$	$\psi_{0,0} + \psi_{2,0}$	$\psi_{0,2} + \psi_{2,2}$	$\psi_{1,3}$	$\psi_{1,5}$	$\psi_{1,7}$	$\psi_{1,1}$
$\psi_{1,5}$	$\psi_{1,7}$	$\psi_{1,1}$	$\psi_{1,3}$	$\psi_{0,6} + \psi_{2,6}$	$\psi_{0,0} + \psi_{2,0}$	$\psi_{0,2} + \psi_{2,2}$	$\psi_{0,4} + \psi_{2,4}$	$\psi_{1,5}$	$\psi_{1,7}$	$\psi_{1,1}$	$\psi_{1,3}$
$\psi_{1,7}$	$\psi_{1,1}$	$\psi_{1,3}$	$\psi_{1,5}$	$\psi_{0,0} + \psi_{2,0}$	$\psi_{0,2} + \psi_{2,2}$	$\psi_{0,4} + \psi_{2,4}$	$\psi_{0,6} + \psi_{2,6}$	$\psi_{1,7}$	$\psi_{1,1}$	$\psi_{1,3}$	$\psi_{1,5}$
$\psi_{2,0}$	$\psi_{2,2}$	$\psi_{2,4}$	$\psi_{2,6}$	$\psi_{1,1}$	$\psi_{1,3}$	$\psi_{1,5}$	$\psi_{1,7}$	$\psi_{0,0}$	$\psi_{0,2}$	$\psi_{0,4}$	$\psi_{0,6}$
$\psi_{2,2}$	$\psi_{2,4}$	$\psi_{2,6}$	$\psi_{2,0}$	$\psi_{1,3}$	$\psi_{1,5}$	$\psi_{1,7}$	$\psi_{1,1}$	$\psi_{0,2}$	$\psi_{0,4}$	$\psi_{0,6}$	$\psi_{0,0}$
$\psi_{2,4}$	$\psi_{2,6}$	$\psi_{2,0}$	$\psi_{2,2}$	$\psi_{1,5}$	$\psi_{1,7}$	$\psi_{1,1}$	$\psi_{1,3}$	$\psi_{0,4}$	$\psi_{0,6}$	$\psi_{0,0}$	$\psi_{0,2}$
$\psi_{2,6}$	$\psi_{2,0}$	$\psi_{2,2}$	$\psi_{2,4}$	$\psi_{1,7}$	$\psi_{1,1}$	$\psi_{1,3}$	$\psi_{1,5}$	$\psi_{0,6}$	$\psi_{0,0}$	$\psi_{0,2}$	$\psi_{0,4}$

(A.29)

This is the fusion algebra for the 12-particle anyon model that describes the Moore-Read quantum Hall state. The fusion rules may be obtained as a restriction of the product $\text{SU}(2)_2 \times \mathbb{Z}_8$ to those fields $\psi_{i,j}$ for which $i + j = 0 \pmod{2}$. Hence, we may also obtain solutions to the Pentagon and Hexagon equations by restriction of the product solutions to this subset of particles. It turns out that all solutions to the Pentagon and Hexagon are, in fact, obtained in this way. One way to see this is by brute force solution of the equations combined with a simple counting argument.

There are 16 solutions to the Pentagon equations. Only two of these allow for solutions to the Hexagon equations, with 16 solutions in 8 mirror pairs for each, giving a total of 32 Pentagon/Hexagon solutions. None of these solutions are modular. The quantum dimensions and Frobenius-Schur indicators of the particles are the same for

all solutions:

	$\psi_{0,0}$	$\psi_{0,2}$	$\psi_{0,4}$	$\psi_{0,6}$	$\psi_{1,1}$	$\psi_{1,3}$	$\psi_{1,5}$	$\psi_{1,7}$	$\psi_{2,0}$	$\psi_{2,2}$	$\psi_{2,4}$	$\psi_{2,6}$	
d	1	1	1	1	$\sqrt{2}$	$\sqrt{2}$	$\sqrt{2}$	$\sqrt{2}$	1	1	1	1	(A.30)
κ	1	0	1	0	0	0	0	0	1	0	1	0	

It turns out that all 32 anyon models for these fusion rules can be distinguished by their spin factors. On the other hand, when we produce solutions to the Pentagon and Hexagon as charge spectrum restrictions of product of the $SU(2)_2$ and \mathbb{Z}_8 solutions, then we can see, using the spins for $SU(2)_2$ type theories given in Chapters 5.4, 5.6, and A.1.4 and the spins for the $\mathbb{Z}_8^{(w)}$ theories, that we get precisely 32 classes of solutions which can be distinguished using only their spin factors. This means that the 32 solutions we find by brute force solution of the Pentagons and Hexagons are precisely the restrictions of product solutions that we knew we would find, and there are no further solutions.

The anyon model for the Moore-Read state is a charge spectrum restriction of the product $\text{Ising} \times \mathbb{Z}_8^{(1/2)}$ [see Eq. (5.53)]. We give the S-matrix and spins for this model explicitly.

	$\psi_{0,0}$	$\psi_{0,2}$	$\psi_{0,4}$	$\psi_{0,6}$	$\psi_{1,1}$	$\psi_{1,3}$	$\psi_{1,5}$	$\psi_{1,7}$	$\psi_{2,0}$	$\psi_{2,2}$	$\psi_{2,4}$	$\psi_{2,6}$	
s	0	$\frac{1}{4}$	0	$\frac{1}{4}$	$\frac{1}{8}$	$-\frac{3}{8}$	$-\frac{3}{8}$	$\frac{1}{8}$	$\frac{1}{2}$	$-\frac{1}{4}$	$\frac{1}{2}$	$-\frac{1}{4}$	(A.31)

$$\mathcal{DS} = \begin{pmatrix}
 1 & 1 & 1 & 1 & \sqrt{2} & \sqrt{2} & \sqrt{2} & \sqrt{2} & 1 & 1 & 1 & 1 \\
 1 & -1 & 1 & -1 & i\sqrt{2} & -i\sqrt{2} & i\sqrt{2} & -i\sqrt{2} & 1 & -1 & 1 & -1 \\
 1 & 1 & 1 & 1 & -\sqrt{2} & -\sqrt{2} & -\sqrt{2} & -\sqrt{2} & 1 & 1 & 1 & 1 \\
 1 & -1 & 1 & -1 & -i\sqrt{2} & i\sqrt{2} & -i\sqrt{2} & i\sqrt{2} & 1 & -1 & 1 & -1 \\
 \sqrt{2} & i\sqrt{2} & -\sqrt{2} & -i\sqrt{2} & 0 & 0 & 0 & 0 & -\sqrt{2} & -i\sqrt{2} & \sqrt{2} & i\sqrt{2} \\
 \sqrt{2} & -i\sqrt{2} & -\sqrt{2} & i\sqrt{2} & 0 & 0 & 0 & 0 & -\sqrt{2} & i\sqrt{2} & \sqrt{2} & -i\sqrt{2} \\
 \sqrt{2} & i\sqrt{2} & -\sqrt{2} & -i\sqrt{2} & 0 & 0 & 0 & 0 & -\sqrt{2} & -i\sqrt{2} & \sqrt{2} & i\sqrt{2} \\
 \sqrt{2} & -i\sqrt{2} & -\sqrt{2} & i\sqrt{2} & 0 & 0 & 0 & 0 & -\sqrt{2} & i\sqrt{2} & \sqrt{2} & -i\sqrt{2} \\
 1 & 1 & 1 & 1 & -\sqrt{2} & -\sqrt{2} & -\sqrt{2} & -\sqrt{2} & 1 & 1 & 1 & 1 \\
 1 & -1 & 1 & -1 & -i\sqrt{2} & i\sqrt{2} & -i\sqrt{2} & i\sqrt{2} & 1 & -1 & 1 & -1 \\
 1 & 1 & 1 & 1 & \sqrt{2} & \sqrt{2} & \sqrt{2} & \sqrt{2} & 1 & 1 & 1 & 1 \\
 1 & -1 & 1 & -1 & i\sqrt{2} & -i\sqrt{2} & i\sqrt{2} & -i\sqrt{2} & 1 & -1 & 1 & -1
 \end{pmatrix} \tag{A.32}$$

A.1.25 “Projection” of the MR state to 6 particles

The anyon model for the Moore-Read state described in Appendix A.1.24 is not modular. In fact, looking at the S-matrix, we see that the particles occur in pairs which are not distinguishable by full monodromies (these particles have identical rows in the S-matrix). The non-modularity of the theory is an obstruction to the existence of a modular invariant partition function in any CFT realization of these 12-particle fusion rules. Conventional CFT wisdom says that, in order to obtain a CFT with such a partition function, we must identify the fields which have identical rows in the S-matrix. This really means that the primary field which is identified with the vacuum must be added to the chiral algebra. The characters of the new chiral algebra are then in one-to-one correspondence with the classes of identified fields and these new characters should have the proper behavior under modular transformations (in particular, the S-matrix will be invertible). Here, this invertible S-matrix would be given by

$$\mathcal{D}S = \begin{pmatrix} 1 & 1 & 1 & 1 & \sqrt{2} & \sqrt{2} \\ 1 & -1 & 1 & -1 & -i\sqrt{2} & i\sqrt{2} \\ 1 & 1 & 1 & 1 & -\sqrt{2} & -\sqrt{2} \\ 1 & -1 & 1 & -1 & i\sqrt{2} & -i\sqrt{2} \\ \sqrt{2} & -i\sqrt{2} & -\sqrt{2} & i\sqrt{2} & 0 & 0 \\ \sqrt{2} & i\sqrt{2} & -\sqrt{2} & -i\sqrt{2} & 0 & 0 \end{pmatrix} \quad (\text{A.33})$$

In this case, the field $\psi_{2,4}$, which corresponds to the electron, is the field that behaves like the vacuum under monodromy with other fields. Since this field is fermionic, it can actually be distinguished from the vacuum by looking at processes involving exchange, rather than full monodromy and so it is not right to think of the field that creates the electron as physically trivial. Also, if we want to describe the full topological interactions of the theory using an anyon model then it is clear that we must have a charge other than the vacuum corresponding to the electron. Nevertheless, one might hope that the full structure of the 12-particle anyon model may be described conveniently in terms of a 6-particle TQFT whose S-matrix is given by Eq. (A.33),

and some contributions coming from the electron that has been forgotten in that theory. If this is the case then the 6-particle theory involved has to have the fusion rules

$\psi_{0,0}$	$\psi_{2,0}$		$\psi_{1,1}$	$\psi_{0,2}$	$\psi_{2,2}$	$\psi_{1,3}$
$\psi_{2,0}$	$\psi_{0,0}$		$\psi_{1,1}$	$\psi_{2,2}$	$\psi_{0,2}$	$\psi_{1,3}$
$\psi_{1,1}$	$\psi_{1,1}$	$\psi_{0,2} + \psi_{2,2}$	$\psi_{1,3}$	$\psi_{1,3}$	$\psi_{0,0} + \psi_{2,0}$	
$\psi_{0,2}$	$\psi_{2,2}$		$\psi_{1,3}$	$\psi_{2,0}$	$\psi_{0,0}$	$\psi_{1,1}$
$\psi_{2,2}$	$\psi_{0,2}$		$\psi_{1,3}$	$\psi_{0,0}$	$\psi_{2,0}$	$\psi_{1,1}$
$\psi_{1,3}$	$\psi_{1,3}$	$\psi_{0,0} + \psi_{2,0}$	$\psi_{1,1}$	$\psi_{1,1}$	$\psi_{0,2} + \psi_{2,2}$	

(A.34)

which are obtained from the table in Appendix A.1.24 by replacing each particle by its class under the field identifications.

When trying to solve the Pentagon and Hexagon equations for the fusion rules above, one finds an interesting and, perhaps, surprising result: the fusion rules admit 8 solutions to the Pentagon equations, but none of these allow for a solution to the Hexagon equations. In other words, there is no anyon model compatible with the fusion rules given above.

In terms of conformal field theory this means that the primary operators of the theory do not form a closed set under fusion; descendants at odd grades necessarily pop up as the dominant terms in some of the operator products. Here, the important descendants are obviously those created by the electron field, which has been added to the operator algebra. In order to represent the topological properties of the CFT by an anyon model, one must introduce separate anyonic charges for the primary fields and for these descendants. Physically, it seems clear that the topological charge spectrum of the theory is, in fact, that of the anyon model presented in Appendix A.1.24, rather than that of the CFT, which puts bosonic and fermionic states together into supersymmetric sectors, while the anyon model has separate sectors for particles which differ by fusion with a fermion.

A.1.26 $SU(3)_2$ Parafermions, or $\mathbb{Z}_2 \times \mathbb{Z}_2 \times \mathbf{Fib}$

$\psi_{0,0}$	$\psi_{0,1}$	$\psi_{1,0}$	$\psi_{1,1}$	$\epsilon_{0,0}$	$\epsilon_{0,1}$	$\epsilon_{1,0}$	$\epsilon_{1,1}$	
$\psi_{0,1}$	$\psi_{0,0}$	$\psi_{1,1}$	$\psi_{1,0}$	$\epsilon_{0,1}$	$\epsilon_{0,0}$	$\epsilon_{1,1}$	$\epsilon_{1,0}$	
$\psi_{1,0}$	$\psi_{1,1}$	$\psi_{0,0}$	$\psi_{0,1}$	$\epsilon_{1,0}$	$\epsilon_{1,1}$	$\epsilon_{0,0}$	$\epsilon_{0,1}$	
$\psi_{1,1}$	$\psi_{1,0}$	$\psi_{0,1}$	$\psi_{0,0}$	$\epsilon_{1,1}$	$\epsilon_{1,0}$	$\epsilon_{0,1}$	$\epsilon_{0,0}$	
$\epsilon_{0,0}$	$\epsilon_{0,1}$	$\epsilon_{1,0}$	$\epsilon_{1,1}$	$\epsilon_{0,0} + \psi_{0,0}$	$\epsilon_{0,1} + \psi_{0,1}$	$\epsilon_{1,0} + \psi_{1,0}$	$\epsilon_{1,1} + \psi_{1,1}$	
$\epsilon_{0,1}$	$\epsilon_{0,0}$	$\epsilon_{1,1}$	$\epsilon_{1,0}$	$\epsilon_{0,1} + \psi_{0,1}$	$\epsilon_{0,0} + \psi_{0,0}$	$\epsilon_{1,1} + \psi_{1,1}$	$\epsilon_{1,0} + \psi_{1,0}$	
$\epsilon_{1,0}$	$\epsilon_{1,1}$	$\epsilon_{0,0}$	$\epsilon_{0,1}$	$\epsilon_{1,0} + \psi_{1,0}$	$\epsilon_{1,1} + \psi_{1,1}$	$\epsilon_{0,0} + \psi_{0,0}$	$\epsilon_{0,1} + \psi_{0,1}$	
$\epsilon_{1,1}$	$\epsilon_{1,0}$	$\epsilon_{0,1}$	$\epsilon_{0,0}$	$\epsilon_{1,1} + \psi_{1,1}$	$\epsilon_{1,0} + \psi_{1,0}$	$\epsilon_{0,1} + \psi_{0,1}$	$\epsilon_{0,0} + \psi_{0,0}$	

(A.35)

This is the fusion algebra of the $SU(3)_2$ parafermionic model that describes the topological interactions of the quasiholes of the $\nu = \frac{4}{7}$ spin singlet Hall state proposed in Ref. [61], up to Abelian contributions from $U(1)$ factors for spin and charge (see Chapter 5.8). There are 8 unitary solutions to the Pentagon equations. These correspond to the products of the Fib solution with the 8 solutions for $\mathbb{Z}_2 \times \mathbb{Z}_2$. Of these 8 Pentagon solutions, 4 allow for solutions to the Hexagon equations, with 16 Hexagon solutions each, for a total of 64 unitary Pentagon/Hexagon solutions. These are precisely the products of the 32 solutions we obtained for $\mathbb{Z}_2 \times \mathbb{Z}_2$ with the 2 solutions we obtained for Fib. As with $\mathbb{Z}_2 \times \mathbb{Z}_2$, many of these solutions correspond to the same anyon model, because they can be obtained from each other by the permuting the particles with nontrivial $\mathbb{Z}_2 \times \mathbb{Z}_2$ charge. Taking this into account, we see that there are 24 non-isomorphic anyon models, in 12 mirror pairs. As usual, only products of modular theories are modular, yielding 6 non-isomorphic unitary modular theories, in 3 mirror pairs. The $SU(3)_2$ parafermionic CFT itself is described by the $D'(Z_2) \times \mathbf{Fib}^{-1}$ anyon model. We tabulate the dimensions, spins, and Frobenius-Schur

indicators for this model (the S-matrix can also be calculated from this data).

$c = \frac{6}{5}$					$\mathcal{D} = 2\sqrt{\phi + 2}$			
	$\psi_{0,0}$	$\psi_{0,1}$	$\psi_{1,0}$	$\psi_{1,1}$	$\epsilon_{0,0}$	$\epsilon_{0,1}$	$\epsilon_{1,0}$	$\epsilon_{1,1}$
d	1	1	1	1	ϕ	ϕ	ϕ	ϕ
s	0	$\frac{1}{2}$	$\frac{1}{2}$	$\frac{1}{2}$	$\frac{3}{5}$	$\frac{1}{10}$	$\frac{1}{10}$	$\frac{1}{10}$
κ	1	1	1	1	1	1	1	1

(A.36)

Bibliography

- [1] D. Lestel, C. Herzfeld, Topological apes: Knots tying and untying and the origins of mathematics, in: P. Grialou, G. Longo, M. Okada (Eds.), *Image and Reasoning*, Vol. 1, Tokyo: University of Keio Press, 2005, pp. 147–162.
- [2] C. Herzfeld, D. Lestel, Knot tying in great apes: etho-ethnology of an unusual tool behavior, *Social Science Information* 44 (2005) 621–653.
- [3] I. Newton, *Philosophiæ Naturalis Principia Mathematica*, London, 1687.
- [4] P. Ehrenfest, *Proc. Amsterdam Acad.* 20 (1917) 200.
- [5] P. Ehrenfest, Welche Rolle spielt die Dreidimensionalität des Raumes in den Grundgesetzen der Physik?, *Ann. Physik* 61 (1920) 440.
- [6] F. R. Tangherlini, Schwarzschild field in n dimensions and the dimensionality of space problem, *Nuovo Cimento* (10) 27 (1963) 636–651.
- [7] W. Büchel, Warum hat der Raum drei Dimensionen?, *Physikalische Blätter* 19 (1963) 547–549, English translation in [153].
- [8] S. N. Bose, Plancks Gesetz und Lichtquantenhypothese, *Zeits. f. Physik* 26 (1924) 178–181.
- [9] A. Einstein, Quantentheorie des einatomigen idealen Gases, in: *Sitzungsber. Kgl. Preuss. Akad. Wiss.*, 1924, pp. 261–267.
- [10] E. Fermi, Zur Quantelung des idealen einatomigen Gases, *Zeits. f. Physik* 36 (1926) 902.
- [11] P. A. M. Dirac, On the theory of quantum mechanics, *Proc. Roy. Soc.* A112 (1926) 661–677.

- [12] M. Born, Zur Quantenmechanik der Stoßvorgänge, *Zeits. f. Physik* 37 (1926) 863–867.
- [13] E. Fadell, L. Neuwirth, Configuration spaces, *Math. Scand.* 10 (1962) 111–118.
- [14] R. P. Feynman, Space-time approach to non-relativistic quantum mechanics, *Rev. Mod. Phys.* 20 (1948) 367–387.
- [15] M. G. G. Laidlaw, C. M. DeWitt, Feynman functional integrals for systems of indistinguishable particles, *Phys. Rev. D* 3 (1971) 1375–1378.
- [16] H. S. Green, A generalized method of field quantization, *Phys. Rev.* 90 (1953) 270–273.
- [17] K. Drühl, R. Haag, J. E. Roberts, On parastatistics, *Commun. Math. Phys.* 18 (1970) 204–226.
- [18] J. M. Leinaas, J. Myrheim, On the theory of identical particles, *Nuovo Cimento B* 37B (1977) 1.
- [19] E. Artin, Theorie der Zöpfe, *Abh. math. Sem. Hamburg* 4 (1926) 47–72.
- [20] F. Wilczek, Magnetic flux, angular momentum, and statistics, *Phys. Rev. Lett.* 48 (1982) 1144–1146.
- [21] F. Wilczek, Quantum mechanics of fractional-spin particles, *Phys. Rev. Lett.* 49 (1982) 957–959.
- [22] G. A. Goldin, R. Menikoff, D. H. Sharp, Comments on “General Theory for Quantum Statistics in Two Dimensions”, *Phys. Rev. Lett.* 54 (1985) 603.
- [23] T. D. Imbo, J. March-Russell, Exotic statistics on surfaces, *Phys. Lett. B* 252 (1990) 84–90.
- [24] G. Moore, N. Seiberg, Polynomial equations for rational conformal field theories, *Phys. Lett. B* 212 (1988) 451–460.

- [25] G. Moore, N. Seiberg, Classical and quantum conformal field theory, *Commun. Math. Phys.* 123 (1989) 177–254.
- [26] E. Witten, Quantum field theory and the Jones polynomial, *Comm. Math. Phys.* 121 (1989) 351–399.
- [27] K. Fredenhagen, K. H. Rehren, B. Schroer, Superselection sectors with braid group statistics and exchange algebras, *Commun. Math. Phys.* 125 (1989) 201–226.
- [28] J. Fröhlich, F. Gabbiani, Braid statistics in local quantum theory, *Rev. Math. Phys.* 2 (1990) 251–353.
- [29] V. G. Turaev, *Quantum Invariants of Knots and 3-Manifolds*, Walter de Gruyter, Berlin, New York, 1994.
- [30] C. Kassel, *Quantum Groups*, Springer-Verlag, New York, Berlin, Heidelberg, 1995.
- [31] B. Bakalov, A. Kirillov, *Lectures on Tensor Categories and Modular Functors*, Vol. 21 of University Lecture Series, American Mathematical Society, 2001.
- [32] R. Prange, S. M. Girvin (Eds.), *The Quantum Hall effect*, Springer-Verlag, New York, 1987.
- [33] A. Karlhede, S. A. Kivelson, S. L. Sondhi, The quantum Hall effect: The article, in: V. J. Emery (Ed.), *Correlated Electron Systems*, World Scientific, Singapore, 1992, lectures presented at the 9th Jerusalem Winter School for Theoretical Physics.
- [34] S. Das Sarma, A. Pinczek, *Perspectives in quantum Hall effects: Novel quantum liquids in low-dimensional semiconductor structures*, Wiley, New York, 1997.
- [35] Z. Ezawa (Ed.), *Quantum Hall effects, field theoretical approach and related topics*, World Scientific, Singapore, 2000.

- [36] J. P. Eisenstein, H. L. Stormer, The fractional quantum Hall effect, *Science* 248 (1990) 1510–1516.
- [37] H. L. Stormer, D. C. Tsui, A. C. Gossard, The fractional quantum Hall effect, *Rev. Mod. Phys.* 71 (1999) S298–S305.
- [38] K. von Klitzing, G. Dorda, M. Pepper, New method for high-accuracy determination of the fine-structure constant based on quantized Hall resistance, *Phys. Rev. Lett.* 45 (1980) 494–497.
- [39] D. C. Tsui, H. L. Stormer, A. C. Gossard, Two-dimensional magnetotransport in the extreme quantum limit, *Phys. Rev. Lett.* 48 (1982) 1559–62.
- [40] V. J. Goldman, B. Su, Resonant tunneling in the quantum Hall regime: Measurement of fractional charge, *Science* 267 (1995) 1010–1012.
- [41] V. J. Goldman, J. Liu, A. Zaslavsky, Fractional statistics of Laughlin quasiparticles in quantum antidots, *Phys. Rev. B* 71 (2005) 153303.
- [42] F. E. Camino, W. Zhou, V. J. Goldman, Realization of a Laughlin quasiparticle interferometer: Observation of fractional statistics, *Phys. Rev. B* 72 (2005) 075342, [cond-mat/0502406](#).
- [43] F. E. Camino, W. Zhou, V. J. Goldman, Aharonov–Bohm superperiod in a Laughlin quasiparticle interferometer, *Phys. Rev. Lett.* 95 (2005) 246802, [cond-mat/0504341](#).
- [44] F. E. Camino, W. Zhou, V. J. Goldman, Transport in the Laughlin quasiparticle interferometer: Evidence for topological protection in an anyonic qubit, *Phys. Rev. B* 74 (2006) 115301, [cond-mat/0606742](#).
- [45] F. E. Camino, W. Zhou, V. J. Goldman, $e/3$ Laughlin quasiparticle primary-filling $\nu = 1/3$ interferometer, *Phys. Rev. Lett.* 98 (2007) 076805, [cond-mat/0610751](#).

- [46] F. E. Camino, W. Zhou, V. J. Goldman, Experimental realization of a primary-filling $e/3$ quasiparticle interferometer (2006), cond-mat/0611443.
- [47] G. Moore, N. Read, Nonabelions in the fractional quantum Hall effect, Nucl. Phys. B 360 (1991) 362–396.
- [48] R. B. Laughlin, Anomalous quantum Hall effect: an incompressible quantum fluid with fractionally charged excitations, Phys. Rev. Lett. 50 (1983) 1395–8.
- [49] R. Willett, J. P. Eisenstein, H. L. Stormer, D. C. Tsui, A. C. Gossard, J. H. English, Observation of an even-denominator quantum number in the fractional quantum Hall effect, Phys. Rev. Lett. 59 (1987) 1776–9.
- [50] W. Pan, J.-S. Xia, V. Shvarts, D. E. Adams, H. L. Stormer, D. C. Tsui, L. N. Pfeiffer, K. W. Baldwin, K. W. West, Exact quantization of the even-denominator fractional quantum Hall state at $\nu = 5/2$ Landau level filling factor, Phys. Rev. Lett. 83 (1999) 3530–3, cond-mat/9907356.
- [51] J. P. Eisenstein, K. B. Cooper, L. N. Pfeiffer, K. W. West, Insulating and fractional quantum Hall states in the first excited Landau level, Phys. Rev. Lett. 88 (2002) 076801, cond-mat/0110477.
- [52] J. S. Xia, W. Pan, C. L. Vicente, E. D. Adams, N. S. Sullivan, H. L. Stormer, D. C. Tsui, L. N. Pfeiffer, K. W. Baldwin, K. W. West, Electron correlation in the second Landau level: A competition between many nearly degenerate quantum phases, Phys. Rev. Lett. 93 (2004) 176809, cond-mat/0406724.
- [53] N. Read, E. Rezayi, Beyond paired quantum Hall states: Parafermions and incompressible states in the first excited Landau level, Phys. Rev. B 59 (1999) 8084–8092, cond-mat/9809384.
- [54] R. H. Morf, Transition from quantum Hall to compressible states in the second Landau level: new light on the $\nu = 5/2$ enigma, Phys. Rev. Lett. 80 (1998) 1505–8, cond-mat/9809024.

- [55] E. H. Rezayi, F. D. M. Haldane, Incompressible paired Hall state, stripe order, and the composite fermion liquid phase in half-filled Landau levels, *Phys. Rev. Lett.* 84 (2000) 4685–4688, [cond-mat/9906137](#).
- [56] C. Nayak, F. Wilczek, $2n$ -quasihole states realize 2^{n-1} -dimensional spinor braiding statistics in paired quantum Hall states, *Nucl. Phys. B* 479 (1996) 529–53, [cond-mat/9605145](#).
- [57] J. K. Slingerland, F. A. Bais, Quantum groups and nonabelian braiding in quantum Hall systems, *Nucl. Phys. B* 612 (2001) 229–290, [cond-mat/0104035](#).
- [58] N. Read, D. Green, Paired states of fermions in two dimensions with breaking of parity and time-reversal symmetries and the fractional quantum Hall effect, *Phys. Rev. B* 61 (2000) 10267–10297, [cond-mat/9906453](#).
- [59] D. A. Ivanov, Non-Abelian statistics of half-quantum vortices in p-wave superconductors, *Phys. Rev. Lett.* 86 (2001) 268–271, [cond-mat/0005069](#).
- [60] A. Stern, F. von Oppen, E. Mariani, Geometric phases and quantum entanglement as building blocks for non-Abelian quasiparticle statistics, *Phys. Rev. B* 70 (2004) 205338, [cond-mat/0310273](#).
- [61] E. Ardonne, K. Schoutens, A new class of non-Abelian spin-singlet quantum Hall states, *Phys. Rev. Lett.* 82 (25) (1999) 5096–5099, [cond-mat/9811352](#).
- [62] A. Y. Kitaev, Fault-tolerant quantum computation by anyons, *Ann. Phys.* 303 (2003) 2, [quant-ph/9707021](#).
- [63] A. Kitaev, Anyons in an exactly solved model and beyond, *Ann. Phys.* 321 (2006) 2–111, [cond-mat/0506438](#).
- [64] M. H. Freedman, A magnetic model with a possible Chern-Simons phase, *Commun. Math. Phys.* 234 (2003) 129–183, [quant-ph/0110060](#).

- [65] M. Freedman, C. Nayak, K. Shtengel, K. Walker, Z. Wang, A class of P, T -invariant topological phases of interacting electrons, *Ann. Phys.* 310 (2004) 428–492, [cond-mat/0307511](#).
- [66] M. Freedman, C. Nayak, K. Shtengel, Extended Hubbard model with ring exchange: A route to a non-Abelian topological phase, *Phys. Rev. Lett.* 94 (2005) 066401, [cond-mat/0312273](#).
- [67] M. Freedman, C. Nayak, K. Shtengel, Line of critical points in $2+1$ dimensions: Quantum critical loop gases and non-Abelian gauge theory, *Phys. Rev. Lett.* 94 (2005) 147205, [cond-mat/0408257](#).
- [68] V. G. Turaev, O. Y. Viro, State sum invariants of 3-manifolds and quantum 6j-symbols, *Topology* 31 (1992) 865–902.
- [69] M. A. Levin, X.-G. Wen, String-net condensation: A physical mechanism for topological phases, *Phys. Rev. B* 71 (2005) 045110, [cond-mat/0404617](#).
- [70] P. Fendley, E. Fradkin, Realizing non-Abelian statistics in time-reversal-invariant systems, *Phys. Rev. B* 72 (2005) 024412, [cond-mat/0502071](#).
- [71] L. Fidkowski, From string nets to nonabelions (2006), [cond-mat/0610583](#).
- [72] B. Douçot, L. B. Ioffe, J. Vidal, Discrete non-Abelian gauge theories in Josephson-junction arrays and quantum computation, *Phys. Rev. B* 69 (2004) 214501, [cond-mat/0302104](#).
- [73] S. D. Sarma, C. Nayak, S. Tewari, Proposal to stabilize and detect half-quantum vortices in strontium ruthenate thin films: Non-Abelian braiding statistics of vortices in a $p_x + ip_y$ superconductor, *Phys. Rev. B* 73 (2006) 220502, [cond-mat/0510553](#).
- [74] S. Tewari, S. D. Sarma, C. Nayak, C. Zhang, P. Zoller, Quantum computation using vortices and majorana zero modes of a $p_x + ip_y$ superfluid of fermionic cold atoms, *Phys. Rev. Lett.* 98 (2007) 010506, [quant-ph/0606101](#).

- [75] V. Gurarie, L. Radzihovsky, A. V. Andreev, Quantum phase transitions across a p -wave Feshbach resonance, *Phys. Rev. Lett.* 94 (2005) 230403, *cond-mat/0410620*.
- [76] N. R. Cooper, N. K. Wilkin, J. M. F. Gunn, Quantum phases of vortices in rotating Bose–Einstein condensates, *Phys. Rev. Lett.* 87 (2001) 120405, *cond-mat/0107005*.
- [77] N. R. Cooper, Exact ground states of rotating Bose gases close to a Feshbach resonance, *Physical Review Letters* 92 (2004) 220405, *cond-mat/0107005*.
- [78] E. H. Rezayi, N. Read, N. R. Cooper, Incompressible liquid state of rapidly rotating bosons at filling factor $3/2$, *Phys. Rev. Lett.* 95 (2005) 160404, *cond-mat/0507064*.
- [79] J. Preskill, Fault-tolerant quantum computation, in: H.-K. Lo, S. Popescu, T. P. Spiller (Eds.), *Introduction to Quantum Computation*, World Scientific, 1998.
- [80] R. W. Ogburn, J. Preskill, Topological quantum computation, *Lect. Notes in Comp. Sci.* 1509 (1999) 341–356.
- [81] M. H. Freedman, Quantum computation and the localization of modular functors, *Found. Comput. Math.* 1 (2001) 183–204, *quant-ph/0003128*.
- [82] M. H. Freedman, M. J. Larsen, Z. Wang, A modular functor which is universal for quantum computation, *Commun. Math. Phys.* 227 (2002) 605–622, *quant-ph/0001108*.
- [83] M. Freedman, A. Kitaev, M. Larsen, Z. Wang, Topological quantum computation, *quant-ph/0101025* (2001).
- [84] C. Mochon, Anyons from nonsolvable finite groups are sufficient for universal quantum computation, *Phys. Rev. A* 67 (2003) 022315, *quant-ph/0206128*.

- [85] C. Mochon, Anyon computers with smaller groups, *Phys. Rev. A* 69 (2004) 032306, [quant-ph/0306063](#).
- [86] S. Das Sarma, M. Freedman, C. Nayak, Topologically protected qubits from a possible non-Abelian fractional quantum Hall state, *Phys. Rev. Lett.* 94 (2005) 166802, [cond-mat/0412343](#).
- [87] M. Freedman, C. Nayak, K. Walker, Towards universal topological quantum computation in the $\nu = 5/2$ fractional quantum Hall state (2005), [cond-mat/0512066](#).
- [88] M. Freedman, C. Nayak, K. Walker, Tilted interferometry realizes universal quantum computation in the Ising TQFT without overpasses (2005), [cond-mat/0512072](#).
- [89] S. Bravyi, Universal quantum computation with the $\nu = 5/2$ fractional quantum Hall state, *Phys. Rev. A* 73 (2006) 042313, [quant-ph/0511178](#).
- [90] N. E. Bonesteel, L. Hormozi, G. Zikos, S. H. Simon, Braid topologies for quantum computation, *Phys. Rev. Lett.* 95 (2005) 140503, [quant-ph/0505065](#).
- [91] S. H. Simon, N. E. Bonesteel, M. H. Freedman, N. Petrovic, L. Hormozi, Topological quantum computing with only one mobile quasiparticle, *Phys. Rev. Lett.* 96 (2006) 070503, [quant-ph/0509175](#).
- [92] L. Hormozi, G. Zikos, N. E. Bonesteel, S. H. Simon, Topological quantum compiling, *Phys. Rev. B* 75 (2007) 165310, [quant-ph/0610111](#).
- [93] Y. Aharonov, D. Bohm, Significance of electromagnetic potentials in the quantum theory, *Phys. Rev.* 115 (1959) 485–491.
- [94] V. B. Braginsky, Y. I. Vorontsov, *Usp. Fiz. Nauk* 41–62 (1974) 114, [*Sov. Phys. Uspekhi* 17, 644 (1975)].
- [95] J. Preskill, Topological quantum computation, lecture notes (2004).
URL <http://www.theory.caltech.edu/~preskill/ph219/topological.ps>

- [96] S. Mac Lane, *Categories for the Working Mathematician*, 2nd Edition, Graduate Texts in Mathematics, Springer-Verlag, New York, 1998.
- [97] B. Buchberger, Ein Algorithmus zum Auffinden der Basiselemente des Restklassenringes nach einem nulldimensionalen Polynomideal, Ph.D. thesis, English translation in [154] (1965).
- [98] B. Buchberger, Ein algorithmisches Kriterium für die Lösbarkeit eines algebraischen Gleichungssystems, *Aequationes mathematicae* 4 (1970) 374–383, English translation in [155].
- [99] P. Etingof, D. Mikshych, V. Ostrik, On fusion categories, *Ann. Math.* 162 (2005) 581–642.
- [100] L. Zehnder, Ein neuer interferenzrefractor, *Zeitschr. f. Instrkde.* 11 (1891) 275–285.
- [101] L. Mach, Über einer interferenzrefractor, *Zeitschr. f. Instrkde.* 12 (1892) 89–93.
- [102] P. Bonderson, K. Shtengel, J. K. Slingerland, Decoherence of anyonic charge in interferometry measurements, *Phys. Rev. Lett.* 98 (2007) 070401, [quant-ph/0608119](#).
- [103] B. J. Overbosch, F. A. Bais, Inequivalent classes of interference experiments with non-Abelian anyons, *Phys. Rev. A* 64 (2001) 062107, [quant-ph/0105015](#).
- [104] A. Zeilinger, General properties of lossless beam splitters in interferometry, *Am. J. Phys.* 49 (1981) 882–883.
- [105] P. Bonderson, K. Shtengel, J. K. Slingerland, Probing non-Abelian statistics with quasiparticle interferometry, *Phys. Rev. Lett.* 97 (2006) 016401, [cond-mat/0601242](#).
- [106] Y. Ji, Y. Chung, D. Sprinzak, M. Heiblum, D. Mahalu, H. Shtrikman, An electronic Mach–Zehnder interferometer, *Nature* 422 (2003) 415–418, [cond-mat/0303553](#).

- [107] I. Neder, M. Heiblum, Y. Levinson, D. Mahalu, V. Umansky, Coherence and phase in an electronic Mach–Zehnder interferometer: An unexpected behavior of interfering electrons (2005), cond-mat/0508024.
- [108] I. Neder, M. Heiblum, Y. Levinson, D. Mahalu, V. Umansky, Unexpected behavior in a two-path electron interferometer, *Phys. Rev. Lett.* 96 (2006) 016804.
- [109] C. L. Kane, Telegraph noise and fractional statistics in the quantum Hall effect, *Phys. Rev. Lett.* 90 (2003) 226802, cond-mat/0210621.
- [110] T. Jonckheere, P. Devillard, A. Crepieux, T. Martin, Electronic Mach–Zehnder interferometer in the fractional quantum Hall effect, *Phys. Rev. B* 72 (2005) 201305(R), cond-mat/0503617.
- [111] K. T. Law, D. E. Feldman, Y. Gefen, Electronic Mach-Zehnder interferometer as a tool to probe fractional statistics, *Phys. Rev. B* 74 (2006) 045319, cond-mat/0506302.
- [112] D. E. Feldman, A. Kitaev, Detecting non-Abelian statistics with an electronic Mach–Zehnder interferometer, *Phys. Rev. Lett.* 97 (2006) 186803, cond-mat/0607541.
- [113] C. Fabry, A. Pérot, Sur les franges des lames minces argenteées et leur application à la mesure de petites épaisseurs d’air, *Ann. Chim. Phys.* 12 (1897) 459–501.
- [114] C. de C. Chamon, D. E. Freed, S. A. Kivelson, S. L. Sondhi, X. G. Wen, Two point-contact interferometer for quantum Hall systems, *Phys. Rev. B* 55 (1997) 2331–43, cond-mat/9607195.
- [115] E. Fradkin, C. Nayak, A. Tsvetik, F. Wilczek, A Chern-Simons effective field theory for the Pfaffian quantum Hall state, *Nucl. Phys. B* 516 (1998) 704–18, cond-mat/9711087.
- [116] A. Stern, B. I. Halperin, Proposed experiments to probe the non-abelian $\nu = 5/2$ quantum Hall state, *Phys. Rev. Lett.* 96 (2006) 016802, cond-mat/0508447.

- [117] P. Bonderson, A. Kitaev, K. Shtengel, Detecting non-Abelian statistics in the $\nu = 5/2$ fractional quantum Hall state, Phys. Rev. Lett. 96 (2006) 016803, cond-mat/0508616.
- [118] E. Grosfeld, S. H. Simon, A. Stern, Switching noise as a probe of statistics in the fractional quantum Hall effect, Phys. Rev. Lett. 96 (2006) 226803, cond-mat/0602634.
- [119] C.-Y. Hou, C. Chamon, “Wormhole” geometry for entrapping topologically protected qubits in non-Abelian quantum Hall states and probing them with voltage and noise measurements, Phys. Rev. Lett. 97 (2006) 146802, cond-mat/0603142.
- [120] P. Fendley, M. P. Fisher, C. Nayak, Dynamical disentanglement across a point contact in a non-Abelian quantum Hall state, Phys. Rev. Lett. 97 (2006) 036801, cond-mat/0604064.
- [121] P. Fendley, M. P. Fisher, C. Nayak, Edge states and tunneling of non-Abelian quasiparticles in the $\nu = 5/2$ quantum Hall state and p+ip superconductors, Phys. Rev. B 75 (2007) 045317, cond-mat/0607431.
- [122] S. B. Chung, M. Stone, Proposal for reading out anyon qubits in non-Abelian $\nu = 12/5$ quantum Hall state, Phys. Rev. B 73 (2006) 245311, cond-mat/0601594.
- [123] L. Fidkowski, Double point contact in the $k=3$ Read–Rezayi state (2007), arXiv:0704.3291.
- [124] E.-A. Kim, Aharonov-bohm interference and fractional statistics in a quantum hall interferometer, Phys. Rev. Lett. 97 (2006) 216404, cond-mat/0604359.
- [125] B. Rosenow, B. I. Halperin, Influence of interactions on flux and back-gate period of quantum Hall interferometers, Phys. Rev. Lett. 98 (2007) 106801, cond-mat/0611101.

- [126] D. J. Thouless, Y. Gefen, Fractional quantum Hall effect and multiple Aharonov–Bohm periods, *Phys. Rev. Lett.* 66 (1991) 806–809.
- [127] X. G. Wen, Theory of the edge states in fractional quantum Hall effects, *Intl. J. Mod. Phys. B* 6 (1992) 1711–62.
- [128] J. B. Miller, I. P. Radu, D. M. Zumbuhl, E. M. Levenson-Falk, M. A. Kastner, C. M. Marcus, L. N. Pfeiffer, K. W. West, Fractional quantum Hall effect in a quantum point contact at filling fraction $5/2$ (2007), [cond-mat/0703161](#).
- [129] R. Dijkgraaf, C. Vafa, E. Verlinde, H. Verlinde, The operator algebra of orbifold models, *Commun. Math. Phys.* 123 (1989) 485–526.
- [130] R. Dijkgraaf, V. Pasquier, P. Roche, Quasi Hopf algebras, group cohomology and orbifold models, *Nucl. Phys. B (Proc. Suppl.)* 18B (1990) 60–72.
- [131] F. A. Bais, P. van Driel, M. de Wild Propitius, Quantum symmetries in discrete gauge theories, *Phys. Lett. B* 280 (1992) 63–70, [hep-th/9203046](#).
- [132] J. Wess, B. Zumino, Consequences of anomalous Ward identities, *Phys. Lett. B* 37 (1971) 95.
- [133] E. Witten, Global aspects of current algebra, *Nucl. Phys. B* 223 (1983) 422–432.
- [134] V. F. R. Jones, A polynomial invariant for knots via von Neumann algebras, *Bull. Am. Math. Soc.* 12 (1985) 103–111.
- [135] G. Kuperberg, unpublished.
- [136] M. H. Freedman, M. J. Larsen, Z. Wang, The two-eigenvalue problem and density of jones representation of braid groups, *Commun. Math. Phys.* 228 (2002) 177–199.
- [137] G. Moore, N. Seiberg, Taming the conformal zoo, *Phys. Lett. B* 220 (1989) 422–430.

- [138] D. Gepner, Field identification in coset conformal field theories, *Phys. Lett. B* 222 (2) (1989) 207–212.
- [139] A. B. Zamolodchikov, V. Fateev, Nonlocal (parafermion) currents in two-dimensional conformal quantum field theory and self-dual critical points in z_N -symmetric statistical systems, *Soviet Physics - JETP* 62 (1985) 215–225.
- [140] D. Gepner, Z. Qiu, Modular invariant partition functions for parafermionic field theories, *Nucl. Phys. B* 285 (1987) 423–453.
- [141] P. Bonderson, J. K. Slingerland, in preparation.
- [142] A. S. Schwarz, The partition function of degenerate quadratic functional and Ray-Singer invariants, *Lett. Math. Phys.* 2 (1978) 247–252.
- [143] J. F. Schonfeld, A mass term for three-dimensional gauge fields, *Nucl. Phys. B* 185 (1981) 157.
- [144] S. Deser, R. Jackiw, S. Templeton, Topologically massive gauge theories, *Ann. Phys.* 140 (1982) 372–411.
- [145] R. Dijkgraaf, E. Witten, Topological gauge theories and group cohomology, *Commun. Math. Phys.* 129 (1990) 393–429.
- [146] X. G. Wen, A. Zee, Classification of Abelian quantum Hall states and matrix formulation of topological fluids, *Phys. Rev. B* 46 (1992) 2290–301.
- [147] F. D. M. Haldane, Fractional quantization of the Hall effect: A hierarchy of incompressible quantum fluid states, *Phys. Rev. Lett.* 51 (1983) 605–608.
- [148] B. I. Halperin, Statistics of quasiparticles and the hierarchy of fractional quantized Hall states, *Phys. Rev. Lett.* 52 (1984) 1583–6.
- [149] J. K. Jain, Composite fermion approach for the fractional quantum Hall effect, *Phys. Rev. Lett.* 63 (1989) 199–202.

- [150] D. Gepner, New conformal field theories associated with Lie algebras and their partition functions, Nucl. Phys. B 290 (1987) 10.
- [151] Z. Wang, Classification of TQFTs, talk at the KITP conference on Topological Phases and Quantum Computation, Santa Barbara (2006).
URL http://online.itp.ucsb.edu/online/qubit_c06/
- [152] D. Gepner, A. Kapustin, On the classification of fusion rings, Phys. Lett. B 349 (1995) 71–75, hep-th/9410089.
- [153] I. M. Freeman, Why is space three-dimensional?, Am. J. Phys. 37 (12) (1969) 1222–1224, based on W. Büchel: “Warum hat der Raum drei Dimensionen?,” Physikalische Blätter 19, 12, pp. 547–549 (December 1963).
- [154] B. Buchberger, An algorithm for finding the basis elements in the residue class ring modulo a zero dimensional polynomial ideal, Ph.D. thesis (2006).
- [155] B. Buchberger, An algorithmic criterion for the solvability of algebraic systems of equations 251 (1998) 535–545.